CURE KINETICS OF WOOD PHENOL-FORMALDEHYDE SYSTEMS

By

JINWU WANG

A dissertation submitted in partial fulfillment of

the requirements for the degree of

DOCTOR OF PHILOSOPHY

WASHINGTON STATE UNIVERSITY

Department of Civil and Environmental Engineering

May 2007

To the Faculty of Washington State University:

The members of the Committee appointed to examine the dissertation of JINWU WANG find it satisfactory and recommend that it be accepted.

_____

Co-Chair

_____

Co-Chair

_____

_____

ACKNOWLEDGEMENT

Many years' effort and the gracious assistance of many individuals converge in this dissertation. I would like to express my sincere appreciation and deep gratitude to my co-advisors, Dr. Marie-Pierre G. Laborie and Dr. Michael P. Wolcott, for their financial support, academic suggestions, and discussion. Thanks also to my committee members, Dr. Armando A. McDonald and Dr. Jinwen Zhang, for their examination of my dissertation and their suggestions.

I would like to extend my appreciation to those faculty, staff, and students who were willing to discuss interesting questions and help me learn instrument operations. These individuals include: Dr. David P. Harper, Dr. Tieqi Li, Dr. J. Andy Soria, Scott Lewis, Bob Duncan, Janet Duncan, Pat Smith, Dr. Donald A. Bender, Dr. Pizhong Qiao, Dr. Vikram Yadama, Dr. Gregory Helms, and Dr. Dan Mitchell. Thanks also to Judy for always being there to offer help. Graduate and post-doctoral fellows who accompanied me through this course of study and made daily life interesting are: Barun Gupta, Sudip Chowdhury, Jun Qian, Melchor Maranan, Eric Rude, Elvie Brown, William Gacitua, Dr. Yu Geng, and Dr. Long (Edward) Jiang.

Finally, I thank my daughter Yun, my son Kai, and my wife, Xingwu for their support and love.

CURE KINETICS OF WOOD PHENOL-FORMALDEHYDE SYSTEMS

Abstract

by Jinwu Wang, Ph.D.
Washington State University
May 2007

Co-Chairs: Marie-Pierre G. Laborie and Michael P. Wolcott

This project aims to develop kinetic models for chemical and mechanical cure development and correlate chemical and mechanical degrees of cure in order to create a comprehensive cure model that encompasses both of these tasks. With these objectives, the cure processes of two commercial phenol-formaldehyde (PF) resol resins with differing molecular weights were evaluated using differential scanning calorimetry (DSC) and dynamic mechanical analysis (DMA) under isothermal and linear heating regimes. For both resins, cure was characterized in the neat state with DSC, in mixtures of PF/wood flour with DSC, and as a bondline between two wood substrates with DMA.

The synergy of DSC and DMA techniques picked up the phase transitions of PF curing processes and characterization were comparable between the two techniques. During a DSC temperature scan, PF resols typically exhibited two exotherms, while in wood/PF mixtures another small exotherm appeared in a lower temperature range, indicating the impact of wood/PF interactions. In contrast, DMA offered a quantitative view of the adhesion mechanics from which the glass transition of uncured resin, gelation, and vitrification points were inferred. An analytical solution was developed to estimate the *in situ* shear modulus of the adhesive layer

during the curing process, a change estimated from 0.01 to 16MPa. The maximum storage modulus and the ratio of maximum to minimum storage modulus were recommended for direct evaluation of wood-PF system.

Model-fitting kinetics of nth order and autocatalytic models can be reasonably applied to the DSC data, while autocatalytic, Prout-Tompkins, and Avrami-Erofeev models have been successfully applied to describe cure development in the DMA. The activation energy of PF curing processes in the neat state was around 85-100 kJ/mol and decreased to 50-70 kJ/mol in the presence of wood. However, it was the model-free kinetics of the Kissinger-Akhira-Sunnose, Friedman and Vyazovkin methods that offered insight into the cure mechanisms of commercial PF resoles and predicted the cure development under isothermal and linear heating regimes for both mechanical and chemical degrees of cure. Mechanical cure development has been correlated with chemical advancement in an empirical equation analog to the Weibull cumulative function. After either mechanical or chemical cure development is characterized, the other can be estimated through connection of the correlation equation between the mechanical and chemical degrees of cure.

TABLE OF CONTENTS

Page

LST OF TABLES

LIST OF FIGURES

Chapter 1 Project Introduction

BACKGROUND

During hot-pressing of wood-based composites, the press schedule is predominantly controlled by two parameters, bond strength development and internal gas pressure. Short pressing times are desirable from an economical standpoint but can result in low bond strength and panel delamination upon press opening. In order to assist in understanding and optimizing hot-pressing conditions for wood –based composites, several researchers have developed hot-pressing models that predict mat temperature, moisture, internal pressure, and density developments as a function of the input hot-pressing parameters (Zombori *et al*. 2003; Thoemen & Humphrey 2003; Dai *et al*. 2005). These hot-pressing models have either ignored bond strength development or have used an arbitrary cure kinetic model to portray bond strength development. In order to improve the accuracy of hot-pressing models, bond strength development models need to be incorporated. In the literature, the cure kinetics of thermosets resins has been mainly modeled based on chemical advancement (He *et al*. 2003; Lei and Wu 2006). However, both chemical and mechanical cure progression are needed to describe bond development. Indeed, the kinetics of chemical cure is not linearly related to the bond strength development. Therefore this research proposes to consider both chemical and mechanical cure in designing kinetic models of bond strength development that are suitable for hot-pressing models.

Phenol-formaldehyde (PF) resins are widely used in wood-based composites

manufacture. It is well established that wood has an influence on the cure kinetics of PF resins (Chow 1969; Pizzi *et al*. 1994). Therefore the models for bond strength development need to account for the influence of wood. The research is proposed for PF as the adhesive system.

Generally, there are three methods to investigate the cure kinetics of PF resins: in neat state, in mixture with wood flour, or in thin film between wood substrate. The cure kinetic of PF resins in a neat state have been the subject of many cure kinetic studies (Kay and Westwood 1975; Park *et al*. 1999; He *et al*. 2003), yet the best model for predicting PF dynamic and isothermal cure has not been established. Clearly there is an need for researchers to compare and contrast several commonly used kinetic models for predicting degree of cure and cure rate of PF resins so that models that are most adequate for incorporation in hot-pressing models be determined.

Although cure development of neat PF resins can provide useful information for resin formulators, it is *in situ* cure development in the presence of wood can assist to disclose the cure mechanism and investigate the effects of wood presence on cure kinetics. There are substantial physical and chemical interaction between wood and PF resins (Pizzi *et al*. 1994). The porous structure of wood may preferentially absorb some PF components or the resin with a specific molecular weight range (Furuno *et al*. 2004); the covalent bond may also form between wood and PF molecular chains (Chow 1969). This presents a question whether the kinetic models appropriate for neat resins are also working for the wood-adhesive systems.

As in literature, wood-PF interactions are maximized and conveniently

researched with the mixtures of wood flour and PF (Chow 1969; Pizzi *et al*. 1994; He *et al*. 2005; Lei an Wu 2006). However, PF resin is used as adhesives and is usually applied as a thin film between two wood substrates, thus it does not have same intricate contact with wood as in the form of powder. Questions are raised whether the adhesive is 'same material' in neat bulk form and in powder mixtures as when presents as a thin adhesive layer between wood substrates. Besides wood-PF interactions and preferential absorption along the interface, residual internal stresses are more likely to be present in the adhesive when it is cured between substrates. These factors might obviously alter the kinetics of PF chemical reaction by which the adhesive hardens and influence the mechanical properties of the *in situ* cured resin compared to the bulk adhesive. Cure kinetics and *in situ* property formation processes are important for setting up optimum process parameters. These aspects are undoubtedly worthy of further investigation. A sandwiched structure with an adhesive layer between two wood substrates was favored in investigating the wood-adhesive bondline development since the sandwiched geometry more closely resembles the practical application of the adhesives when compared to the mixture in PF/wood flour. The *in situ* shear and flexural modulus development of the adhesive layer during cure is different from bulk property formation process and is one of basic material parameters needed to construct an useful hot-pressing model.

Another question is how physical and mechanical properties change with the chemical degree of cure. Curing is intended to advance the PF molecules into a highly crosslinked network to achieve a high durability of the products; curing is also meant

to develop physical and mechanical strength in the products. The kinetics of chemical advancement of the adhesive layer is not necessarily linearly related with developing rate of mechanical properties. In literature, the cure kinetics of thermosets such as PF resin is most modeled based on chemical advancement (He *et al*. 2003; Lei and Wu 2006). The relationship of chemical and mechanical advancements remains unclear. However, both are needed to describe bondline development completely so that a cure model for hot-pressing can encompass information on both. Usually, the phenolic has developed enough stiffness and durability in use before it has sufficient strength at pressing temperature to permit pressing opening. So pressing time is determined such that developed interface adhesion is enough to withstand internal pressure or stresses imposed by changes in wood thickness spring back at the time of press opening. The relationship of degree of cure and mechanical properties can assist to determine exactly when this occurs, thus stop pressing in time to short the press cycle. Curing process continues to achieve higher crosslinking density by stacking the boards together by virtue of residual heat long after pressing. For this purpose, it is worthwhile to investigate the relationship between mechanical development and chemical advancement.

OBJECTIVES

In this perspective, the overall goal of this research is to develop a protocol to obtain cure kinetic data, provide a practical kinetic analysis and model methodology, and recommend appropriate models for predicting cure behavior of PF resins in terms

of mechanical cure and chemical cure. The chemical advancement in reaction heat evolution will be monitored with differential scanning calorimetry (DSC); and the mechanical property evolution will be monitored by dynamical mechanic analysis (DMA) through a sandwich beam with an adhesive layer between two wood substrates. The chemical advancement and mechanical develop rate will be correlated so that a cure model for PF resins can encompass information on both. These objectives fit in the broader aim to incorporate a cure kinetic model into a hot-pressing model for wood-based composites. The specific objectives of this research are:

(1) To evaluate and compare the ability of most common kinetic models for a) revealing the cure process of commercial PF resins and b) predicting the dynamic and isothermal cure behavior.

(2) To investigate the influence of individual wood constituents and wood itself on the kinetics of PF chemical cure.

(3) To explore dynamic mechanical analysis (DMA) as a procedure to directly evaluate bond strength development in a sandwich beam consisting of an adhesive layer between two wood veneers.

(4) To model PF mechanical cure development by DMA

(5) To correlate the mechanical property development by DMA and chemical degree of cure by DSC.

ORGANIZATION OF THE DISSERTATION

The dissertation is divided into nine chapters, including this introductory chapter. Chapters two through eight are written as a stand-alone paper each consisting of an introduction, objectives, methodology, results, and a conclusion. All chapters are connected by using the same two PF resins for addressing one aspect of the objectives presented in this introduction chapter. In chapter two the chemical structures and molecular weights of the two PF resins are characterized with ^{1}H- and ^{13}C-nuclear magnetic resonance as well as gel permeation chromatography to provide a basic knowledge of the materials used in all chapters. Chapter three introduces and compares the applications and limitations of model-fitting kinetics to characterize the chemical cure of the PF resoles. Chapter four examines the potential of model-free kinetics for gaining insight on the cure mechanisms of PF resoles and for predicting chemical cure development under isothermal and constant heating rate regimes. Chapter five investigates the effects of wood content and wood species on chemical cure development of PF resins. Chapter six demonstrates a DMA technique for directly evaluating wood-adhesive system, by estimating the the *in situ* shear modulus of a PF adhesive layer in a sandwich beam Chapter seven examines the feasibility of characterizing cure development events such as gelation and vitrification points and obtaining mechanical cure kinetic data using DMA. The cure kinetic data are modeled with three model-fitting equations. In chapter eight the mechanical cure modeled by DMA and the chemical cure modeled by DSC are correlated. The cure kinetics is modeled with model-free kinetics. Finally, Chapter nine summarizes the conclusions

of this project. Scheme 1 is a schematic diagram showing connections of various topics.

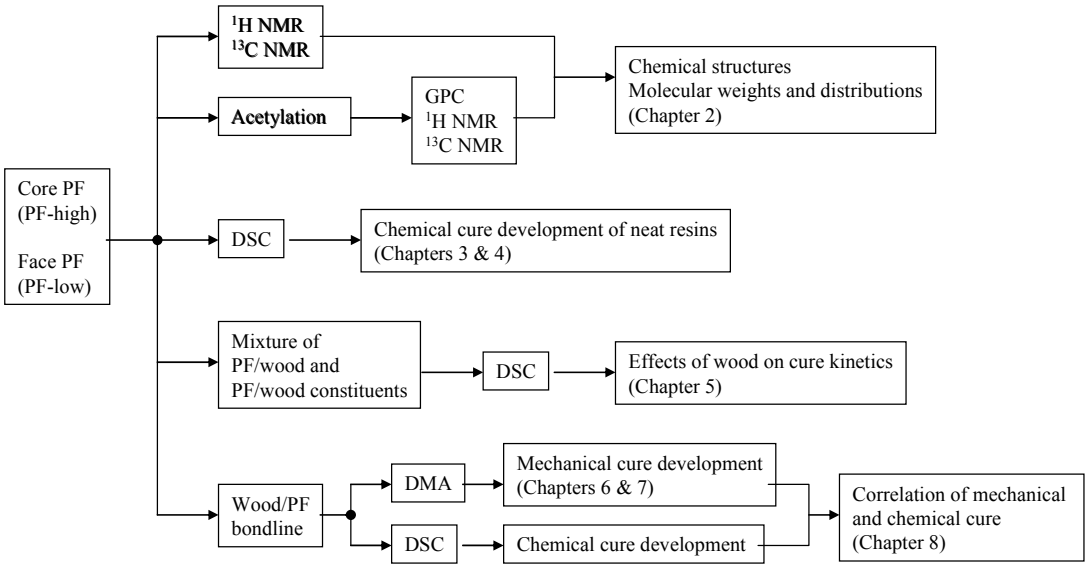

Scheme 1 A schematic diagram of linkage between various topics presented in this research.

REFERENCES

Chow, S.-Z. A kinetic study of the polymerization of phenol-formaldehyde resin in the presence of cellulosic materials. *Wood Science (1969), 1*(4), 215-221.

Dai, C.; Yu, C.; Zhou, X. Heat and mass transfer in wood composite panels during hot pressing. part II. Modeling void formation and mat permeability. *Wood and Fiber Science (2005), 37*(2) 242-257

Furuno, T.; Imamura, Y.; Kajita, H. The modification of wood by treatment with low molecular weight phenol-formaldehyde resin: a properties enhancement with neutralized phenolic-resin and resin penetration into wood cell walls. *Wood Science and Technology (2004), 37*(5), 349-361.

He, G.; Riedl, B.; Ait-kadi, A. Model-free kinetics: curing behavior of phenol formaldehyde resins by Differential Scanning Calorimetry. *Journal of Applied Polymer Science (2003), 87*, 433 -440.

Kay, R.; Westwood, A. R. Differential scanning calorimetry (DSC) investigations on

condensation polymers. I. Curing. *European Polymer Journal (1975), 11*(1), 25-30

Lei, Y.; Wu, Q. Cure kinetics of aqueous phenol-formaldehyde resins used for oriented strandboard manufacturing: effect of wood flour. *Journal of Applied Polymer Science (2006), 102*(4), 3774-3781.

Park, B.-D.; Riedl, B.; Bae, H.-J.; Kim, Y. S. Differential scanning calorimetry of phenol - formaldehyde (PF) adhesives. *Journal of Wood Chemistry and Technology (1999), 19*(3), 265-286

Pizzi, A.; Mtsweni, B.; Parsons, W. Wood-induced catalytic activation of PF adhesives. Auto-polymerization vs. PF/wood covalent bonding. *Journal of Applied Polymer Science (1994), 52*(13), 1847-1856.

Thoemen, H.; Humphrey, P. E. Modeling the continuous pressing process for wood-based composites. *Wood and Fiber Science (2003), 35*(3), 456-468.

Zombori, B. G.; Kamke, F. A. Watson, L. T. Simulation of the internal conditions during the hot-pressing process. *Wood and Fiber Science (2003), 35*(1), 2-23.

Chapter 2 Quantitative Analysis of Phenol-formaldehyde Resins with ^{13}C-, ^{1}H-NMR and Gel Permeation Chromatography

ABSTRACT

The chemical structure and molecular weight distributions of phenol-formaldehyde (PF) resol resins have been correlated with resin performance and have provided useful information for resin formulations and applications. In this research, the chemical structure and molecular weights of two commercial PF resins with different molecular weights were characterized by ^{1}H- and quantitative ^{13}C-NMR spectroscopy and gel permeation chromatography (GPC) in their neat and acetylated states. Results from all three techniques showed that the two PF resins were distinctive in their relative quantities of methylene bridge structures, methylol groups, and molecular weight distributions and that one PF resin was more advanced than the other. The average molecular weight of the acetylated lower molecular weight resin determined by GPC corresponded with those obtained with ^{1}H and ^{13}C-NMR spectra. However, GPC analysis of the higher molecular weight resin (on the acetylated) tended to over-estimate the molecular weight.

Key words: ^{1}H-NMR, quantitative ^{13}C-NMR spectroscopy; gel permeation chromatography; phenol–formaldehyde resin; molecular weight.

INTRODUCTION

Phenol-formaldehyde (PF) resins are widely used in the manufacture of wood-based composites. A measure of the molecular weights of PF resins is important for quality control during synthesis, for predicting properties of the cured resin and following reaction kinetics (Dargaville *et al*. 1997). Molecular weight distributions have been correlated with composite performance (Wilson *et al*. 1979, Nieh and Sellers 1991). It is therefore critical to accurately characterize resin structure and molecular weight. Gel permeation chromatography (GPC) is the most widely used method for characterizing molecular weight distributions of PF resins. Tetrahydrofuran (THF), the solvent most frequently used as an eluent, dissolves only lower molecular weight fractions of PF resins and not higher ones (Wellons and Gollob 1980). High molecular weight PF resins have been traditionally acetylated in order to become soluble in THF and amenable to GPC analysis. PF resins can also be treated with an ion-exchange resin to remove sodium ions and become soluble in THF. Even after treatment with an ion-exchange resin (Yazaki *et al*. 1994), the advanced PF resins are not completely soluble in THF or other organic solvents.

Furthermore, it has been shown that the average molecular weights of ion-exchange treated PF resin are lower than those measured on acetylated PF resins (Yazaki *et al*. 1994). Riedl *et al*. (1988) identified binary solvents that were suitable for GPC analysis of low molecular weight PF resins. In particular, THF modified with a small amount of trichloroacetic acid system produced good results, with minimal association and high solubility. Therefore, although GPC analysis can be effectively

used for low molecular weight PF resins, resins with high molecular weight and high alkalinity must be acetylated prior to dissolution in THF for GPC analysis. However, intermolecular associations of acetylated PF species in THF result in an overestimation of the actual molecular weights (Wellons and Gollob 1980; Yazaki *et al*. 1994).

In addition to the GPC technique, researchers can use nuclear magnetic resonance (NMR) in solution to estimate molecular weights. The number average molecular weights for PF resins can be calculated using Woodbrey's formulae (Woodbrey *et al*. 1965) on the basis of ^{1}H-NMR spectra. Yazaki *et al* (1994) have confirmed the validity of the formulae by applying it to a model compound, which has a molecular weight of 320 g/mol. On the other hand, ^{13}C-NMR spectroscopy provides a qualitative evaluation of the chemical structures of PF resins (Holopainen *et al*. 1997). The large chemical shift range of ^{13}C-NMR allows the identification of many functional groups of PF resins that overlap in the ^{1}H-NMR spectra (McGraw *et al*. 1989). Owing to the nuclear overhauser effect (NOE), ^{13}C-NMR spectra are not quantitative and may not be used for molecular weight determination. However, Luukko *et al*. (1998) and Rego *et al*. (2004) demonstrated that the quantitative ^{13}C-NMR analyses of PF resols are possible using inverse gated-decoupling and a shiftless paramagnetic relaxation reagent. This suggests that molecular weight distribution may be computed from both ^{13}C-NMR and ^{1}H-NMR.

The objectives of this work are to 1) characterize the chemical structures and molecular weights of two commercial PF resins with GPC, ^{1}H- and quantitative

^{13}C-NMR , and to 2) compare the estimates of molecular structure and molecular weights as determined by ^{1}H-NMR, quantitative ^{13}C-NMR, and GPC. For these purposes, ^{1}H-NMR and ^{13}C-NMR spectral analyses were made on both neat resins and acetylated resins, while GPC analysis was only made on acetylated resins.

EXPERIMENTAL

Materials

Face and core resol PF resins used for the face and core layers of oriented strand boards were obtained from a commercial company and stored in a freezer at -20 ^{o}C. The core PF resin has higher viscosity, pH value and lower solid content than the face PF resin (Figure 2.1). Resins were characterized as received and also after acetylation.

Table 2.1 Features of the core PF and face PF resins.

	Core PF	**Face PF**
NV, %	45.0	54.5
Specific Gravity	1.195 – 1.215	1.220
Viscosity, cps	175 – 300	100 – 225
NaOH, %	5.53 – 5.73	2.96 – 3.16
Free Phenol, %	< 1.0	< 0.2
Free Formaldehyde, %	< 0.2	<0.2
pH	11.0 – 11.5	9.8 – 10.2

Acetylation of PF resins

Prior to GPC analysis, the PF resins were acetylated in order to afford solubility in THF (Yazaki *et al*. 1994). Approximately 15 g of liquid PF resin was acetylated in a 1:1 (79.10 g and 102.09 g) molar mixture of pyridine: acetic anhydride placed in an ice-bath for an initial 2-hour period, followed by a 72-hour period at room temperature. After 74 hours of reaction time, the reaction mixture was poured into ice-water (400mL) and stirred for 20 minutes. The white precipitate was collected, washed with water (4x400mL), and dissolved in chloroform. The organic solvent layer was washed with water (4 x200mL). The organic phase was dried with anhydrous sodium sulfate and then filtered. The chloroform was removed by rotational evaporation in vacuum at 40 °C. The dried residue was dissolved in a small amount of acetone, to which water (30mL) was added, and evaporated in vacuum at 40 °C by the rotavapour. The residuals were further dried under high vacuum overnight to yield approximately 5g acetylated PF resins.

GPC analysis of the acetylated PF resins

Viscotek 270 was coupled with a Waters HPLC unit and Jordi Gel polydivinylbenzene mixed bed column with a right angle, refractive index and differential viscometer detectors. Polystyrene standards were used for calibration. Acetylated PF resins were dissolved in THF at a concentration of 3.6 mg/ml. Aliquots, 200µl in size were injected in the column that had THF as the mobile phase with a flow rate of 0.5 ml/min. 4 replicates have been conducted.

^{1}H- and quantitative ^{13}C-NMR analyses of the acetylated resins

Based on solubility criteria and solvent chemical shifts, chloroform-d was selected as a solvent for solution NMR analysis of the acetylated PF resins. Chloroform also served as a chemical shift reference. In order to reduce the testing time with ^{13}C-NMR, Chromium (III) acetylacetonate ($Cr(C_5H_7O_2)_3$) of 97% purity from Aldrich was added in 20 mM concentration in the NMR tube as a relaxation reagent (Lukko *et al*. 1998). ^{1}H-NMR and ^{13}C-NMR spectra were recorded on a Bruker AMX-300 spectrometer operating at 75.5 MHz. The operating parameters for ^{1}H-NMR were as follows: acquisition time: 4.95 s; pulse width: 9.7 s; pulse delay: 2 s; number of scans: 16. The inverse gated-decoupling technique was used to eliminate the nuclear overhauser effect (NOE) for quantitative ^{13}C-NMR. Typical spectra of resins were run with a 45^{o} pulse. Preliminary tests were run to optimize the delay time, acquisition time, and the number of scans. Specific times and numbers of scans were then selected (8 s delay, 0.6 s acquisition, 2560 scans) to measure the spectra of the acetylated and neat resins for quantitative analysis with three sample repetitions.

^{1}H- and quantitative ^{13}C-NMR analyses of the neat resins

In order to investigate the effect of acetylation on the molecular weights measurements, the neat resins were also analyzed by ^{1}H- and ^{13}C–NMR in deuterium oxide (D_2O, 99.9%) with 0.5% DSS (Sodium 2, 2-dimethyl-2-silapentane-5-sulfonate from Cambridge Isotope) as an internal reference. Due to the insolubility of

Chromium (III) acetylacetonate in D_2O, Gadolinium (III) chloride hexahydrate of 99.99% (from Aldrich) was used as the relaxation reagent with a concentration around 1 mM for ^{13}C-NMR. A preliminary test with 20 mM of Gadolinium showed that at this concentration, the spin-spin relaxation time T_2 greatly decreased, indicating that insufficient points were picked to give the correct spectrum. The ^{1}H-NMR and ^{13}C-NMR spectra of neat resins in D_2O solution were recorded on a Varian Inova 500 spectrometer at 125.6 Hz. ^{1}H- and ^{13}C-NMR parameters were similar with those for the acetylated resins.

RESULTS AND DISCUSSION

Molecular weights of the acetylated PF resins by GPC analyses

The typical GPC chromatogram from the viscometer detector is shown in Figure 2.1, and chromatograms by the right angle and refractive index detectors are similar. GPC gives relatively reliable data for the molecular weight distributions of two PF resins. Both resins consist of three fractions. The first PF fraction eludes its largest oligomers between 8.6 and 11.3 ml for the core PF and between 9.9 to 11.3 ml for the face PF, indicating that the core resin has a higher molecular weight fraction than the face resin. The two other fractions, likely dimmers (peak at 11.5 ml) and monomers of hydroxymethylated phenols (peak at 12.1 ml), are similar for both resins. The core PF resin also has a broader molecular weight distribution compared to the face PF resin. Average molecular weights (Mn and Mw) and polydispersity index

(Mw/Mn) calculated from the GPC results are presented in Table 2.2. The measured molecular weights confirm that the core resin has a broader molecular weight distribution and higher molecular weights than the face resin.

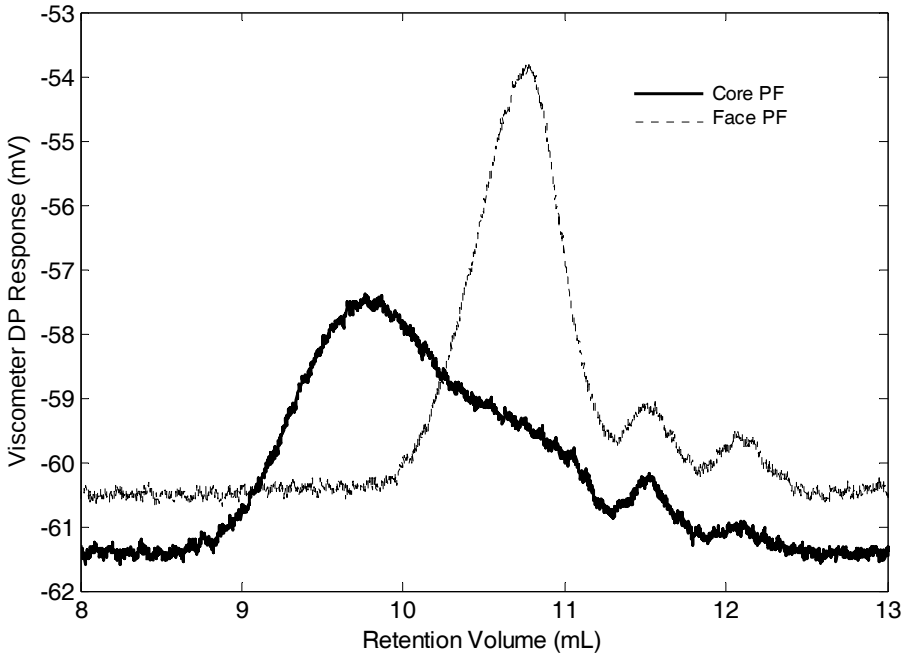

Figure 2.1 GPC chromatogram for core and face PF resin obtained from the differential viscometer detector.

Table 2.2 Molecular weights of acetylated resins by GPC

	M_n (g/mol)	M_w (g/mol)	M_w/M_n
Face PF	439	621	1.41
Core PF	3893	6576	1.72

M_n: number average molecular weight, M_w: weight average molecular weight.

Chemical structures and molecular weights of the acetylated PF resins by ^{1}H- and ^{13}C-NMR

Species in the resins

The typical species in PF resins are hydroxymethylated phenols (HMPs) that may be mono-di or trisubstituted at the ortho and para positions, and their dimmers and oligomers (**scheme 1**) (Bouajila *et al*. 2002).

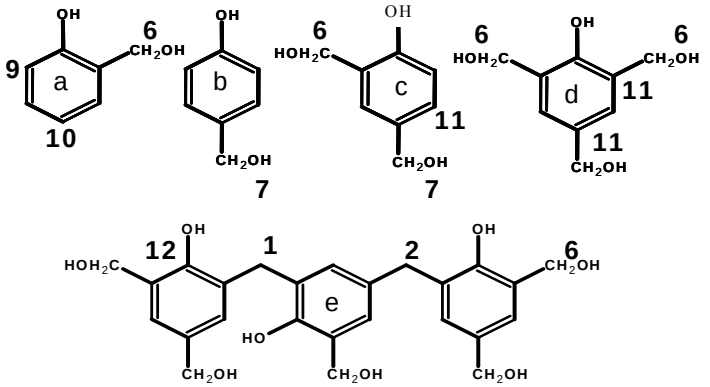

Scheme 1. Typical PF species and carbon numbering for identification.

After acetylation, the hydroxyls are substituted by the acetoxy group (**Scheme 2**).

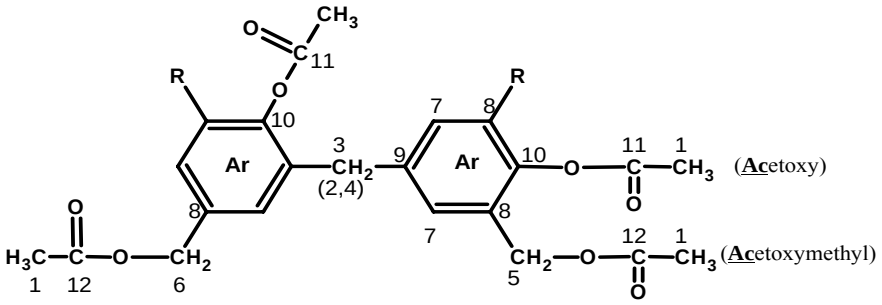

Scheme 2 Acetylated PF dimmer and numbering of functional carbons for identification.

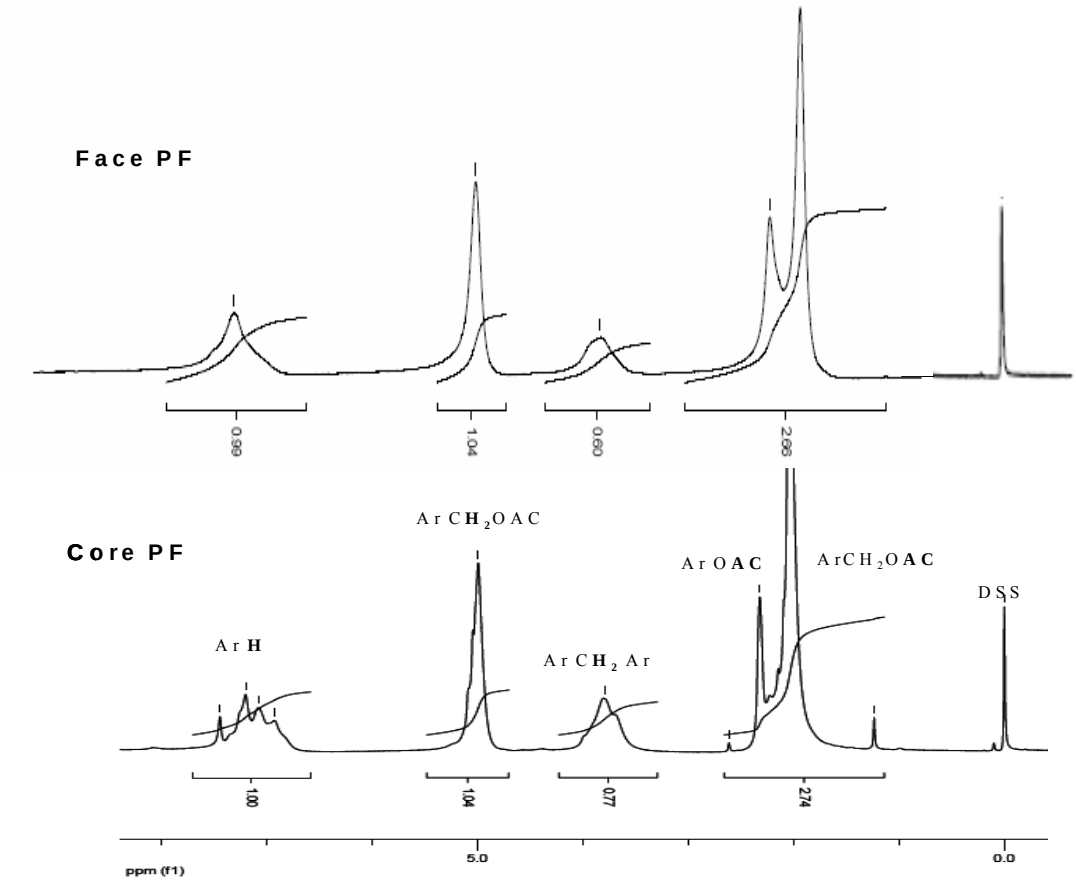

Figure 2.2 ^{1}H-NMR spectra of the acetylated face PF and core PF resins in $CDCl_3$; Ar: aromatic ring, Ac: acetoxy group.

Chemical shift assignments of the acetylated PF resins by ^{1}H-NMR

^{1}H-NMR spectra of acetylated face and core PF resins are shown in Figure 2.2. The spectra of both resins are similar. Certain clusters of protons in functional groups are well resolved for the acetylated resins and can be assigned to specific chemical shift regions (Woodbrey 1965; Steiner 1975; McGraw *et al*. 1989). With this resolution in chemical shifts and the ability to quantify functional groups in ^{1}H-NMR, molecular weights can be calculated for two acetylated resins using Woodbrey's

formulae (Woodbrey *et al*. 1965). In that objective, integration of specific chemical shift regions was performed as presented in Table 2.3.

Table 2.3 ^{1}H-NMR chemical shift of acetylated resins in $CDCl_3$

Nature of the proton	Chemical Shift region (ppm)
Ar**H**	7.67-6.58
ArC**H**$_2$OAc	5.3-4.60
ArC**H**$_2$Ar	4.03-3.42
ArO**Ac**	2.33-2.13
Ar(CH$_2$O)**Ac**	2.07-1.62

Ar: aromatic ring, Ac: acetoxy group

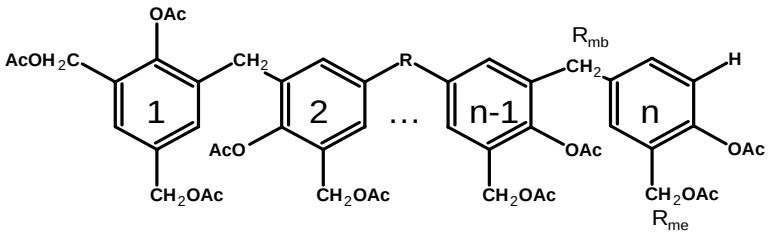

Scheme 3 Linear structure assumption for the acetylated PF resins, Ac: acetoxy groups.

In general, molecular size of resol resin was rather small. It was assumed that the methylene bridges did not bond the aromatic rings into cyclic structures but predominated in linear structures (**Scheme 3**). Hence, the average number of aromatic

rings per molecule chain, *n*, i.e. degree of polymerization, may be calculated from Eq. (1) (Woodbrey *et al*. 1965; Yazaki *et al*. 1994).

$$n = \frac{1}{1 - R_{mb}} \tag{1}$$

where R_{mb} in Eq. (1) and R_{me} in Scheme 3 represent the contents of methylene bridges and methylols per phenolic ring, respectively. For the ^{1}H-NMR spectra of the acetylated resins in CD_4Cl, R_{mb} and R_{me} can be calculated from integrals of ^{1}H-NMR spectra of the acetylated resins in Table 2.3 as follows:

$$R_{me} = \frac{3\int \mathrm{ArCH_2OAc}}{2\int \mathrm{ArOAc}}; \quad R_{mb} = \frac{3\int \mathrm{ArCH_2Ar}}{2\int \mathrm{ArOAc}} \tag{2}$$

From the degree of polymerization, the number average molecular weight for the acetylated resins, the number average molecular weight of acetylated resins, Mn(Ac), can then be calculated with Eq.(3).

$$Mn(Ac) = n * [131 + (5 - R_{me} - R_{mb}) + 73 * R_{me} + 14 * R_{mb}] \tag{3}$$

The first item in the square bracket of Eq. (3) (i.e. 131) represents the molecular weight of the aromatic ring with an acetoxy group. The second item in parentheses represents the molecular weight of hydrogen that remained on the aromatic ring. The

third item represents the molecular weight of acetoxymethyl, and the last item represents molecular weight of methylene bridge $–CH_2-$. Functional groups and molecular weights thus calculated from the ^{1}H-NMR spectra are summarized in Table 2.4. All integration values are expressed per phenolic unit (p.p.u). The core PF has a higher content of methylene bridges, a higher degree of polymerization and molecular weights, but a lower content of methylol, indicating that the core PF resin was more advanced.

Table 2.4 Summary of characteristic structures and molecular weights of two acetylated PF resins based on ^{1}H-NMR spectra in $CDCl_3$.

	Methylol R_{me} (p.p.u)	Methylene Bridge R_{mb} (p.p.u)	Degree of Polymerization (n)	Molecular Weight (M_n)
Core PF	1.18 (0.017)	0.79 (0.014)	4.87 (0.32)	1122 (72)
Face PF	1.37 (0.011)	0.66 (0.00096)	2.90 (0.006)	704 (3)

M_n: number average molecular weight; p.p.u.: per phenolic unit.

Chemical shift assignments of the acetylated PF resins by ^{13}C-NMR

^{13}C-NMR chemical Shifts of the acetylated PF resols in chloroform-d were assigned in Figure 2.3 and summarized in Table 2.5 according to literature (McGraw *et al*. 1989; Yazaki *et al*. 1994). ^{13}C-NMR probed the spectrum of o-o, o-p, and p-p methylene bridges in the region of 20-40 ppm separately for the acetylated resin. The

core PF resin clearly presented the signals of o-o methylene bridges at 30-32 ppm while the signal for the face PF resin was weak at this region.

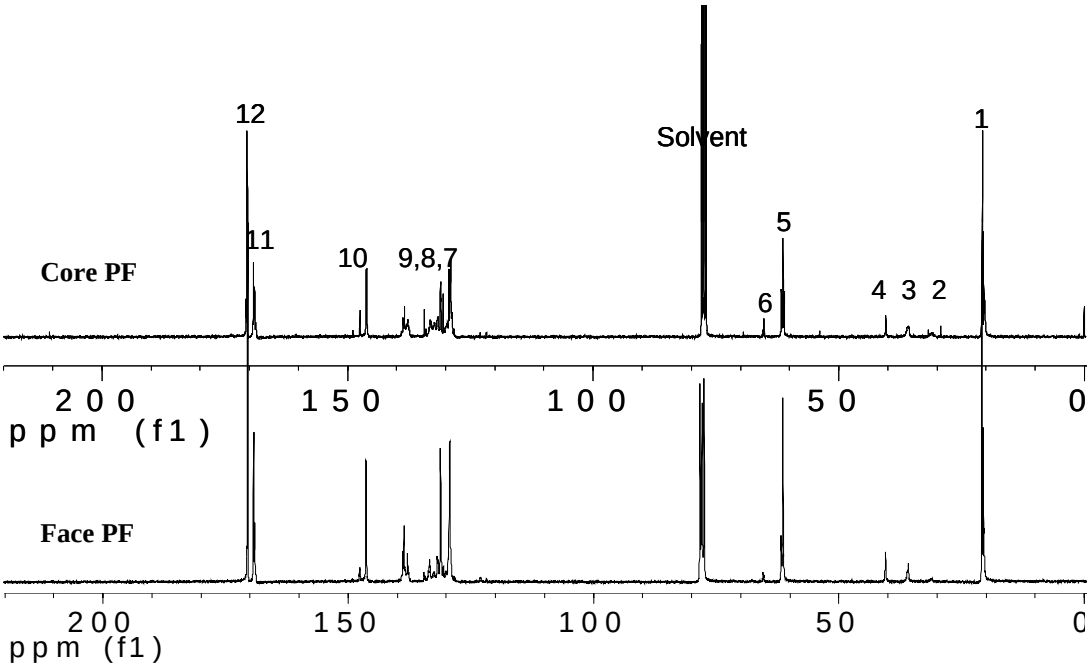

Figure 2.3 ^{13}C-NMR spectra of the core and face PF resins in $CDCl_3$ with carbon assignments shown in scheme 2.

Optimization of ^{13}C-NMR parameters for quantitative analysis

Differential NOE among the ^{13}C nuclei and the long spin-lattice relaxation times (T_1) of PF carbons prevent quantitative analysis of PF structures using ^{13}C-NMR spectra. Inverse gated-decoupling technique was used to eliminate NOE variations. However, due to loss of part of the NOE, the number of scans is too high to obtain a reasonable signal-to-noise ratio. Note that there was a build-up of the

NOE-effect during the acquisition period when decoupling was active. In order to

Table 2.5 ^{13}C-NMR chemical shifts of the acetylated PF resol resin in chloroform-d.

Assignment of the carbons	Chemical shift (ppm)
Acetyl methyls (1)	20-22
Ortho-ortho methylene (2)	30-32
Ortho–para methylene bridges (3)	36-37
Para–para methylene bridges (4)	40-42
Hemiacetal of formalin	54, 89 (trace)
Ortho methylol methylene (5)	61-63
Para methylol methylene (6)	65-66
Phenolic hemiformals	68 (trace)
Chloroform-d (solvent)	77
Free *ortho* carbon	121 (trace)
Free *para* carbon	122 (trace)
Meta, substituted *ortho, para* (7, 8)	128-135
para-benzyl (9)	137-139
Acetylated phenoxy carbon (10)	146-149
Phenolic acetyl carbonyl (11)	169-170
Methylol acetyl carbonyl (12)	170-172

***** Number in parenthesis corresponds to Scheme 2 and Figure 2.3**.**

suppress this NOE-effect, the relaxation delay time must be at least 5 times larger than T_1 for ^{13}C (Luukko *et al*. 1998). For resols, the longest T_1 relaxation times are those of the quaternary aromatic carbons (in the order of 15 s) (Rego *et al*. 2004) and result in preparation delays of at least 75 s, which need a prohibitive 53 h measuring time for

2560 repetitive scans. The use of shiftless paramagnetic relaxation reagents of Chromium (III) acetylacetonate and Gadolinium (III) chloride hexahydrate decreased the longest carbon spin-lattice relaxation T_1 to approximately 0.35-0.40 s, which reduced measuring time to 3.4 h when the number of scans was set at 2560. Furthermore, several preliminary tests were run on the acetylated PF resins to find optimum combinations of delay time, acquisition time and the number of scans. Two different regions were used to determine whether the resin spectrum was quantitative. First, the ratio of the integration value of the phenolic carbon to the integration value of other aromatic carbons should theoretically be 1:5. The other method of determining the quantitative of the NMR analysis was to compare the integration values of the two sharp signals of acetyl methyl, $-CH_3$ at 20 ppm (1 in Figure 2.3) and quaternary carbon of carbonyl C=O at 169~172 ppm (11+12 in Figure 2.3) and the ratio should be 1:1. With the delay time at 8 s, the acquisition time at 0.6 s, and the number of scans at 2560, these ratios were around 1:5 and 1:1 (Table 2.6), indicating reliable quantitative measurement.

Table 2.6 The ratios of phenolic to other aromatic carbons (1:5) and acetyl methyl to acetyl carbonyl carbons (1:1).

	10/(7+8+9)	(12+11)/1
Theoretical	1:5	1:1
Measured Face PF	1:5.01	1:1.04
Measured Core PF	1:4.99	1.02:1

The numbers are corresponding to those in Figure 2.3

Table 2.7 Summary of characteristic structures and molecular weights of two acetylated PF resins based on ^{13}C-NMR spectra in $CDCl_3$.

	Methylol R_{me} (p.p.u)	Methylene Bridge R_{mb} (p.p.u)	Degree of Polymerization (n)	Molecular Weight (M_n)
Core PF	1.23 (0.045)	0.64 (0.005)	2.74 (0.038)	636 (0.025)
Face PF	1.42 (0.045)	0.49 (0.003)	1.97 (0.12)	481 (21)

M_n: number average molecular weight; p.p.u.: per phenolic unit.

Molecular weights of the acetylated PF resins by ^{13}C-NMR

The number average molecular weights for two acetylated resins were calculated using Woodbrey's Eq. (3) (1965) on the basis of ^{1}H-NMR spectra as mentioned above. In this research, this method was also applied to the ^{13}C-NMR spectra to calculate molecular weight using Eq. (3) following same principal. In this case, the R_{mb} and R_{me} were directly obtained from respective integrals of signals by setting the integral value of phenolic carbon region as unity (R_{mb} = 2+3+4, R_{me} = 5+6 in Table 2.5**)**. Characteristic structures and calculated molecular weights were summarized in Table 2.7. All integration values were expressed per phenolic unit (p.p.u). The calculated degree of polymerization and molecular weight for the core PF resin were larger than those of face PF resins, indicating that the core PF resin was more advanced. The core resin has more methylene bridges and less methylol

substitution than the face resin. This is in accordance with the results from ^{1}H-NMR spectra.

Chemical structures and molecular weights of the neat PF resins by ^{13}C- and ^{1}H-NMR

Chemical shift assignment of the neat PF resins by ^{1}H-NMR

^{1}H-NMR spectra of the neat core PF resin is shown in Figure 2.4**.** The spectra of the neat face PF resins are similar. The designations of integrals and their corresponding chemical structures and shifts are presented in Table 2.8 (Woodbrey *et al*. 1965; Yazaki *et al*. 1994). The values of A1 cannot be measured experimentally for resoles and were determined by calculation from other experimental integrals (Woodbrey *et al*. 1965). The number molecular weight was then calculated for two neat resins based on integral values of ^{1}H-NMR spectra.

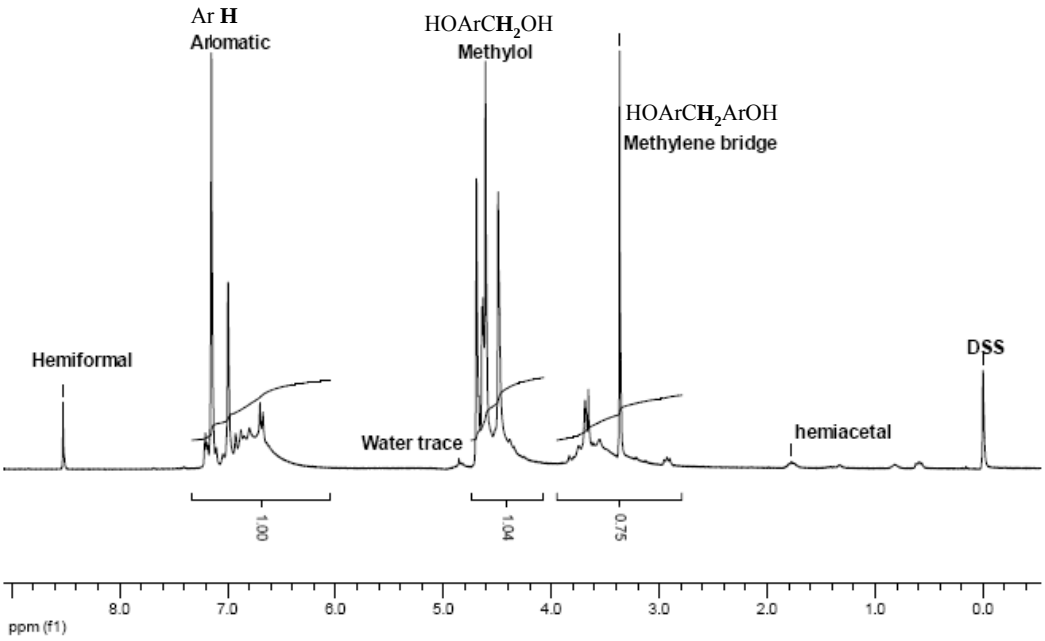

Figure 2.4 ^{1}H-NMR spectrum of the neat core PF resin in D_2O.

Table 2.8 ^{1}H-NMR chemical shift of neat resins in D_2O (Woodbrey *et al*. 1965).

Assignment	Shift (ppm)	Integral
ArO**H**		A1
Ar**H**	7.40–6.30	A2
o-HOArC**H**$_2$OH	4.76–4.54	A4
p-HOArC**H**$_2$OH	4.50–4.20	A5
o,o_, o,p_-HOArC**H**$_2$ArOH	3.90–3.71	A6
p,*p*_-HOArC**H**$_2$ArOH	3.67–3.00	A7

*A*1 = (1/5)[*A*2+(*A*3/4) +(1/2)(*A*4 +*A*5) + *A*6 + *A*7], Ar: aromatic ring.
(*Notes: symbol A used here for convenient of calculation of A1*)

Molecular weights of the neat PF resins by ^{1}H-NMR

For the neat PF resins, the acetoxy groups (Ac in Scheme 3) should be substituted with hydrogen. Then the number average molecular weight of the neat resin, Mn(OH), could be calculated by Eq. (4) and Eq. (5) based on ^{1}H-NMR spectra of the neat resin.

$$Mn(OH) = n * [89 + (5 - R_{me} - R_{mb}) + 31 * R_{me} + 14 * R_{mb}] \quad (4)$$

$$R_{me} = \frac{(A6 + A7)}{2A1}, \quad R_{mb} = \frac{(A4 + A5)}{2A1} \quad (5)$$

where A1, A4, A5, A6, and A7 are integrals of ^{1}H-NMR spectra of the neat resins in Table 2.8. Characteristic structures and molecular weights were summarized in Table 2.9. Consistently, the calculated degree of polymerization and molecular weight for

the core PF resin were larger than those of face PF resins. This indicates that the core PF resin was more advanced.

Table 2.9 Summary of characteristic structures and molecular weights of two neat PF resins based on ^{1}H-NMR spectra in D_2O.

	Methylol R_{me} (p.p.u)	Methylene Bridge R_{mb} (p.p.u)	Degree of Polymerization (n)	Molecular Weight (Mn)
Core PF	1.49 (0.066)	0.72 (0.025)	3.67 (0.31)	541 (41)
Face PF	1.29 (0.034)	0.61 (0.015)	2.55 (0.10)	357 (17)

Chemical shift assignment of the neat PF resins by ^{13}C-NMR

Figure 2.5 displays the typical ^{13}C-NMR spectra of two neat resins in D_2O. Typical chemical shifts were recognized according to the literature and summarized in Table 2.10 (Holopainen *et al*. 1997; Luukko *et al*. 1998, Rego *et al*. 2004). The most diagnostic carbon atoms found in the ^{13}C-NMR spectra of the neat PF resins are the phenolic carbons, which are directly bonded to a hydroxyl group. Due to variations of its environment, the chemical shifts of phenolic carbon were located between 153 and 168 ppm. The wider the distribution of molecular weight, the larger the range of chemical shifts of phenolic carbons were (Holopainen *et al*. 1997). Comparison of the spectra of two resins found that the chemical shifts of phenolic carbons of the core PF resin had shifted to the lower field than those of the face PF. The range of chemical

shifts of phenolic carbon is broader for the core PF resin implying its higher condensation alkalinity and higher molecular weight compared to face PF resin.

Free *ortho* and *para* carbons occur at 119 ppm and 121 ppm, respectively, and can be used to follow the progress of resin cure where more and more ortho and para positions become progressively substituted with formaldehyde residues. For these two resins, the intensity of free ortho and para carbons for the core PF resin is smaller than that for the face PF resin. The o-o' bridge at 30 ppm that was nicely resolved at the ^{13}C-NMR spectra of the acetylated resins (Figure 2.3) was not observed in neat resins here. Mcgraw *et al*. (1989) assumed that the o-p' and o-o methylene bridges appeared together as a cluster of signals due to a strong down field shift of the o-o' methylene. The signals in this region were stronger for the core PF than for the face PF resin.

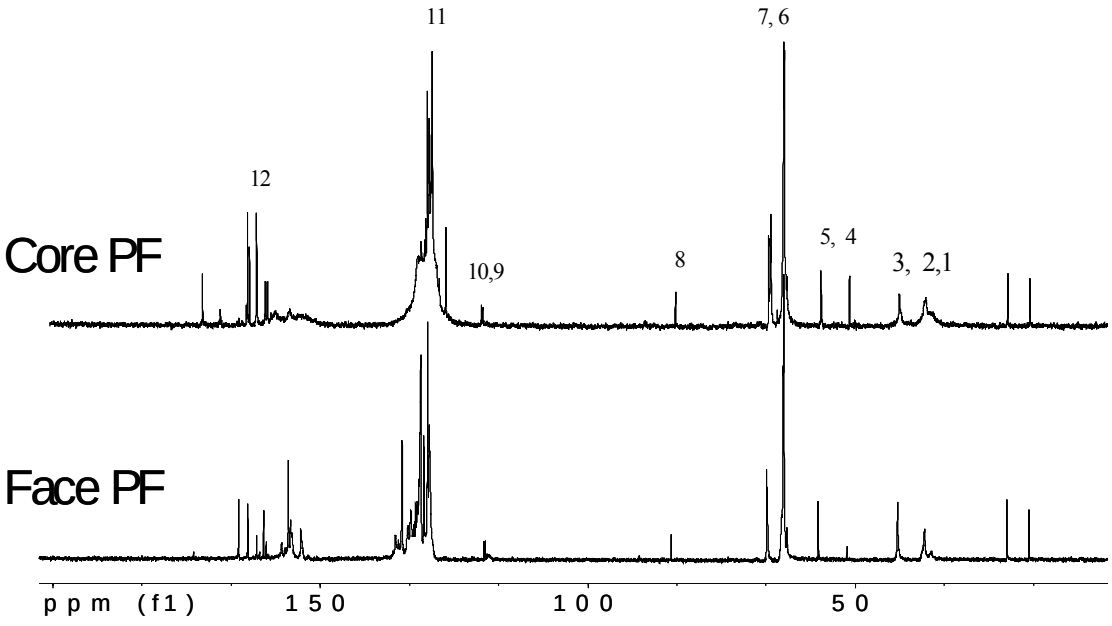

Figure 2.5 ^{13}C NMR spectra of the core and face PF resins in D_2O solvent. GPC has shown that the core PF has a higher molecular weight than that of the face resin.

Table 2.10 ^{13}C-NMR chemical shifts of PF resins in D_2O solvent.

Assignment of the carbons	Chemical shift (ppm)
ortho–para methylene bridges (1*) *ortho–para* methylene bridges (2)	34–36
para–para methylene bridges (3)	40–41
Methanol (4)	51
hemiacetal of formalin (5)	56
ortho methylol (6)	60–63
para methylol (7)	64–66
oxymethylene of formaldehyde oligomers (8)	84
free *ortho* (9)	119
free *para* (10)	121
meta, substituted *ortho*, substituted *para* (11)	124–133
phenoxy region (12)	150-168

*the numbers are corresponding to that in **Figure 2**.

Molecular weights of the neat PF resins by ^{13}C-NMR

The ^{13}C-NMR spectra of the neat resins were recorded under the parameters, which meet the requirement for quantitative analysis as discussed for the acetylated resins. R_{mb} and R_{me} were directly obtained from respective integrals of signals by setting integral value of phenolic carbon region as unity (R_{mb} = 1+2+3, R_{me} = 6+7 in

Table 2.10). Hence, Eq. (4) was used to calculate the molecular weights as presented in Table 2.11.

Table 2.11 Summary of characteristic structures and molecular weights of two neat PF resins based on ^{13}C-NMR spectra in D_2O.

	Methylol R_{me} (p.p.u)	Methylene Bridge R_{mb} (p.p.u)	Degree of Polymerization (n)	Molecular Weight (Mn)
Core PF	1.57 (0.019)	0.75 (0.018)	4.1 (0.28)	615 (45)
Face PF	1.60 (0.015)	0.57 (0.013)	2.31 (0.069)	344 (12)

Mn: number average molecular weight; p.p.u.: per phenolic unit.

Comparison of different methods

Each method of obtaining molecular weights with NMR techniques yielded consistent results: the core PF had a higher content of methylene bridge per phenolic unit, a higher degree of polymerization and molecular weights, but a lower content of methylol per phenolic unit. Table 2.12 summarizes the molecular weights of the neat resins obtained from the ^{1}H- and ^{13}C-NMR spectra, as well as the molecular weights of the neat resins, which were calculated from the spectra of the acetylated resins by removing the acetoxy groups.

For the neat resin, there was no significant difference between the molecular weights obtained from the ^{1}H- and ^{13}C-NMR spectra. However, the molecular weight

of the neat resin derived from ^{1}H-NMR spectra of the acetylated resins was larger than that derived from ^{13}C-NMR spectra of the acetylated resin. There are better agreements of the molecular weights from ^{1}H-NMR spectra than those from ^{13}C-NMR. It seems that the molecular weights derived from ^{13}C-NMR spectra of the acetylated resins were incorrect**,** as shown in Table 2.12. The molecular weights obtained from ^{1}H-NMR spectra of the acetylated resins were larger than those from the neat resins. Acetylation increased the molecular weight slightly (Wellons and Gollob 1980; Yazaki *et al*. 1994). In this sense, ^{1}H-NMR had a better quantitative analysis for the resin structure than ^{13}C-NMR despite every effort to obtain quantitative ^{13}C-NMR spectra.

By comparing the molecular weight from ^{1}H-NMR and ^{13}C-NMR (Table 2.13), it can be seen that for the lower molecular weight resins, the GPC and NMR techniques yield similar results. Larger discrepancies are found for the higher molecular weight resin. There were reports that GPC analysis of the acetylated higher molecular weight resin tended to over-estimate the molecular weight ((Wellons and Gollob 1980; Yazaki *et al*. 1994). However, Steiner (1975) found that ^{1}H- NMR was relatively insensitive when the molecular weight of the resins was large. For example, the assumption of linear structure for Woodbrey's formula may not hold true at high molecular weight. Hence, the molecular weight calculated by NMR technique may also have a loophole. Therefore, for the core PF resin, it is unclear which technique is more credible. Perhaps the real value of molecular weight of the core PF lies between those obtained by GPC and NMR.

Table 2.12 Comparison of number average molecular weight (M_n) and degree of polymerization (n) of the neat resins by ^{1}H- and ^{13}C-NMR.

	Core PF				Face PF			
	Acetylated*		Neat		Acetylated*		Neat	
	^{1}H	^{13}C	^{1}H	^{13}C	^{1}H	^{13}C	^{1}H	^{13}C
M_n	665	386	541	615	422	287	357	344
n	4.87	2.74	3.67	4.1	2.90	1.97	2.55	2.31

*M_n and n of the neat resins were calculated from spectra of the acetylated resins by taking out of acetoxy groups.

Table 2.13 Comparison of number average molecular weight (M_n) and degree of polymerization (n) of the acetylated PF resins by ^{1}H- and ^{13}C-NMR and GPC.

	Acetylated Core PF			Acetylated Face PF		
	^{1}H	^{13}C	GPC	^{1}H	^{13}C	GPC
M_n	1122	636	3893	704	481	439
n	4.87	2.74	16.4	2.90	1.97	1.85

CONCLUSION

Both ^{1}H-NMR and ^{13}C-NMR spectroscopy proved to be valuable techniques in a detailed analysis of acetylated and neat resins. Chemical shifts of PF resins could be assigned according to the literature. With ^{13}C-NMR for the neat resins in D_2O, the

phenolic carbon region from 150-160 ppm was an informative spectrum for analyzing the varieties of its environments. The broader distribution of the core PF resin in this region implied its advanced structures as compared with the face PF resin. ^{13}C-NMR probed the spectrum of o-o, o-p, and p-p methylene bridges in the region of 20-40 ppm separately for the acetylated resin. The core PF resin clearly presented the signals of o-o methylene bridges at 30-32 ppm while the signal for the face PF resin was weak at this region. Inverse-gated decoupling and addition of relaxation reagents of Chromium (III) acetylacetonate and Gadolinium (III) chloride hexahydrate into NMR solvents were effective for use in quantitative analysis with ^{13}C-NMR for the resin chemical structures. The quantitative analyses with ^{1}H- and ^{13}C-NMR have demonstrated that the core PF resin has a higher methylene bridge content per phenolic unit, degree of polymerization, and molecular weights but lower methylol content per phenolic unit than the face PF resins.

Although ^{13}C-NMR had a higher spectrum resolution and gave more detailed information for the PF chemical function groups, quantitative analysis with ^{13}C-NMR was not more effective than that with ^{1}H-NMR. GPC chromatograms clearly showed that both resins have three fractions of molecular weights and the core PF is more advanced than the face PF resin. For the face PF resin with a low molecular weight, GPC and NMR gave values of molecular weight at the same order, while GPC gave a much higher molecular weight for the core PF resin than NMR. This work suggests that both GPC and ^{1}H- and ^{13}C-NMR are useful qualitative tools for differentiating the resins. However, the accuracy of these methods for determining the molecular weight

distribution of PF resins should be investigated further.

Achnowledgement: GPC test was conducted at the Forest Products Department at

University of Idaho under assistance of Dr. J. Andy Soria.

REFERENCES

Bouajila, J., Raffin, G., Waton, H., Sanglar, C., Paisse, J. O., Grenier-Loustalot, M. F. Phenolic resins - characterizations and kinetic studies of different resols prepared with different catalysts and formaldehyde/phenol ratios (I). *Polymers & Polymer Composites,(2002) 10* (5), 341-359.

Dargaville, T. R.; Guerzoni, F. N.; Looney, M. G.; Shipp, D. A.; Solomon, D. H.; Zhang, X. Determination of molecular weight distributions of novolac resins by gel permeation chromatography. *Journal of Polymer Science A: Polymer Chemistry (1997), 35*, 1399–1407.

Holopainen, T.; Alvila, L.; Rainio, J.; Pakkanen, T. T**.;** Tuula, T. Phenol-formaldehyde resol resins studied by 13C-NMR spectroscopy, gel permeation chromatography, and differential scanning calorimetry. *Journal of Applied Polymer Science* (*1997), 66* (6), 1183-1193.

Luukko, P. A.; Holopainen, T.; Rainio, J.; Pakkanen, T.T. Optimizing the conditions of quantitative 13C-NMR spectroscopy analysis for phenol-formaldehyde resol resins. *Journal of Applied Polymer Science (1998), 69* (9), 1805-1812.

McGraw, G. W.; Landucci, L. L.; Ohara, S.; Hemingway, R. W. Proton and carbon-13 NMR studies on phenol-formaldehyde prepolymers for tannin-based adhesives. *Journal of Wood Chemistry and Technology (1989), 9* (2), 201-217.

Nieh, W. L. S.; Sellers, T., Jr.. Performance of flakeboard bonded with three phenol-formaldehyde resins of different mole ratios and molecular weights. *Forest Products Journal (1991), 41*(6), 49-53.

Riedl, B.; Calve, L.; Blanchette, L. Size - exclusion chromatography of spray-dried phenol -formaldehyde resins on different columns and solvent systems. *Holzforschung (1988), 42* (5), 315-318.

Rego, R., Adriaensens, P. J., Carleer, R. A., & Gelan, Jan M. (2004). Fully quantitative carbon-13NMR characterization of resol phenol-formaldehyde pre-polymer resins. *Polymer (2004), 45* (1), 33-38.

Steiner, P. R. Phenol – formaldehyde wood adhesive characterization by proton magnetic resonance spectroscopy. *Journal of Applied Polymer Science (1975)*, *19* (1), 215-225.

Wellons, J. D.; Gollob, L. GPC and light scattering of phenolic resins - problems in determining molecular weights. *Wood Science (1980)*, *13* (2), 68-74.

Wilson, J. B.; Jay, G. L.; Krahmer, R. L. Using resin properties to predict bond strength of oak particleboard. *Adhesives Age (1979)*, *22* (6), 26-30.

Woodbrey, J. C.; Higginbottom, H. P.; Culbertson, H. M. Proton magnetic resonance study on the structure of phenol-formaldehyde resins. *Journal of Polymer Science, Part A: General Papers (1965), 3*(3), 1079-1106.

Yazaki, Y.; Collins, P. J.; Reilly, M. J.; Terrill, S. D.; Nikpour, T. Fast - curing phenol - formaldehyde (PF) resins. Part 1 Molecular weight distribution of PF resins. *Holzforschung (1994), 48* (1), 41-48.

Chapter 3 Comparison of Model-fitting Kinetics for Predicting the Cure Behavior of Commercial Phenol-formaldehyde Resins

ABSTRACT

Phenol-formaldehyde (PF) resins have been the subject of many model-fitting cure kinetic studies, yet the best model for predicting PF dynamic and isothermal cure has not been established. The objective of this research is to compare and contrast several commonly used kinetic models for predicting degree of cure and cure rate of PF resins. Toward this objective, the n^{th}-order Borchardt-Daniels (n^{th}-BD), ASTM E698 (E698), autocatalytic Borchardt-Daniels (Auto-BD), and modified autocatalytic methods (M-Auto) are evaluated on two commercial PF resins containing different molecular weight distributions and thus cure behaviors. The n^{th}-BD, E698 and M-Auto methods all produce comparable values of activation energies while Auto-BD method yields aberrant values. For dynamic cure prediction, all models fail to predict reaction rate, while degree of cure is reasonably well predicted with all three methods. As a whole, the n^{th}-BD method best predicts degree of cure for both resins as assessed by mean squared error of prediction.

Key words: resins, activation energy, modeling, kinetics (polym.), differential scanning calorimetry (DSC)

INTRODUCTION

Several hot-pressing models of engineered wood-based composites have been developed to predict properties such as moisture content and internal pressure during mat-solidification in the past decades ((Bolton and Humphrey 1988; Thoemen and Humphrey 2003; Dai and Yu 2004; Zombori *et al*. 2004). Such models are important to design and optimize hot-pressing parameters during the manufacture of engineered wood-based composites. During panel consolidation, the heat of resin polymerization plays an important role. Yet hot-pressing models have either used an arbitrary kinetic model or have not incorporated the resin cure kinetics (Bolton and Humphrey 1988; Thoemen and Humphrey 2003; Dai and Yu 2004; Zombori *et al*. 2004), hence limiting their application. In order to improve the accuracy of hot-pressing models, cure kinetics needs to be incorporated. During a DSC temperature scan phenol-formaldehyde (PF) resoles typically exhibit two exotherms (Holopainen *et al*. 1997). Although a subject of controversy the first exotherm is often ascribed to hydroxymethylphenols formation and condensation while the second exotherm is attributed to dimethylene ether linkages decomposition into methylene linkages between phenolic moieties (Holopainen *et al*. 1997). To model resin cure kinetics, model-fitting (MF) (Harper *et al.* 2001) and model-free kinetics (Wang *et al*. 2005) can be used in combination with differential scanning calorimetry (DSC) (Prime 1997). For commercial PF resins, model-free kinetics has recently demonstrated excellent modeling and prediction abilities for both degree of cure and reaction rate during dynamic and isothermal cure (Wang *et al*. 2005). However model-free kinetics

involves complex computations that may not be easily implemented in a comprehensive hot-pressing model. Indeed, hot-pressing models require solving simultaneously two governing partial differential equations, one on heat transfer and one on mass transfer (Zomborie *et al*. 2004). As a result, an explicit cure kinetic model can be more easily incorporated into the solving process. In contrast, MF methods assume a definite reaction model facilitating simple computations with kinetic parameters such as activation energy, reaction order and pre-exponential factor. As such, they remain of interest when an approximate prediction of cure development is needed, and will be easily incorporated into a hot-pressing model. In fact, MF kinetics has long been used to characterize and compare the cure kinetics of different PF resins (Kay and Westwood 1975; Rials 1992; Vazquez *et al*. 2002; Park *et al*. 2002). In particular, the n^{th} order model with the Borchardt-Daniels (ASTM E 2041) and the ASTM E 698 methods have been widely utilized. Yet different kinetic methods often generate different kinetic parameters (Alonso *et al*. 2004). For instance, the n^{th} order with the Borchardt-Daniels method was reported to yield activation energy values that are 30% higher than those obtained with the Ozawa or Kissinger equations used in ASTM E698 (Alonso *et al*. 2004). These observations raise a concern about which MF method is best suited to model the cure kinetics of different commercial resins including the PF varieties studied in this research. More importantly, the prediction ability of MF methods for phenolic resin cure has not been established. The choice of an MF method to predict PF cure kinetics for incorporating into hot-pressing models is, therefore, not evident. In this perspective, the objective of

this study is to determine and compare the suitability of four MF kinetic methods to model and predict the cure kinetics of PF resins. The specific models studied include the n^{th} order with Borchardt-Daniels, autocatalytic model with Borchardt-Daniels, ASTM E698 and modified autocatalytic methods (Harper et al. 2001).

EXPERIMENTAL

Materials

Two PF resole resins tailored for use in face and core layers of oriented strand board (OSB) production were obtained from a commercial source (Wang *et al*. 2005). The face resin displayed a weight-average molecular weight (M_w) of 621 g/mol and a polydispersity (M_w/M_n) of 1.4. This resin was subsequently identified as PF-low. The core resin possessed a M_w = 6576 g/mol and M_w/M_n =1.72 and was labeled as PF-high. Resin solids contents for the PF-low and PF-high resins were 54.5% and 45.0%, respectively. In addition, elemental analysis (Nelson and Sommers 1982) showed the presence of 3.7 and 3.9 wt % nitrogen for PF-high and PF-low respectively, suggesting the presence of urea in both resins.

Differential Scanning Calorimetry

A Mettler-Toledo DSC 822e was used to perform dynamic and isothermal cure experiments. Approximately 13.5mg of resin was placed in a 30 µl high pressure gold-plated crucible. Dynamic temperature scans were conducted from 25°C to 250°C

at 4 heating rates: 2, 5, 10 and 20°C/min. In all DSC scans, nitrogen was used as a purge gas at a flow rate of 80 ml/min. Six replicate measurements were performed for each heating rate. Four randomly selected measurements were used to extract kinetic parameters and remaining two measurements were used to compare with predictions. In addition, the first replicate was re-scanned at 10^{o}C/min immediately following the first scan to assure complete cure. Both degree of cure (α) and reaction rate ($d\alpha/dt$) were determined at a specific cure time (t) by normalizing the partial heat of reaction ($\Delta H(t)$), and heat flow (dH/dt) by the total heat of reaction (ΔH), respectively:

$$\alpha = \frac{\Delta H(t)}{\Delta H} \tag{6}$$

$$\frac{d\alpha}{dt} = \frac{dH/dt}{\Delta H} \tag{7}$$

The cure kinetic parameters for the n^{th} order with Borchardt-Daniels, autocatalytic model with Borchardt-Daniels, ASTM E698 and modified autocatalytic methods were extracted form the cure and cure rate data using linear least-squares fitting routines programmed in MATLAB. The resulting kinetic parameters were then used to predict and compare dynamic cure with experimental data at 4 different heating rates. To further validate the methods for isothermal cure, isothermal DSC runs were conducted at 120°C for different times. A cure temperature of 120°C was representative of PF cure under typical hot-pressing conditions for the panel core (Zombori *et al*. 2004) and it also allowed easy observation of cure development with DSC. The DSC cell was preheated to 120°C and approximately 13.5 mg of PF resin

was inserted and cured for different times. The sample was then quickly removed from the DSC and quenched in liquid nitrogen. The residual heat of reaction of the partially cured samples (ΔH_R) was obtained from a subsequent ramp scan at 10°C/min from 25 to 250°C. The time dependence of the degree of cure at 120 °C was obtained by normalizing the difference of total and residual heat of reaction with total heat of reaction ($\alpha=(\Delta H-\Delta H_R)/\Delta H$) as a function of cure time. The total heat of reaction was taken as the average reaction heat previously measured in dynamic tests of fresh resins. The time dependence of the degree of cure at 120°C was compared with predictions from the MF methods.

Model-Fitting algorithms

During a reaction process, the overall reaction rate can be modeled as:

$$\frac{d\alpha}{dt} = A\exp(-E/RT)\,f(\alpha) \tag{8}$$

where t (s) is the time, A (s^{-1}) the pre-exponential factor**,** E (J/mol) the activation energy , R (8.314 J/mol·K) the universal gas constant, T(K) the absolute temperature and f(α) the reaction model. Two reaction models are commonly used for simple reactions; these are the n^{th} order $f(\alpha) = (1-\alpha)^n$ and the autocatalytic model $f(\alpha) = \alpha^m(1-\alpha)^n$ in which m+ n is called the order of reaction. Under isothermal conditions, in n^{th} order kinetics, the rate of conversion is proportional to the concentration of unreacted material. Reaction rate therefore reaches its maximum at

the onset of reaction and then decreases until the reaction is complete (ASTM E2041). In autocatalyzed kinetics on the other hand, both the reactant and product are catalysts so that a maximum reaction rate is obtained during the course of the reaction (Prime 1997). Both models can be applied to dynamic experiments (Martin and salla 1992).

Using the n^{th} order and autocatalytic models Eq. (8) can be rearranged into Eq. (4) and (5) respectively:

$$\ln\left(\frac{d\alpha}{dt}\right) = \ln(A) + n\ln(1-\alpha) - \frac{E}{RT} \tag{9}$$

$$\ln\left(\frac{d\alpha}{dt}\right) = \ln(A) + m\ln(\alpha) + n\ln(1-\alpha) - \frac{E}{RT} \tag{10}$$

From one DSC dynamic scan, the values of α and $d\alpha/dt$ and corresponding temperature are used to solve Eqs. (9) and (10) by multiple linear regression. Kinetic parameters, A, E and n for the n^{th} order model (n^{th}-BD) and A, m, n, and E for the autocatalytic model (Auto-BD) are thus determined (ASTM E2041; Borchardt and Daniels 1957). This DSC analysis is usually designated as the Borchardt-Daniels method or the single heating rate method; it is attractive because all the kinetic parameters are derived from one single dynamic DSC scan. With this method however, kinetics parameters are heating rate dependent and they are subject to signal noise, solvent effect and unresolved baselines (Dunne *et al*. 2000).

The kinetic parameters can also be determined from multiple heating rate scans. Specifically, in the case of a constant heating rate, $\beta=dT/dt$, Eq. (8) can be

rearranged into the integral form $g(\alpha)$:

$$g(\alpha) = \int_0^{\alpha} \frac{d\alpha}{f(\alpha)} = \frac{A}{\beta} \int_{T_0}^{T} \exp(-E/RT)dT \tag{11}$$

Because Eq. (11) has no exact analytical solution, Doyle (Doyle 1961; 1962) proposed two approximations for g(α), which can be rearranged into (Ozawa 1965; Flynn and Wall 1966):

$$\ln\left(\frac{\beta}{T^2}\right) = \ln\left(\frac{RA}{Eg(\alpha)}\right) - \frac{E}{RT} \tag{12}$$

$$\log(\beta) = \log\left(\frac{AE}{R}\right) - \log g(\alpha) - 2.315 - \frac{0.4567E}{RT} \tag{13}$$

The peak temperature (T_{ipeak}) dependency on heating rate (β_i) can thus be used to calculate the activation energy (Kissinger 1956; Shulman and Lochte 1968; Wang *et al*. 1995). Assuming an iso-fractional peak temperature (Horowitz and Metzger 1963), a linear regression of ln (β_i/T^2_{ipeak}) or log (β_i) against $1/T_{ipeak}$ across several heating rates yields the activation energy with Kissinger Eq. (14) (Kissinger 1957) or Ozawa Eq. (15) (Ozawa 1965; Shulman and Lochte 1968) respectively.

$$E = \frac{Rd[-\ln(\beta/T^2_{peak})]}{d(1/T_{peak})} \tag{14}$$

$$E = -2.19R\frac{d(\log\beta)}{d\left(1/T_{peak}\right)} \tag{15}$$

Ozawa equation yields slightly higher E values than those obtained by Kissinger equation (ASTM E 698; Alonso *et al*. 2004). The calculated activation energy by Ozawa equation can be refined as suggested by ASTM E698 to be comparable with that by Kissinger equation. This modified version of Ozawa equation is designated as E698 method. For PF resins, Alonso *et al* (2004) found less than 4% variation in the estimates of E between the two equations. In addition, the estimates of E by E698 method are lower than those from the Borchardt-Daniels method (Alonso *et al*. 2004; Park *et al*. 1999). To calculate the pre-exponential factor A, a definite reaction model must be assumed. For n^{th} order reactions, Kissinger (1957) proposed:

$$A = \frac{\beta E \exp(E/RT_{peak})}{RT_{peak}^2 n(1-\alpha_{peak})^{n-1}} \tag{16}$$

Assuming a first order reaction, A is easily obtained from Eq. (16) by substituting the intermediate heating rate and its corresponding peak temperature. Hence, with the E698 method, E can be determined regardless of the reaction model while A can only be measured for n^{th} order reactions.

Another method has been developed to calculate autocatalytic kinetic parameters from multiple heating rate DSC scans (Harper *et al*. 2001; Lam 1987; Chung 1984). This method assumes that the degree of cure at the exothermic peak

(α_{peak}) is heating rate-dependent and relates to the reaction orders m and n. The relationship between degree of cure at peaks and reaction orders is given by setting the optimum criteria in Eq.(10):

$$m = \frac{\alpha_{peak}}{1-\alpha_{peak}} n \,. \tag{17}$$

For any specific kinetic process, α_{peak} is obtained experimentally, thus constraining the values of m and n by Eq. (17). Another constraint arises from the integral function for the autocatalytic model in Eq. (18):

$$g(\alpha) = \int_0^{\alpha} \frac{d\alpha}{\alpha^m (1-\alpha)^n} \tag{18}$$

In this case, the zero value of lower limit of integral imposes a constraint: m must be less than unity for g(α) to be finite (Martin and Salla 1992). It is possible to obtain a unique analytical solution for g(α) when (n + m) sums to an integer higher than 1 and when m < 1 (Martin and Salla 1992). However, for n + m = 1, the kinetic integral g(α) has different solutions for each value of n with m < 1 (Martin and Salla 1992). In this paper, g(α_{peak}) is not solved analytically but rather numerically by assuming a value for the reaction order m + n of 1, 2 and 3 respectively within the constraints of Eq. (17) and that of m<1. Activation energy and pre-exponential factor are then determined simultaneously from the slope and intercept of the log (β_i)+log [g(α_{ipeak})] versus

$1/T_{ipeak}$ plot across several heating rates β_i according to Eq. (13). This method designated as the modified autocatalytic model (M-Auto) is advantageous in that the peak temperature is not assumed iso-fractional (Harper *et al*. 2001). Table 3.1 summarizes the mathematical expressions, parameters and algorithms associated with each of the models used in this paper.

Table 3.1 Summary of kinetic models, parameters and methods used.

Method name	Model f(α)	Kinetic parameters	Method used to extract kinetic parameters
E 698	First order (1-α)	A, E	ASTM E 698, multiple heating rates
n^{th}-BD	n^{th} order $(1-\alpha)^n$	A, E, n	ASTM E 2041, single heating rate with Borchardt-Daniels method
Auto-BD	Autocatalytic model $\alpha^m(1-\alpha)^n$	A, E, m, n	Single heating rate with Borchardt-Daniels method
M-Auto			Multiple heating rates

RESULTS AND DISCUSSION

PF Cure analysis

The commercial PF resins exhibit two distinct exotherms that shift to higher temperatures with increasing heating rate (Figure 3.1). PF-high displays an additional exothermic shoulder between the two major exotherms (Figure 3.1). In PF-high, the

highest molecular weight fractions react rapidly so that the maximum exotherm appears early for PF-high (Detlefsen 2002). The PF-high resin reaches similar degree of cure ca. 10°C earlier than that required for the PF-low resin (Figure 3.1). As expected, DSC appears sensitive to differences in reaction exotherms and cure development of different resins.

Table 3.2 Summary of PF cure peak temperature, degree of cure at peaks in parenthesis and heat of reaction across 4 heating rates*.

	β (°C/min)	2	5	10	20
PF-low	T_1 (°C) (α_1)	119 (0.31)	130(0.30)	137 (0.29)	153 (0.26)
	T_2 (°C) (α_2)	131(0.59)	142(0.57)	151 (0.54)	163 (0.46)
	ΔH (kJ/kg)	406	427	425	424
PF-high	T_1 (°C) (α_1)	108 (0.23)	118 (0.23)	128 (0.24)	135 (0.19)
	T_2 (°C) (α_2)	137 (0.82)	149 (0.83)	159 (0.81)	169 (0.78)
	ΔH (kJ/kg)	365	363	373	361

*6 replicates, the standard error ≤ 2.65 for all variables.

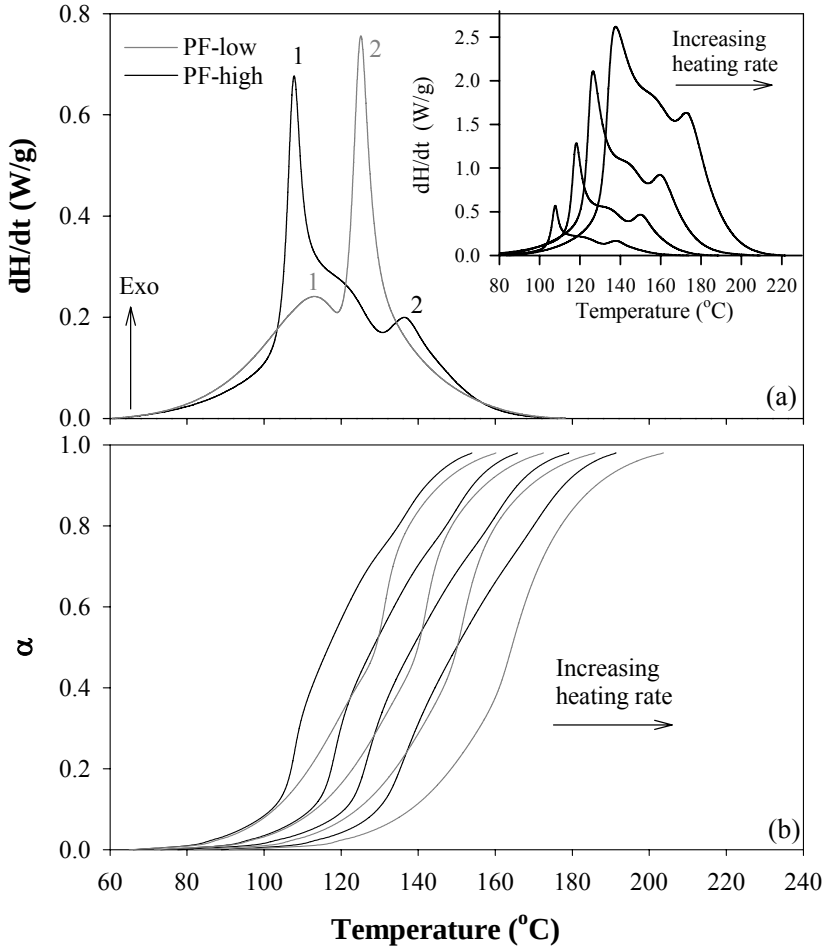

Figure 3.1 (a) DSC heat flow (dH/dt) at 2 °C/min and (b) degree of cure (α) for PF-low and PF-high. The number 1 and 2 designate exotherm peak 1 and peak 2. Insert in (a) highlights the influence of heating rate (2, 5, 10, and 20 °C/min) on the cure of PF-high.

Similar values for the total heat of reaction (ΔH) are measured at all heating rates for each resin. As expected the more advanced PF-high resin releases less heat corresponding to the cure reaction (365 ±5 kJ/kg) than does the PF-low resin (420 ± 9 kJ/kg) (Table 3.1). In addition, the peak temperatures were found to be approximately

iso-fractional regardless of heating rate (Table 3.2).

Table 3.3 Kinetic parameters for the PF-low and PF-high Resins obtained from the model-fitting kinetic methods.

Method			PF-low			PF-high			
			E (kJ/mol)	ln A (1/s)	n	E (kJ/mol)	ln A (1/s)	n	$R^2 \geq$
n^{th}-BD[a]		2°C/min	94	22	1.15	99	24	1.14	0.93
		5°C/min	96	23	1.15	99	24	1.13	
		10°C/min	99	23	1.11	99	24	1.13	
		20°C/min	104	25	1.18	105	25	1.23	
E 698		Peak 1	87	21	1.00	99	26	1.00	0.99
		Peak 2	97	23	1.00	98	23	1.00	
M-Auto	Peak1	m+n=1	83	19	0.71	94	23	0.78	0.99
	Peak1	m+n=2	84	20	1.42	96	24	1.55	
Auto-BD[a]		5°C/min	15	-1	0.82	-1	-6	0.66	0.93

a: average of 4 replicates at each heating rate, standard deviation ≤ 2.90

Kinetic parameters from model-fitting kinetics

Table 3.3 summarizes the kinetic parameters obtained by the MF kinetics from dynamic test data for the two PF resins. The Auto-BD leads abnormal kinetic parameters and is therefore not applicable for PF resins. The Auto-BD method is unable to account for all intrinsic properties of the autocatalytic model, i.e. the

constraints of m and n (Eqs. (17) and (18)) are not met with this method.

The n^{th}-BD, E698 and M-Auto methods generate consistent activation energies and pre-exponential factors for both resins (Table 3.3). These parameters are in the 83-105 kJ/mol and 19-26 s^{-1} ranges respectively and are in agreement with the literature (Kay and Westwood 1975) and with model-free kinetics methods (Wang *et al*. 2005). With all three methods, slightly higher activation energy is found for PF-high than that for PF-low, consistent with the higher advancement of PF-high (Vazquez *et al*. 2002).

The advantage of the E698 and M-Auto methods over the n^{th}-BD method is that kinetic parameters can be determined for individual exotherm. The M-Auto method is only applicable when a reaction order (m) is small. When the M-Auto method can be applied, it generates activation energies slightly lower than those measured with the E698 method (Table 3.3). Recall that the E698 method neglects the dependence of α_{peak} on heating rates whereas this dependence is included in the M-Auto method (Harper *et al*. 2001). For the two PF resins used in this study, there are only small variations for degree of cure at peaks across heating rates. As a result, both methods lead small differences in activation energies for the two resins. The n^{th}-BD method gives cure kinetic parameters for the overall cure process at each heating rate, which are very similar to those obtained from maximum peaks with E698. A trend towards higher activation energies with increasing heating rates for the PF-low resins is observed (Table 3.3). The higher activation energies measured at 20 ^{o}C/min suggests that this heating rate is less appropriate to characterize PF cure. This discrepancy is

likely due to the higher thermal lag manifested at the higher heating rate. The n^{th}-BD method is generally observed to overestimate the kinetic parameters when compared with the E 698 method (Alonso *et al*. 2004; Park *et al*. 1999). However, with the exception of the 20 ^{o}C/min, this overestimate is not apparent in this study. It is clear that the n^{th}-BD and E698 methods can provide consistent kinetic parameters, and the M-Auto method is limited to small reaction orders while the Auto-BD method is inapplicable.

Predicting cure for dynamic conditions

Dynamic cure development was predicted by substituting values of activation energy, pre-exponential factor, reaction orders, and arbitrary heating rates for the corresponding n^{th} order model or autacatalytic model into Eq. (8). The equations were then solved using the Runge-Kutta method (Dormand and Prince 1980) implemented in a MATLAB program. All kinetic parameters from Table 3.3 can be used to predict cure behavior. Further, with the E698 method two reactions can be modeled as independent and/ or consecutive reactions (Eq. 19) (Flynn and Wall 1966). Two reactions can also be modeled as parallel and competing (Eq. 20) (Vyazovkin 2001). In both cases, the overall reaction rate is obtained by substituting the kinetic

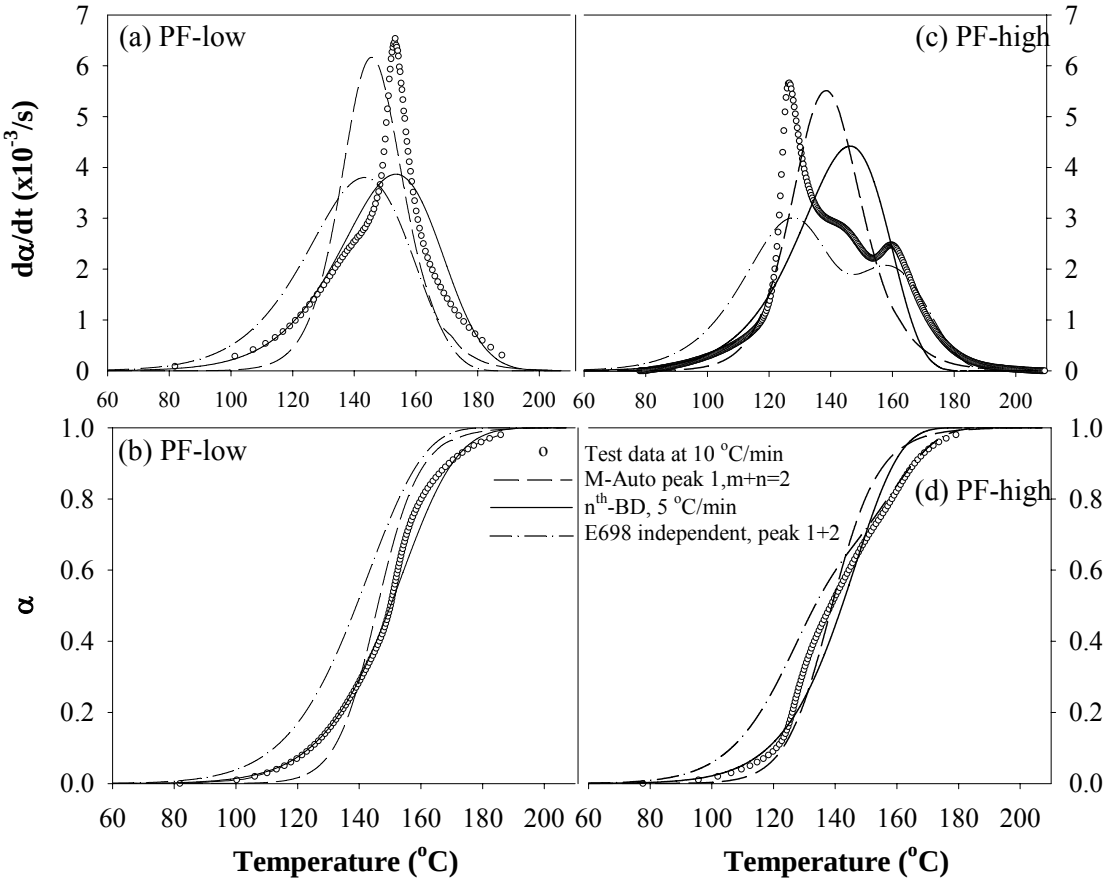

Figure 3.2 Comparison of the test data at 10 °C/min and MF predictions of PF-low and PF-high for reaction rate (dα/dt) and degree of cure (α).

parameters obtained from individual peak 1 and 2 as indicated by the subscripts in Eqs. (19) and (20).

$$\frac{d\alpha}{dt} = w_1 \frac{d\alpha_1}{dt} + w_2 \frac{d\alpha_2}{dt} = w_1 A_1 \exp\left(\frac{-E_1}{RT}\right)(1-\alpha_1) + w_2 A_2 \left(\frac{-E_2}{RT}\right)(1-\alpha_2) \tag{19}$$

$$\frac{d\alpha}{dt} = A_1 \exp\left(\frac{-E_1}{RT}\right)(1-\alpha) + A_2 \exp\left(\frac{-E_2}{RT}\right)(1-\alpha) \tag{20}$$

where w_i is the fraction of each reaction. In this study peak deconvolution allowed an estimate of relative heat of reaction for the two main exotherms at around $w_i = 0.5$. Within E 698 method, predictions are compared with parameters (A, E) obtained for peak 1 and peak 2 respectively, and also compared with combinations of two distinct exotherms as described in Eqs (19) and (20). The predictions are best when two independent or consecutive reactions (Eq. (19)) are assumed as indicated by the lowest mean squared error of prediction (MSEP) (Rawlings *et al*. 1998).

Figure 3.2 shows the test data and predictions of reaction rate and degree of cure for both resins by parameters from each one of the E698, n^{th}- BD and M-auto, which are best among each method as evidenced by the lowest MSEP in Table 3.4. Clearly, the MF kinetic models studied predict the degree of cure for PF resins better than the reaction rate. The failure to accurately model reaction rate of PF cure likely stems from the limitation of most MF kinetics to one reaction and the fact that PF cure involves multiple reactions as evidenced by the multiple exotherms in the PF-low and PF-high thermograms. When two independent or consecutive reactions (Eq.(19)) are assumed with E 698 method, two peaks are captured for the reaction rate of PF-high (Figure 3.2c). This method also predicts PF-high degree of cure very accurately after 70% conversion (Figure 3.2d). Over the entire cure process however, the n^{th}-BD method produces the best predictions of degree of cure as evidenced by the lowest MSEP (Table 3.4). This is true for both resins. As a conclusion, none of the models evaluated accurately predict the reaction rate of the PF cure studied. However, the degree of cure is accurately predicted with the n^{th}-BD method. But the MSEP values

for this method are higher than those obtained with the model-free kinetics Kissinger-Akahira-Sunose (KAS) method in a parallel study (Wang *et al*. 2005). This indicates that overall, model-free kinetics methods are better than MF method for dynamic predictions.

Table 3.4 Mean squared errors of prediction (MSEP) for both dynamic and isothermal conditions at specific degree of cure and data points (in parentheses).

Predicted variable	Model	PF-low	PF-high
Dynamic (10^{o}C/min) temperature at α $(^{o}C)^2$	M-Auto peak 1,m+n=2	51.2 (99)	40.1 (99)
	n^{th}-BD, 5 ^{o}C/min	4.6 (99)	14.9 (99)
	E 698 independent, peak 1+2	128.7 (99)	63.9 (99)
	KAS	3.0 (99)	0.30 (99)
Dynamic (10 ^{o}C/min) reaction rate at α 10^{-6} $(1/s)^2$	M-Auto peak 1,m+n=2	1.8 (99)	2.0 (99)
	n^{th}-BD, 5 ^{o}C/min	2.1 (99)	1.9 (99)
	E 698 independent, peak 1+2	2.6 (99)	0.6 (99)
	KAS	0.1 (99)	0.06 (99)
Isothermal (120^{o}C) cure time at α $(min)^2$	M-Auto peak 1,m+n=2	67.9 (11)	55.1 (13)
	n^{th}-BD, 5 ^{o}C/min	32.4 (11)	11.5 (13)
	E 698 independent, peak 1+2	68.6 (11)	24.0 (13)
	KAS	12.0 (11)	19.4 (13)

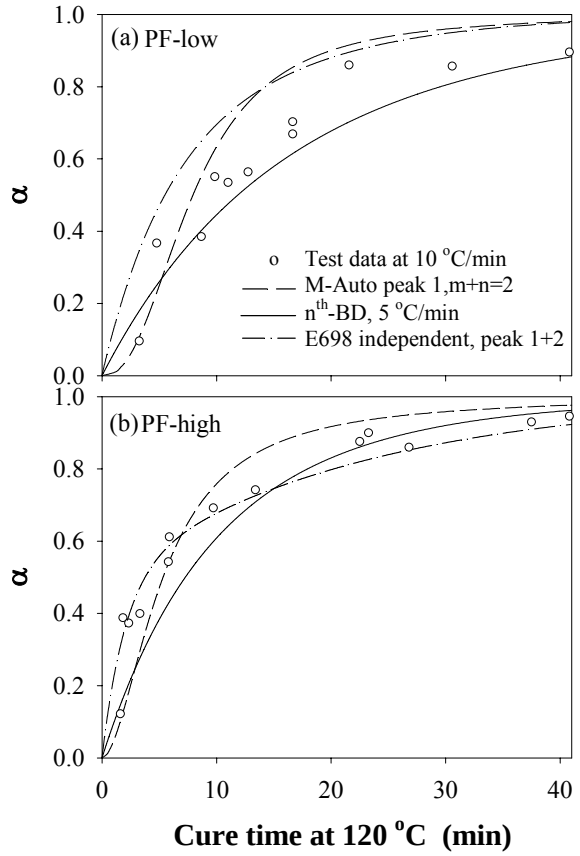

Figure 3.3 Experimental degree of cure (α) at 120°C and MF predictions for (a) PF-low and (b) PF-high.

Predicting cure for isothermal conditions

The ability to predict isothermal cure from dynamic scan data is significant because dynamic tests are more repeatable and easily conducted compared to isothermal tests. In addition, such predictions provide further validation of the models. The predictions of isothermal cure development from all three models are compared to experimental data in Figure 3.3. For PF-low, n^{th}-BD is more accurate than others (Figure 3.3a). However, for PF-high, the E698 with an assumption of two independent

reactions (Eq. (19)) is more accurate during the early curing period while n^{th}-BD predicts a little better towards the end of cure. Across the cure regime studied, the n^{th}-BD model performs better as evidenced by MSEP (Table 3.4). Generally, n^{th}-BD method is the best prediction model of isothermal cure. Comparing with model-free kinetics KAS method in a parallel study (Wang *et al*. 2005), the MSEP with n^{th}-BD is the same order with that by KAS for PF-high, and higher for PF-low (Table 3.4); supporting the notion that the model-free kinetics KAS model is more accurate for isothermal prediction than n^{th}-BD method.

CONCLUSION

The applicability of model-fitting kinetics for predicting cure development of PF resins is compared. The Auto-BD is inappropriate for kinetic modeling of commercial PF resins. The activation energy obtained by n^{th}-BD, E698 and M-Auto methods are comparable. All methods give inaccurate predictions of reaction rate while providing reasonable predictions for degree of cure in both dynamic and isothermal conditions. For a high molecular weight PF resin the E698 independent method provides an excellent local prediction of degree of cure above 70% under dynamic conditions, and works better at the early curing period under isothermal conditions. Altogether, the n^{th}-BD method performs better than the other methods. Yet, the n^{th}-BD predictions are not as good as those by model-free kinetics. On the other hand, they can be easily incorporated in a complex hot-pressing model. Considering that n^{th}-BD method requires only one single heating rate, this method is recommended

for simple kinetic modeling of PF resins.

REFERENCES

Alonso, M. V.; Oliet, M.; Peres, J. M.; Rodriguez, F.; Echeverria, J. Determination of curing kinetic parameters of lignin-phenol-formaldehyde resol resins by several dynamic differential scanning calorimetry methods. *Thermochimica Acta (2004), 419*, 161-167.

ASTM E 698-01 Standard test method for Arrhenius kinetic constants for thermally unstable materials. ASTM International: West Conshohocken, USA.

ASTM E2041-03 Standard method for estimating kinetic parameters by differential scanning calorimeter using the Borchardt and Daniels method. ASTM International: West Conshohocken, USA.

Bolton, A. J.; Humphrey, P. E. The hot pressing of dry-formed wood-based composites. Part I. A review of the literature, identifying the primary physical processes and the nature of their interaction. *Holzforschung (1988), 42*(6), 403-6.

Borchardt, H. J.; Daniels, F. Application of differential thermal analysis to the study of reaction kinetics. *Journal of the American Chemical Society (1957), 79*, 41-46.

Dai, Chunping; Yu, Changming. Heat and mass transfer in wood composite panels during hot-pressing: Part I. A physical-mathematical model. *Wood and Fiber Science (2004), 36*(4), 585-597.

Detlefsen, W.D. Phenolic resins: Some chemistry, technology, and history. In: M. Chaudhury, A.V. Pocius (Eds.), Surfaces, Chemistry and Applications. (2002), 869-945. Elsevier: Amsterdam.

Dormand, J. R.; Prince, P. J. A family of embedded Runge-Kutta formulae. *Journal of Computational and Applied Mathematics (1980), 6*, 19-26.

Chung, T. S. Cure mechanism of a modified nitrile epoxy adhesive. *Journal of Applied Polymer Science (1984), 29*(12 Pt. 2), 4403-6

Doyle, C. D. Kinetic analysis of thermogravimetric data. *Journal of Applied Polymer Science (1961), 5*, 285-92.

Doyle, C. D. Estimating isothermal life from thermogravimetric data. *Journal of Applied Polymer Science (1962), 6*(24), 639-42.

Dunne, R. C.; Sitaraman, S. K.; Luo, S.; Rao, Y.; Wong, C. P.; Estes, W. E.; Gonzalez, C. G.; Coburn, J. C.; Periyasamy, M. Investigation of the curing behavior of a novel epoxy photo-dielectric dry film (ViaLux 81) for high density interconnect applications. *Journal of Applied Polymer Science (2000), 78*, 430-437

Flynn, J. H.; Wall, L. A. General treatment of the thermogravimetry of polymers. *Journal of Research of the National Bureau of Standards, Section A: Physics and Chemistry (1966), 70*(6), 487-523. .

Harper, D. P.; Wolcott, M. P.; Rials, T. G. Evaluation of the cure kinetics of the wood/pMDI bondline. *International Journal of Adhesion & Adhesives (2001)*, *21*, 137-144.

Holopainen, T.; Alvila, L.; Rainio, J.; Pakkanen, T. T. Phenol formaldehyde resol resins studied by ^{13}C NMR spectroscopy, gel permeation chromatography, and differential scanniong calorimetry. *Journal of Applied Polymer Science (1997), 66*, 1183-1193.

Horowitz, N. H.; Metzger, G. A New Analysis of Thermogravimetric Traces. *Analytical Chemistry (1963), 35*, 1464-1468.

Kay R.; Westwood A.R. Differential scanning calorimetry (DSC) investigations on condensation polymers. I. Curing. *European Polymer Journal (1975), 11*(1), 25-30

Kissinger, H. E. Variation of peak temperature with heating rate in differential thermal analysis. *Journal of Research of the National Bureau of Standards (1956), 57,* 217-221.

Kissinger, H. E. Reaction kinetics in differential thermal analysis. *Analytical Chemistry (1957), 29*, 1702-1706.

Lam, P. W. K. The characterization of thermoset cure behavior by differential canning calorimetry. Part I: Isothermal and dynamic study. *Polymer Composites (1987), 8*, 427-436

Luukko, P.; Alvila, L.; Holopainen, T.; Rainio, J.; Pakkanen, T. T. Effect of alkalinity on the structure of phenol-formaldehyde resol resins. *Journal of Applied Polymer Science (2001), 82*(1), 258-262.

Martin, J. L.; Salla, J. M. Models of reaction commonly employed in the curing of thermosetting resins. *Thermochimica Acta (1992), 207*, 279-304.

Nelson, D. W.; Sommers, L. E. In Methods of soil analysis, Part 2. Chemical and microbiological properties, second ed., Page, A.L., Ed.; American Society of

Agronomy, Madison, WI, 1982, Chap. 29.

Ozawa, T. A new method of analyzing thermogravimetric data. *Bulletin of Chemistry Society, Japen (1965)*, 38, 1881-1887.

Park, B.-D.; Riedl, B.; Bae, H.-J.; Kim, Y. S. Differential scanning calorimetry of phenol - formaldehyde (PF) adhesives. *Journal of Wood Chemistry and Technology (1999), 19*(3), 265-286.

Park, B.-D.; Riedl, B.; Kim, Y. S.; So, W. T. Effect of synthesis parameters on thermal behavior of phenol-formaldehyde resol resin. *Journal of Applied Polymer Science (2002), 83*(7), 1415-1424.

Prime RB. Thermosets. In: Turi EA, editor. Thermal characterization of polymeric materials. New York: Academic Press, 1997:435–569.

Rawlings, J. O.; Pantula, S. G.; Dickey, D. A. Applied Regression Analysis, second ed.; Springer: New York, 1998.

Rials, T. G. Cure analysis of phenol - formaldehyde resins by microdielectric spectroscopy. *ACS Symposium Series (1992), 489*(Viscoelasticity Biomater.), 282-294.

Shulman, G. P.; Lochte, H. W. Thermal degradation of polymers. V. Derivation of thermogravimetric and kinetic data from mass spectrometric thermal analysis. *Journal of Macromolecular Science, Part A (1968), 2*, 411-420.

Thoemen, H.; Humphrey, P. E. Modeling the continuous pressing process for wood-based composites. Wood and Fiber Science (2003), 35(3), 456-468.

Vazquez, G.; Gonzalez-Alvarez, J.; Lopez-Suevos, F.; Freire, S.; Antorrena, G. Curing kinetics of tannin-phenol-formaldehyde adhesives as determined by DSC. *Journal of Thermal Analysis and Calorimetry (2002), 70(1)*, 19-28.

Vyazovkin, S. Modification of the integral isoconversional method to account for variation in the activation energy. *Journal of Computational Chemistry (2001), 22*(2), 178-183.

Wang, Y.-H.; Hong, Y.-L.; Hong, J.-L. Cure kinetics of a flexible aromatic dicyanate with Schiff base structure. *Journal of Applied Polymer Science (1995), 58*(9), 1585-92.

Wang, Jinwu; Laborie, Marie-Pierre G.; Wolcott, Michael P. Comparison of model-free kinetic methods for modeling the cure kinetics of commercial phenol-formaldehyde resins. *Thermochimica Acta (2005), 439*(1-2), 68-73.

Zombori, B. G.; Kamke, F. A. Watson, L. T. Simulation of the internal conditions during the hot-pressing process. *Wood and Fiber Science (2003), 35*(1), 2-23.

Chapter 4 Comparison of Model-free Kinetic Methods for Modeling the Cure Kinetics of Commercial Phenol-formaldehyde Resins

ABSTRACT

For many industrial processes it is important to model the cure kinetics of phenol-formaldehyde resoles. Yet the applicability of common model-free kinetic algorithms for the cure of phenolic resins is not known. In this study the ability of the Friedman, Vyazovkin and Kissinger-Akahira-Sunose (KAS) model-free-kinetics algorithms to model and predict the cure kinetics of commercial resoles is compared. The Friedman and Vyazovkin methods generate consistent activation energy dependences on conversion compared to the KAS method. In addition, the activation energy dependency on conversion is of higher amplitude with these two methods than with the KAS method. Hence, the Friedman and Vyazovkin methods are more adequate for revealing the cure steps of commercial PF resoles. Conversely, the KAS algorithm is easily amenable to dynamic cure predictions compared to the Friedman and Vyazovkin methods. Isothermal cure is equally well predicted with the three. As a result, the KAS algorithm is the method of choice for modeling and predicting the cure kinetics of commercial phenolic resoles under various temperature programs.

Key words: phenol-formaldehyde, model-free algorithms, differential scanning calorimetry (DSC), cure prediction.

INTRODUCTION

Phenolic resins are widely used as binders in the composites industry, for thermal insulation and molding compounds (Knop and Pilato 1985). As for any thermosets controlling the degree of cure and cure kinetics is critical to designing the manufacturing process and the performance of the end-product. For characterizing cure kinetics differential scanning calorimetry (DSC) is the technique of choice (Prime 1997). During a DSC temperature scan phenol-formaldehyde (PF) resoles typically exhibit two exotherms (Luukko *et al*. 2001; Holopainen *et al*. 1997). Although a subject of controversy the first exotherm is often ascribed to hydroxymethylphenols (HMPs) formation and condensation while the second exotherm is attributed to dimethylene ether linkages decomposition into methylene linkages between phenolic moieties (Luukko *et al*. 2001; Holopainen *et al*. 1997). In addition, commercial PF resoles for wood-based composites are often modified with up to 20 % wt urea (Kim *et al*. 1996) such that their cure may not be adequately modeled with traditional model-fitting kinetic methods (Vyazovkin and Wight 1997). On the other hand, model-free kinetics (MFK) is well suited to portray the kinetics of complex reactions such as the cure of PF resins (Vyazovkin and Wight 1997; Sbirrazzuoli *et al*. 1997). MFK does not assume any definite form of the reaction and allows for variations in activation energy as the reaction progresses (Vyazovkin and Wight 1997). In fact, both PF and phenol-urea-formaldehyde (PUF) resins have been successfully characterized with MFK using the Kissinger-Akahira-Sunose (KAS) algorithm (Kissinger 1957; Sunose and Akahira 1971; He *et al*. 2003a; He and Riedl

2003). For PF resoles, changes in activation energy with degree of cure, E_α, helped distinguish two-stages in a highly condensed PF resin. In the first stage E_α increase with degree of cure was ascribed to consecutive and competitive reactions. Following this chemical regime, a decrease in E_α was ascribed to a diffusion-controlled regime (He *et al*. 2003a). The KAS algorithm could also be used to predict the isothermal cure of PF resins from dynamic tests (He *et al*. 2003a). Owing to additional cure reactions involving urea, PUF resins exhibited a more complex E_α curve than PF resins (He and Riedl 2003). Finally, the effects of water and wood on the cure kinetics of PF resins have also been examined with the KAS method (He *et al*. 2003b; He and Riedl 2004). While at low conversion water contributed to reversible cure reactions, it acted as a plasticizer at higher conversion and thus delayed the diffusion control regime enabling more complete cure (He *et al*. 2003a). Wood was found to accelerate the addition reactions in PF resoles while retarding the condensation reactions (He and Riedl 2004).

To date, all MFK studies on phenolic systems have utilized the KAS algorithm although isoconversional algorithms such as the Vyazovkin (1997; 2001) and Friedman methods (Friedman 1964) are also available. The objective of this research is to evaluate and compare the ability of the Friedman, Vyazovkin and KAS methods for 1) revealing the cure process and 2) predicting the dynamic and isothermal cure behavior of commercial PF resole resins from dynamic test data. In this objective, the cure kinetics of two commercial PF resoles that differ in molecular weight is evaluated with the three MFK methods.

EXPERIMENTAL

Materials

Two PF resoles, tailored as adhesives for oriented strand boards, were obtained from a commercial source. The resins were frozen and stored at -20^{o}C until use. To determine molecular weights, the resins were acetylated with 1:1 pyridine and acetic anhydride (Yazaki *et al*. 1994) and analyzed by gel permeation chromatography (GPC) in tetrahydrofuran. The GPC system consisted of a Viscotek 270 coupled to a Waters HPLC unit and Jordi Gel polydivinylbenzene mixed bed column with triple detectors. One resin had a weight-average molecular weight (M_w) of 621 g/mol and a polydispersity (M_w/M_n) of 1.41; it was labeled as PF-low. The other resin displayed an M_w = 6576 g/mol and M_w/M_n =1.72; it was labeled as PF-high. The resin solid contents were 54.5% and 45.0% for PF-low and PF-high respectively. In addition, elemental analysis (Nelson and Sommers 1982) showed the presence of 3.7 and 3.9 wt % nitrogen for PF-high and PF-low respectively, indicating the presence of urea in both resins.

Differential Scanning Calorimetry

A Mettler-Toledo DSC 822^{e} was used to perform dynamic and isothermal cure experiments. Approximately 13.5mg of resin was placed in a 30µl high pressure gold-plated crucible. Dynamic temperature scans were conducted at 5 heating rates 2, 5, 10, 20 and 25°C/min from 25°C to 250°C (He *et al*. 2003a). Nitrogen was used as a purge gas at a flow rate of 80 ml/min. For each heating rate six replicate

measurements were performed. In addition the first replicate was scanned again at 10^{o}C/min immediately after the first scan. This second scan ensured complete cure during the first heating scan as evidenced by the absence of residual cure. DSC thermograms were then processed with the Mettler-Toledo STAR^{e} V7.2 software to extract the degree of cure, α, reaction rate, $d\alpha/dt$, and corresponding temperature, T_{α}, in the $0 \leq \alpha \leq 0.99$ range. Both α and $d\alpha/dt$ were determined at a specific cure time, t, by normalizing the partial heat of reaction, $\Delta H(t)$, and heat flow, dH/dt, respectively by the total heat of reaction ΔH:

$$\alpha = \frac{\Delta H(t)}{\Delta H} \tag{21}$$

$$\frac{d\alpha}{dt} = \frac{dH/dt}{\Delta H} \tag{22}$$

MATLAB programs using the linear least square method were then developed to extract cure kinetic parameters according to the Friedman, Vyazovkin and KAS algorithms. The experimental data obtained at 2, 5 and 10°C/ min was then processed with these three programs. Kinetic parameters measured with the KAS algorithm were used to develop and compare dynamic cure predictions with experimental data at 20 and 25°C/min. To further validate the three MFK methods for isothermal cure, isothermal DSC runs were conducted at 120°C for different periods of time. The cure temperature and the cure times were selected based on experimental facility and so as to span the complete cure process. Specifically, the DSC cell was preheated to 120°C and approximately 13.5 mg of PF resin was inserted and cured for different periods of

time. The sample was then quickly removed from the DSC and quenched in liquid nitrogen. The residual heat of reaction of the partially cured samples, ΔH_R, was obtained from a subsequent ramp scan at 10°C/min from 25 to 250°C so that:

$$\alpha(t) = \frac{\Delta H - \Delta H_R}{\Delta H} \tag{23}$$

The total heat of reaction was taken as the average reaction heat previously measured in dynamic tests of fresh resins, 365 (± 5) kJ/kg for PF-high and 420 (± 9) kJ/kg for PF-low. The time dependence of the degree of cure at 120°C was compared with predictions from the three methods.

MFK algorithms

The phenomenological kinetics of cure can be generally described as:

$$\frac{d\alpha}{dt} = A\exp(-E/RT)\, f(\alpha) \tag{24}$$

where f(α) is the reaction model, T(K) the absolute temperature**,** A (s^{-1}) the pre-exponential factor**,** E (kJ/mol) the activation energy and R the universal gas constant. The Friedman (1964), Vyazovkin (1997; 2001) and KAS algorithms (Kissinger 1957; Sunose and Akahira 1971) can then be used to determine the activation energy dependence on degree of cure E_α.

For various heating rates, β_i, the Friedman method directly evaluates Eq. (24) at

a specific degree of cure α:

$$\ln\left(\frac{d\alpha}{dt}\right)_{\alpha i} = \ln(A_\alpha f(a)) - \frac{E_\alpha}{RT_{\alpha i}} \tag{25}$$

A new parameter $C_f(\alpha) = \ln(A_\alpha f(\alpha))$ can introduced so that $C_f(\alpha)$ and E_α are sufficient to fully describe the kinetic behavior:

$$\ln\left(\frac{d\alpha}{dt}\right)_{\alpha i} = C_f(\alpha) - \frac{E_\alpha}{RT_{\alpha i}} \tag{26}$$

For a specific α value and several heating rates β_i, pairs of $(d\alpha/dt)_{\alpha i}$ and $T_{\alpha i}$ are determined experimentally from the DSC thermograms. The parameters E_α and $C_f(\alpha)$ at this specific value of α are then estimated from plots of $\ln (d\alpha/dt)_{\alpha i}$ versus $1/T_{\alpha i}$ (Eq. (26)) across at least three different heating rates. The procedure is repeated for many values of α yielding continuous functions of α for E_α and $C_f(\alpha)$. The interest of the Friedman method is that Eq. (26) does not introduce any approximations and the method is not restricted to the constant heating rate mode. However, as in the case of any kinetic methods involving the differential term $d\alpha/dt$, the Friedman method is subject to significant numerical instability and noise interference (Sbirrazzuoli *et al*. 1997).

As a result, Vyazovkin proposed an alternative algorithm, which is summarized in the following equations. A detailed derivation of the algorithm is provided elsewhere (Vyazovkin 1997; 2001). In Vyazovkin method n scans are performed at different heating programs $T_i(t)$. The activation energy at a specific degree of cure is obtained by minimizing the function $\varphi(E_\alpha)$:

$$\varphi(E_\alpha) = \sum_{i=1}^{n} \sum_{\substack{j=1 \\ (j \neq i)}}^{n} \frac{I[E_\alpha, T_i(t_\alpha)]}{I[E_\alpha, T_j(t_\alpha)]} \tag{27}$$

In Eq. (7) the temperature integral, I, is defined as:

$$I[E_\alpha, T(t_\alpha)] = \int_{t_{\alpha-\Delta\alpha}}^{t_\alpha} \exp\left(\frac{-E_\alpha}{RT(t)}\right) dt \tag{28}$$

Eq. (28) can be solved numerically by integrating the experimental data within small time intervals $\Delta\alpha$. The I values are then substituted into $\varphi(E_\alpha)$, and this function is minimized by Brent's method (Brent 1973) leading to E_α. Again the procedure is repeated for distinct values of α. A new parameter $C_v(\alpha)$ can also be created that complements E_α in fully describing the cure kinetics:

$$C_v(\alpha) = \int_0^\alpha \frac{d\alpha}{Af(\alpha)} = \frac{1}{\beta} \int_{T_0}^{T} \exp\left(\frac{-E_\alpha}{RT}\right) dT \tag{29}$$

Finally in the KAS method, E_α is evaluated by using Doyle's integral approximations in Eq. (30) (Doyle 1961). In this case, Eq. (31) is derived for various heating rates. Again it can be rewritten into Eq. (32) by introducing a new parameter $C_k(\alpha) = \ln (RA_\alpha / E_\alpha\, g(\alpha))$:

$$g(\alpha) = \int_0^\alpha \frac{d\alpha}{f(\alpha)} = \frac{A}{\beta} \int_{T_o}^{T} \exp\left(-\frac{E}{RT}\right) dT \approx \frac{ART^2}{\beta E} \exp(-E/RT) \tag{30}$$

$$\ln\left(\frac{\beta_i}{T_{\alpha i}^2}\right) = \ln\left(\frac{RA_\alpha}{E_\alpha g(\alpha)}\right) - \frac{E_\alpha}{RT_{\alpha i}} \tag{31}$$

$$\ln\left(\frac{\beta_i}{T_{\alpha i}^2}\right) = C_k(\alpha) - \frac{E_\alpha}{RT_{\alpha i}} \tag{32}$$

The experimental determination of E_α and $C_k(\alpha)$ is similar to that of the Friedman method. For each degree of cure α, a corresponding $T_{\alpha i}$ and heating rate are used to plot $\ln (\beta_i/T^2_{\alpha i})$ against $1/T_{\alpha i}$. The parameters E_α and $C_k(\alpha)$ are then determined from the regression slope and intercept respectively.

The Friedman and Vyazovkin methods respectively solve the differential (Eq. (24)) and the integral kinetic forms (Eq. (28)) without approximations. On the other hand, the KAS method utilizes a close-form approximation (Eq. (30)). As a result, the KAS method provides only an estimate of the activation energy compared to the Vyazovkin and Friedman methods (Budrugeac and Segal 2001). In addition, while the Friedman and Vyazovkin methods are applicable to different temperature programs, the KAS method only works for constant heating programs.

RESULTS AND DiSCUSSION

Kinetic parameters from MFK methods

As expected, the commercial PF resoles exhibit two major exotherms that shift to higher temperatures with increasing heating rate (Figure 4.1). In addition, PF-high displays a third intermediate exotherm of small intensity (Figure 4.1). Hence, PF-low

has two discernable cure reactions while three reactions are evident during PF-high cure. Note also that a high degree of cure (54%) is required for PF-low to reach its highest reaction rate while the maximum reaction rate is achieved very early (22% degree of cure) for PF-high. To interpret the differences in stages in the cure of both resins, the E_α dependence on degree of cure can be examined (Sbirrazzuoli and Vyazovkin 2002).

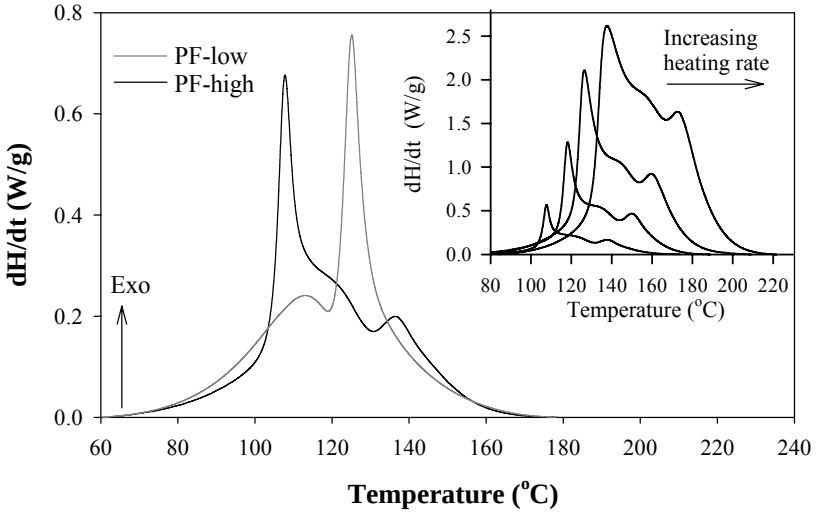

Figure 4.1 DSC thermograms at 2°C/min for the PF-low and PF-high resins. Insert highlights the influence of heating rate (2, 5, 10, and 20 °C/min) on the cure of the PF-high resin.

In Figure 4.2 the dependence of E_α on degree of cure is computed from the Friedman, Vyazovkin and KAS algorithms. The overall range of activation energies between 60 and 120 kJ/ mol is consistent with the values obtained from model fitting

kinetics of PF resins (Ray and Westwood 1975; Park *et al*. 2002). Evident in Figure 4.2 is the superposition of the Friedman and Vyazovkin E_α curves. The KAS method yields similar ascending and descending pattern, yet variations in E_α are smaller and the activation energy curve is shifted to higher conversion (Figure 4.2). Such a consistency between the Friedman and Vyazovkin methods has been previously observed on simulated data of parallel reactions (Vyazovkin 2001). In contrast, the shift and low amplitude of E_α obtained with the KAS method likely stems from the approximation used in this algorithm. Recall that the Friedman and Vyazovkin methods use the point values of the overall reaction rate (Budrugeac and Segal 2001) or small time intervals (Vyazovkin 2001) while the KAS method uses Doyle's approximation (Eq. 30) that describes the history of the system Budrugeac and Segal 2001). Yet Vyazovkin reported that the KAS method provides satisfactory E estimates as long as E/RT is greater than 13 (Vyazovkin and Dollimore 1996). In the case of the commercial PF resoles used in this study, despite an $E/RT > 13$, the KAS method generates an activation energy curve that is shifted to higher conversion and reduced in amplitude. This discrepancy in the case of commercial PF resoles likely stems from violation of the Doyle's assumption of a constant activation energy across the kinetic process (He and Riedl 2003). It results that the Vyazovkin and Friedman methods provide more consistent and accurate E_α functions. With these two methods, E_α is also more sensitive to changes in PF cure mechanisms. Therefore, to gain insight on the cure mechanism of PF resins, the Vyazovkin and Friedman methods are preferred over the KAS method.

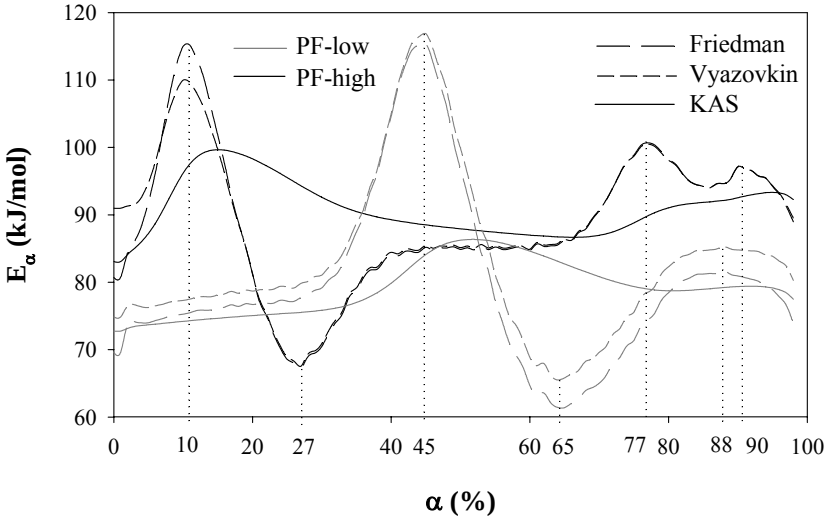

Figure 4.2 Activation energies change with the degree of cure by the Friedman, Vyazovkin and KAS methods for the PF-low and PF-high.

Regardless of the method used the wavy shape of E_α points to the complexity and molecular weight dependency of PF cure kinetics. Indeed it is established that complex reactions involving multiple parallel reactions or changes in the limiting stage cause variations in E_α (Vyazovkin and Lesnikovich 1990; Flynn and Wall 1966; Opfermann 2000). Specifically, an increasing E_α function reveals competition between parallel reactions (He *et al*. 2003a; Vyazovkin and Lesnikovich 1990). Alternatively a concave decreasing E_α curve suggests a reversible stage reaction and a convex decreasing E_α function shows a change in limiting stage (Vyazovkin and Lesnikovich 1990). Therefore the shape of E_α can give some insight on the change in reaction steps (Vyazovkin and Wight 1997).

For PF-low, Friedman and Vyazovkin methods generate two E_α peaks at 45% and 88% degrees of cure (Figure 4.2) in accordance with two detected exotherms (Figure 4.1). E_α shape for PF-low suggests 4 cure stages. The increasing and then concave decreasing E_α curve suggests the presence of competitive reactions up to 45% conversion followed by a reversible stage intermediate up to 65% (Vyazovkin and Lesnikovich 1990; Vyazovkin and Wight 1997). At a degree of cure of 65% parallel reactions reconvene as indicated by the E_α increase until the cure changes from a kinetic to a diffusion-controlled process (Butt 1999) above 88% conversion where E_α decreases in a convex fashion (Vyazovkin and Lesnikovich 1990; Vyazovkin and Wight 1997). This 4-stage cure is more complex than the 3-stage cure of PUF resins previously described based on the KAS algorithm (He and Riedl 2003). Recall however that the KAS method is less sensitive to changes in E_α than the Vyazovkin and Friedman methods used in this study. In fact, the E_α curves obtained from the KAS method for PF-low and PF-high would also suggest a 3-stage cure. In addition in contrast to a single cure exotherm previously detected on PUF resins (He and Riedl 2003); two exotherm peaks are detected on these commercial PF resoles.

Although the specific reactions underlying the four stages cannot be identified solely based on this study, this cure behavior is in line with the individual cure reactions of urea-modified PF resins. PF cure involves a set of parallel reactions with HMPs formation, condensation and the various crosslinking chemistries (Detlefsen 2002). With the addition of urea, condensation of phenol and urea with formaldehyde as well as co-condensation between phenol and urea derivatives are also taking place

(He and Yan 2004). The changing contribution of each reaction to the overall activation energy explains the constant change in activation energy as cure progresses (He and Riedl 2003). Since water is remains in the crucible during cure, the cure process is further complicated (He *et al.* 2003b). At low conversion water contributes to reversible reactions (He *et al.* 2003b). At high conversion, water plasticizes the PF network thus delaying diffusion control and allowing for more complete cure (He *et al.* 2003b).

For PF-high an even more complex cure mechanism is observed with the presence of 2 highest E_α peaks at 10% and 77% conversion but also two small E_α peaks at 40% and 90% degree of cure. The greater complexity likely stems from the detection of 3 exotherms on the DSC thermogram for PF-high (Figure 4.1). In all case PF-high likely exhibits a similar 4-steps pattern as PF-low does. That is competitive condensation reactions occur up to 10%; they are followed by a reversible intermediate stage up to 27 % degree of cure. Competing crosslinking reactions then resume until diffusion rate control occurs at 77 % degree of cure as previously observed on phenolic systems (He *et al*. 2003a; He and Riedl 2003). The E_α peaks shoulders at 40% and 90% may arise from a mathematical artifact.

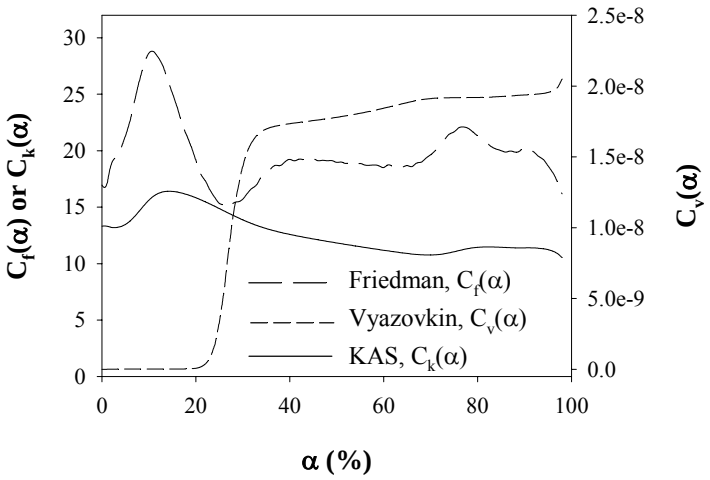

Figure 4.3 Combined parameters of the Friedman, Vyazovkin and KAS methods for PF-high.

Finally, the second MFK parameter needed to model reaction kinetics is the combined complex parameter C(α). The degree of cure dependence of this parameter with all three methods also reflects the changing cure mechanism as shown for PF-high (Figure 4.3). Because this parameter is a modeling tool deprived of distinct physical meaning no inferences are made from its pattern. Next C(α) and E_α obtained from the 3 methods are utilized for assessing MKF predictions during dynamic and isothermal cure of PF resins.

Prediction of dynamic cure of PF resins

Eq. (32) used for the KAS method directly relates temperature and degree of cure (He *et al*. 2003a). Therefore only the KAS method was used to predict the dynamic cure of PF resins. At a selected heating rate $C_k(\alpha)$ and E_α were substituted

into Eq. (32) to predict the temperature associated with discrete values of α. An algorithm based on the Powell dogleg method (Powell 1970) was developed with MATLAB to solve Eq. (32). Relationships between temperature and degree of cure were thus obtained and were easily converted to reaction rate-temperature relationships at specific heating rates. Figure **4.4** compares experimental reaction rate and degree of cure with the KAS predictions for PF-high and PF-low respectively. Recall that the model was built from data at 2, 5, and 10^{o}C/ min only whereas predictions are also made at 20 and 25^{o}C/ min for model validation. Mean squared errors of prediction (MSEPs) (Rawlings *et al*. 1998) were calculated for both dynamic and isothermal MFK predictions (Table 4.1). The MSEP is the average squared difference between independent experimental observations and model predictions for the corresponding values of the independent variable (Rawlings *et al*. 1998). The MSEP values of the KAS predictions for temperature and reaction rate are small, both one order of magnitude lower than those obtained with the best model-fitting kinetics in a parallel study (Wang *et al*. 2006). The KAS method therefore provides excellent dynamic predictions compared to model-fitting kinetics. This is further evidenced in Figure **4.4**, where the KAS algorithm succeeds in capturing the complexity of PF-high thermogram.

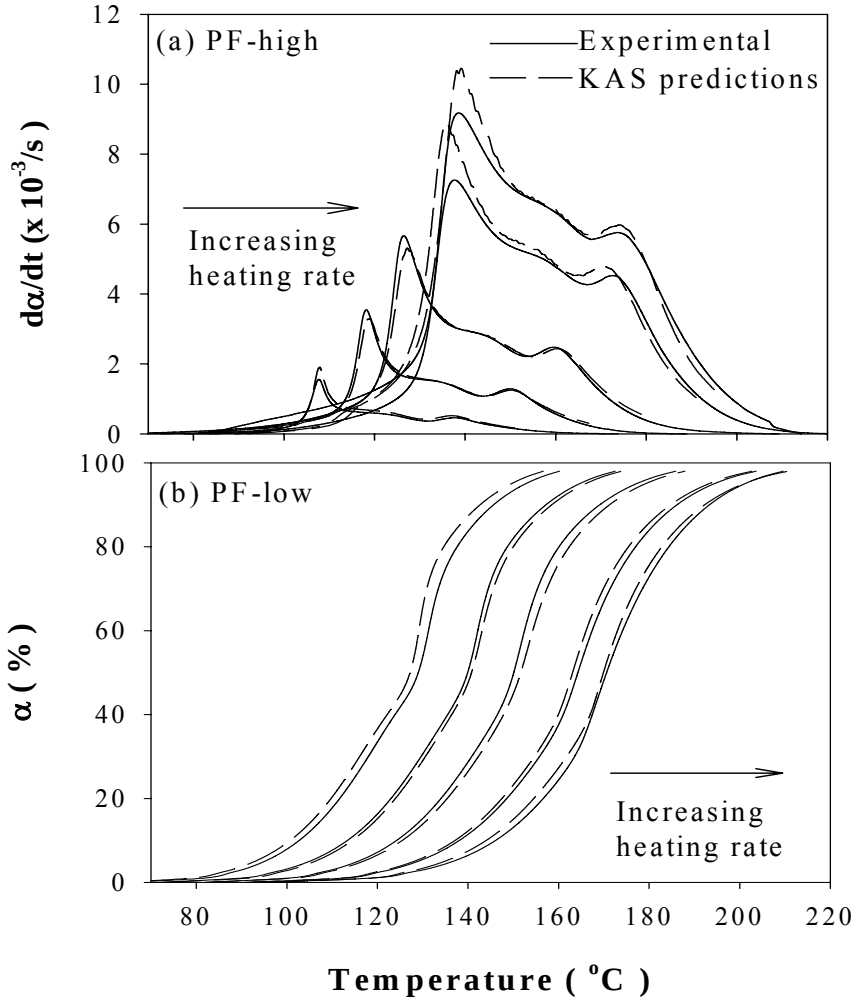

Figure 4.4 Comparisons of experimental data and KAS predictions for dynamic conditions at 2, 5, 10, 20 and 25 ^{o}C/min for (a) the reaction rate of PF-high and (b) the degree of cure of PF-low.

Table 4.1 Mean squared errors of prediction for both dynamic and isothermal conditions at specific degree of cure and data points (in parentheses).

Predicted variable	Model	PF-low	PF-high
Dynamic (10 ^{o}C/min) temperature at α (^{o}C)^2	KAS	2.97 (99)	0.27 (99)
Dynamic (10 ^{o}C/min) reaction rate at α (1/s)^2	KAS	9.82x10^{-8}(99))	6.27x10^{-8}(99)
Isothermal (120^{o}C) cure time at α (min)^2	Friedman Vyazovkin KAS	15.8 (11) 16.7 (11) 12.0 (11)	13.4 (13) 19.1 (13) 19.4 (13)

Prediction of isothermal cure of PF resins

Prediction of isothermal cure from dynamic scans is of scientific and practical interest. First, good prediction of isothermal cure from parameters obtained during dynamic cure clearly validates the models. Second, isothermal cure characterization is notoriously challenging from the experimental standpoint (Widmann 1975). In this study, Friedman, Vyazovkin and KAS algorithms were used to predict the isothermal cure behavior of the two PF resins at 120°C. The premise of isothermal prediction is that pairs of α and the corresponding f(α), g(α), E_α and A values are identical for dynamic and isothermal conditions (Doyle 1962). Hence, MFK parameters can be used to develop a prediction model of the cure time needed to achieve a specific degree of cure, t_α , at a given temperature (T_{iso}).

With Friedman algorithm, Eq. (26) is rewritten to yield:

$$t_\alpha = \int_0^\alpha \exp\left(\frac{E_\alpha}{RT_{iso}}\right)\exp[-c_f(\alpha)]d\alpha \qquad (33)$$

Vyazovkin method yields an integrated equation from Eq. (24) and Eq. (29) at an arbitrary isothermal temperature T_{iso} as:

$$\int_0^t \exp\left(\frac{-E_\alpha}{RT_{iso}}\right)dt = \int_0^\alpha \frac{d\alpha}{Af(\alpha)} = C_v(\alpha) \tag{34}$$

At each small $\Delta\alpha$, the left integral is evaluated numerically with the trapezoid integration rule and the corresponding Δt is calculated. This calculation is reiterated from time 0 on. Thus at an arbitrary isothermal temperature a relationship between t_α and α is established.

Finally, the KAS parameters are used to reorganize Eqs. (24) and (32) into:

$$t_\alpha = \frac{R\exp(E_\alpha / RT_{iso})}{E_\alpha \exp(C_k(\alpha))} \tag{35}$$

Isothermal cure predictions from all three MFK algorithms are compared with experimental data for PF-low and PF-high in Figure 4.5. The small MSEP values (MSEP < 19.4) for both resins and all three models (Table 4.1) indicates the quality of the models compared to those determined in another study (Wang *et al*. 2006) from n-order kinetics (MSEP < 33). Analysis of variance (ANOVA) at an α level of 0.05 detected no differences in the isothermal prediction ability of the three MFK algorithms. Overall, the cure of PF-low and PF-high resins is equally well predicted with MFK methods. Yet, locally the isothermal data for PF-low does not capture the complexity of the cure prediction in the 10-20 minutes range (**Figure 4.5**).

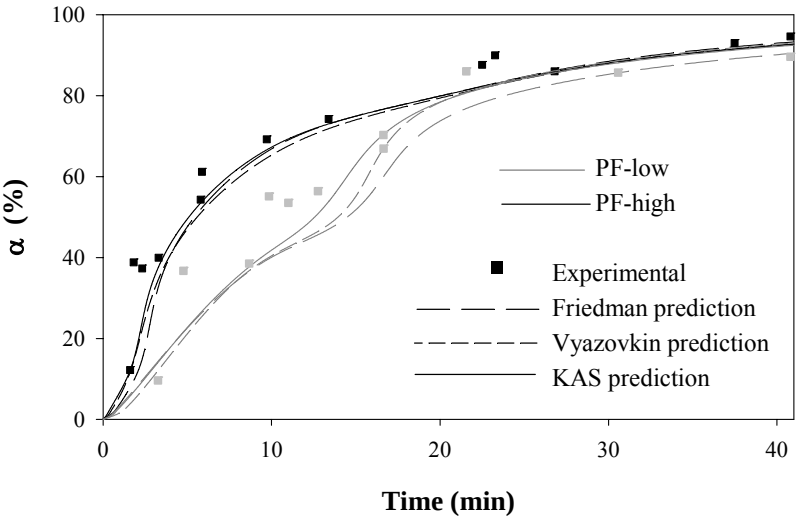

Figure 4.5 Comparison of experimental data with the Friedman, Vyazovkin and KAS predictions of degree of cure of PF-low and PF-high during isothermal cure at 120°C.

CONCLUSION

The cure development of two commercial PF resoles was analyzed by the Friedman, Vyazovkin and KAS model-free kinetics. The three algorithms were compared in their consistency and ability to perform dynamic and isothermal predictions. The Friedman and Vyazovkin methods generated consistent and accurate activation energy dependences on degree of cure. These two algorithms were also the most sensitive to changes in activation energy. Higher consistency and accuracy of the Friedman and Vyazovkin methods compared to the KAS algorithm were ascribed to the use of a close-form approximation of the kinetic equation in the latter algorithm. On the other hand, the KAS algorithm was more amenable to dynamic cure

predictions. For isothermal cure predictions the three MFK algorithms provided equally good predictions. In all cases, predictions with MFK were significantly better than those measured in a parallel study with model-fitting methods. Hence, the Friedman and Vyazovkin methods are best suited for activation energy measurement. These two methods are the most appropriate for gaining insight on the cure mechanisms of commercial PF resoles. Alternatively, the KAS method is best suited for modeling and prediction purposes.

REFERENCES

Brent, R. P. Algorithms for minimization without derivatives. Englewood Cliff, N.J., Prentice-Hall, 1973.

Butt, J. B. Reaction Kinetics and Reaction Design, second ed., Marcel Dekker, Inc., New York, 1999.

Budrugeac, P.; Segal, E. Some methodological problems concerning nonisothermal kinetic analysis of heterogeneous solid-gas reactions. *International Journal of Chemical Kinetics (2001), 33(10)*, 564-573.

Detlefsen, W.D. Phenolic resins: Some chemistry, technology, and history, in: M. Chaudhury, A.V. Pocius (Eds.), Surfaces, chemistry and applications, Elsevier, Amsterdan, 2002, pp. 869-945

Doyle, C. D. Kinetic analysis of thermogravimetric data. *Journal of Applied Polymer Science (1961), 5*, 285-92.

Doyle, C. D. Estimating isothermal life from thermogravimetric data. Journal of Applied Polymer Science (1962), 6(No. 24), 639-42.

Flynn, J. H.; Wall, L. A. General treatment of the thermogravimetry of polymers. *Journal of Research of the National Bureau of Standards, Section A: Physics and Chemistry (1966), 70*(6), 487-523. .

Friedman, H. L. Kinetics of thermal degradation of char-forming plastics from thermogravimetry-application to a phenolic resin. *Journal of Polymer Science (1964),* Volume Date 1963, No. 6(Pt. C), 183-95.

He, G.; Riedl, B.; Ait-kadi, A. Model-free kinetics: Curing behavior of phenol formaldehyde resins by Differential Scanning Calorimetry. *Journal of Applied Polymer Science (2003a), 87*, 433 -440.

He, G.; Riedl, B.; Ait-kadi, A. Curing process of powdered phenol formaldehyde resol resins and the role of water in the curing systems. *Journal of Applied Polymer Science (2003b), 89*, 1371-1378.

He, G.; Riedl, B. Phenol-urea-formaldehyde cocondensed resol resins: their synthesis, curing kinetics, and network properties. *Journal of Polymer Science, Part B: Polymer Physics (2003), 41*(16), 1929-1938.

He, G.; Riedl, B. Curing kinetics of phenol formaldehyde resin and wood-resin interactions in the presence of wood substrates. *Wood Science and Technology (2004), 38*(1), 1432-5225.

He, G.; Yan, N. ^{13}C NMR study on structure, composition and curing behavior of phenol-urea-formaldehyde resole resins. *Polymer (2004), 45*(20), 6813-6822.

Holopainen, T.; Alvila, L.; Rainio, J.; Pakkanen, T. T. Phenol formaldehyde resol resins studied by 13C NMR spectroscopy, gel permeation chromatography, and differential scanniong calorimetry. *Journal of Applied Polymer Science (1997), 66*, 1183-1193.

Kay R.; Westwood, A. R. Differential scanning calorimetry (DSC) investigations on condensation polymers. I. Curing. *European Polymer Journal (1975), 11*(1), 25-30

Kim, M. G., Watt, C.; Davis, C. R. Effects of urea addition to phenol-formaldehyde resin binders for oriented strandboard. *Journal of Wood Chemistry Technology (1996), 16*, 21-29.

Kissinger, H. E. Reaction kinetics in differential thermal analysis. *Analytical Chemistry (1957), 29*, 1702-1706.

Knop, A.; Pilato, L. A.; Phenolic Resins, Springer-Verlag, New York, 1985.

Luukko, P.; Alvila, L.; Holopainen, T.; Rainio, J.; Pakkanen, T. T. Effect of alkalinity on the structure of phenol-formaldehyde resol resins. *Journal of Applied Polymer Science (2001), 82*(1), 258-262.

Nelson, D. W.; Sommers, L. E. In Methods of soil analysis, Part 2. Chemical and microbiological properties, second ed., Page, A.L., Ed.; American Society of Agronomy, Madison, WI, 1982, Chap. 29.

Opfermann, J. inetic analysis using multivariate non-linear regression: I. Basic concepts. *Joural of Thermal Analysis and Calorimetry (2000), 60*(2), 641-658.

Park, B.-D.; Riedl, B.; Kim, Y. S.; So, W. T. Effect of synthesis parameters on thermal behavior of phenol-formaldehyde resol resin. *Journal of Applied Polymer Science (2002), 83*(7), 1415-1424.

Powell, M. J. D. in: P. Rabinowitz, (Ed.), Numerical Methods for Nonlinear Algebraic Equations, Gordon and Breach Science Publishers, London, 1970, pp. 87-114

Prime R. B. Thermosets. In: Turi EA, editor. Thermal characterization of polymeric materials. New York: Academic Press, 1997:435–569.

Rawlings, J. O.; Pantula, S. G.; Dickey, D. A. Applied Regression Analysis, second ed., Springer, New York, 1998.

Sbirrazzuoli, N.; Girault, Y.; Elegant, L. Simulations for evaluation of kinetic methods in differential scanning calorimetry. Part 3 - Peak maximum evolution methods and isoconversional methods. *Thermochimica Acta (1997), 293*(1-2), 25-37.

Sbirrazzuoli, Nicolas; Vyazovkin, Sergey. Learning about epoxy cure mechanisms from iso-conversional analysis of DSC data. *Thermochimica Acta (2002), 388*(1-2), 289-298.

Sunose, T.; Akahira, T. Method of determineing activation deterioration constant of electrical insulating materials. *Research Report, Chiba Inst. Tecnol. (Sci. Tecnol.) (1971), 16*, 22-23.

Vyazovkin, S. V.; Lesnikovich, A. I. An approach to the solution of the inverse kinetic problem in the case of complex processes. 1. Methods employing a series of thermoanalytical curves. *Thermochimica Acta (1990), 165*(2), 273-280.

Vyazovkin, S.; Dollimore, D. Linear and Nonlinear Procedures in Isoconversional Computations of the Activation Energy of Nonisothermal Reactions in Solids. *Journal of Chemical Information and Computer Sciences (1996), 36*(1), 42-45.

Vyazovkin, S. Evaluation of activation energy of thermally stimulated solid-state reactions under arbitrary variation of temperature. *Journal of Computational Chemistry (1997), 18*(3), 393-402.

Vyazovkin, S.; Wight, C. A. Kinetics in solids. *Annual Review of Physical Chemistry (1997), 48*, 125-149.

Vyazovkin, S.; Sbirrazzuoli, N. Kinetic methods to study isothermal and nonisothermal epoxy-anhydride cure. *Macromolecular Chemistry and Physics (1999), 200*(10), 2294-2303.

Vyazovkin, S. Modification of the integral isoconversional method to account for variation in the activation energy. *Journal of Computational Chemistry (2000), Volume Date 2001*, 22(2), 178-183.

Wang, J., M.-P. G. Laborie, and M. P. Wolcott. Comparison of model-fitting kinetic methods for modeling the cure kinetics of commercial phenol–formaldehyde resins. *Journal of Applied Polymer Science (2006),* Accepted.

Widmann, G. Quantitative isothermal DTA studies. *Thermochimica Acta (1975), 11*(3), 331-333.

Chapter 5 The Influence of Wood on the Cure Kinetics of Phenol-formaldehyde Resins

ABSTRACT

The cure kinetics of pure phenol formaldehyde (PF) resins have been investigated extensively. However, it is unclear whether the obtained kinetic parameters can be used to describe and predict cure development in the presence of wood, since wood is known to affect the cure kinetics of PF resins. In this research, differential scanning calorimetry (DSC) was used to investigate the influence of wood and wood constituents on the cure development and kinetics of PF resins. Mixtures of PF resin with southern yellow pine, extracted southern yellow pine, southern yellow pine extractives, cellulose, lignin, and hemicelluloses were evaluated in terms of heat of reaction, onset and end cure temperatures and activation energies using the Borchardt-Daniels nth order (nth-BD) model, Kissinger equation, and Vayazovkin model-free kinetics.

DSC analysis showed that the curing behavior of the PF resin did not change significantly when the wood content was below 20%. When the wood content was above 35%, the thermogram shapes and derived kinetic parameters changed significantly. One new exotherm appeared at low temperatures (ca. 50°), while the main reaction exotherms were not affected. The time-to-completion for wood/PF mixture was also not affected by the presence of wood. When conversion above 70% is of interest in practical application, the models working for pure resin can also be

appropriate as a predictor for PF/wood mixture. The mixture of southern yellow pine extractives at 35 % content level released similar heat in reactions with pure PF resin, while all other substrates reduced the reaction heat significantly, suggesting that the resin did not reach the same cure extent as PF alone. Cellulose and xylan did not change the cure kinetics for PF curing. The catalytic effect of the presence of wood may come from interactions between PF and lignin.

Key words: Differential scanning calorimetry (DSC); kinetic models; southern yellow pine; wood constituents; phenol formaldehyde resin.

INTRODUCTION

The cure behavior and kinetics of neat phenol-formaldehyde (PF) resins have been investigated for decades (Prime 1998). Wang *et al.* (2005, 2006) demonstrated that both model-fitting kinetics and model-free kinetics (MFK) are practical models for describing and predicting the cure of neat PF resins. At the same time, wood has long been known to influence the cure mechanisms and kinetics of PF resins (Chow 1969; Pizzi *et al*. 1994; He and Riedl 2004; He and Yan 2005).

In the presence of wood, the activation energy of the curing process can be considerably altered (Chow 1969; Pizzi *et al*. 1994; He and Yan 2005). Some wood species have no impact on the PF cure, while others increase or decrease the activation energy, accelerating or retarding the cure (Mizumachi and Morita 1975). He

and Riedl (2004) reported that wood accelerated the substitution reactions (hydroxymethylation) and retarded the condensation reactions in the curing processes, further separating the two reactions into two exotherms on a DSC thermogram. Most often, a decrease in activation energy is observed in the presence of wood (Mizumachi and Morita 1975; Pizzi *et al*. 1994). The decrease of activation energy has been ascribed to catalytic activation induced by secondary interactions, such as dipolar forces or hydrogen bonds, between the lignocellulosic substrate and the PF resin (Pizzi *et al*.1994; He and Riedl 2004). Others have postulated that covalent bonds between wood carbohydrates and the resin could form, thus depressing the cure activation energy (Chow 1969; Kottes-Andrews *et al*. 1986). Furthermore, He and Riedl (2004) have shown that wood reduces the total heat of reaction, resulting in lower degrees of cure in PF resins cured in the presence of wood. The wood particles were proposed to physically separate the resin species, hence decreasing their mobility and probability to connect to each other. In line with these results, Laborie and Frazier (2006) noted that PF carbons exhibited lower cross polarization rates in the presence of wood than in the neat state, supporting the thesis of a lower crosslink density and degree of cure for PF resins cured in the presence of wood.

As a result, researchers have evaluated the impact of specific wood constituents on PF cure. Barry *et al*. (1993) noted a correlation between the heat of reaction of PF cure and the lignin content, with higher lignin content corresponding to lower heat of reaction. Chow (1969) reported that the PF chemical conversion decreased with increasing hydroxyl content in the mixture, either due to higher

cellulosic content or higher hydroxyl groups per pyranose unit in the cellulosic compounds. Chow (1969) postulated that the activation energy for forming a resin-carbohydrate bond was less than that for a resin-resin bond, suggesting preferential reaction of phenolics with carbohydrates over self-condensation. Recent research also suggests that the low pH value of wood and extractives is the main cause for changes in activation energy (He and Riedl 2004, He and Yan 2005).

In most of these studies, activation energies were simply computed from the Kissinger equation, which is generally valid for simple reactions where iso-conversional cure peaks are obtained (Kissinger 1957). For complex, multiple reactions as in the case of PF resins (Detlefsen 2002), the Kissinger equation and the nth-BD method are inadequate to disclose mechanisms and may be inaccurate (Wang *et al*. 2005, Vyazovkin & Sbirrazzuoli 2006).

On the other hand, MFK is well-suited to portray the kinetics of complex reactions such as the cure of PF resins (Wang *et al*. 2005). MFK does not assume any definite form of the reaction and allows for variations in activation energy throughout the reaction process. As a result, the cure of PF resins in the presence of wood has been recently characterized with MFK using the Kissinger-Akahira-Sunose (KAS) algorithm (He & Riedl 2004). The study demonstrated that the activation energy-conversion curve for 50% PF/spruce mixtures had a similar pattern to that of pure PF resin. In the early stage of curing, an increase in E_α with conversion was ascribed to consecutive and competitive reactions, after which a decrease in E_α was ascribed to a diffusion-controlled regime. In contrast to the cure thermogram of the neat PF resin,

He and Riedl (2004) and He and Yan (2005) reported that a small peak appeared in the lower temperature range between 60 and 100°C in the DSC curves of PF resin/wood mixtures. This small exotherm was ascribed to hydroxymethylation reactions accelerated by the wood, while the main condensation reactions were retarded. The activation energy-changing pattern obtained by KAS was sensitive to this small exotherm, and a slightly slower increase rate in activation energy below 10% degree of cure was noted in comparison to neat PF (He & Riedl 2004).

The objective of this research was twofold: 1) to evaluate and compare the effectiveness of the Kissinger equation, nth BD, and model-free Vyazovkin method for characterizing the cure kinetics of PF resins in the presence of wood and wood constituents, and 2) to utilize the best-suited kinetic model to determine the influence of wood and wood constituents on the cure of PF resins.

EXPERIMENTAL

Materials

A commercial PF resole was obtained from Georgia-Pacific Company and stored at -20^{o}C until use. The resin had a weight-average molecular weight (M_w) of 6576 g/mol, polydispersity (M_w/M_n) of 1.72. Gel permeation chromatography analysis showed that the resin has three fractions: a main fraction of high molecular weight species and two small fractions of low molecular weight material, monomers and dimers. The resin solid content is 45.0% and pH in the 11.0-11.5 range. In addition,

elemental analysis showed the presence of 3.7 wt % nitrogen for the resin, indicating that urea was present (Wang *et al*. 2005).

Southern yellow pine (SYP) strands with 5% moisture content were obtained from the Huber Wood Engineering. The wood strands were ground into wood flour, passing through 60 mesh screen which corresponded to particles up to 250 μms. In order to evaluate the effect of extracted wood and extractives on the resin cure, part of the SYP was soxhlet extracted with acetone and then water for 72 hours each. Measured extractive content was 3.9% for SYP. The flours of SYP and extracted SYP as well as SYP extractives were then dried under a vacuum at 60 ˚C until constant weight and stored in a desiccator with drierite until use. Cellulose powder was made by grinding filter paper (Whatman) into flour passing through 60 mesh with a Wiley mill machine. Unsulfonated kraft lignin (Indulin® AT) and birchwood xylan powder were obtained from Westvaco and Sigma Aldrich respectively, and used as received.

Mixtures of wood/ PF and wood constituents/ PF were prepared as follows: 2.0 g of liquid resin was manually mixed in a vial with 0.50, 1.1, 2.0, 4.7 g wood flour to yield mixtures having PF: wood weight % ratios of 80/20, 65/35 , 50/50 and 30/70% wood content based on total weights (i.e. liquid resin +wood flour). Similarly, mixtures were prepared with cellulose, lignin, xylan, SYP extractives, and extracted SYP in a 65/35 PF: substrate % weight ratio. The time between the preparation of the mixtures and DSC analysis of all replicates did not exceed 12 hours and did not affect the DSC thermograms.

In order to investigate the effects of wood particle size on the effects of curing,

PF resin was sprayed on both sides of a 1mm-thick oven-dried wood strip with an air brush, resulting in a 70% wood content level. A small disk was trimmed from the resinated wood strip for DSC scanning.

Differential scanning calorimetry

A Mettler-Toledo DSC 822^e was used to perform dynamic and isothermal cure experiments. For dynamic tests, a baseline for moist wood was first obtained by placing 10 mg SYP flour with a moisture content of 25% and 125% into high pressure crucibles and performing a heating scan at 10 °C/min in the DSC. Then wood/PF mixtures were evaluated. Approximately 13.5mg of PF/wood mixtures or neat PF resin were placed in a 30µl high pressure gold-plated crucible. Dynamic temperature scans were conducted at 4 heating rates 2, 5, 10, and 20 °C/min from 25°C to 250°C. For each heating rate, three replicate measurements were performed. The resinated disk was scanned at one heating rate of 5 °C/min from 25°C to 250°C. DSC thermograms were then processed with the Mettler-Toledo STAR^e V7.2 software to extract the degree of cure, α, reaction rate, $d\alpha/dt$, and corresponding temperature, T_α, in the $0 \leq \alpha \leq 0.99$ range. Both α and $d\alpha/dt$ were determined at a specific cure time, t, by normalizing the partial heat of reaction, $\Delta H(t)$, and heat flow, dH/dt, respectively by the total heat of reaction ΔH.

The neat resin was also characterized under isothermal cure conditions. An isothermal cure was performed for different time periods in the DSC cell that had been preheated at 120°C. Following the precure of the neat resin sample in the DSC

cell at 120°C, the sample crucible was quickly removed from the DSC, quenched in liquid nitrogen, and rescanned in the DSC at 10 °C/min to determine residual cure.

Kinetic models

An Arrhenius equation can be used to describe the cure reaction rate of thermosetting resins:

$$\frac{d\alpha}{dt} = A\exp\left(\frac{-E}{RT}\right) f(\alpha) \tag{36}$$

In Eq. (36), α is the conversion and a function of time (t), $f(\alpha)$ the reaction model, T the temperature, A the pre-exponential factor, E the activation energy and R the gas constant. Using the n^{th} order Eq. (36) can be rearranged into Eq. (37):

$$\ln\left(\frac{d\alpha}{dt}\right) = \ln A + n\ln(1-\alpha) - \frac{E}{RT} \tag{37}$$

Kinetic parameters, A, E and n can be extracted by the Borchardt-Daniels procedure with the values of α and $d\alpha/dt$ and corresponding temperature from one DSC dynamic scan (ASTM E 2041, nth-BD).

The kinetic parameters can also be determined from multiple heating rate scans. The peak temperature (T_{ipeak}) dependency on heating rate (β_i) can thus be used to calculate the activation energy. Assuming an iso-fractional peak temperature, a

linear regression of ln (β_i/T^2_{ipeak}) against $1/T_{ipeak}$ across several heating rates yields the activation energy with Kissinger Eq. (38) (Kissinger 1957).

$$E = \frac{Rd[-\ln(\beta / T_{peak}^2)]}{d(1/T_{peak})} \tag{38}$$

With this method, when the peak temperatures are closer to each other across a series of heating rates, the calculated activation energies will increase in value. The n^{th}-BD method gives cure kinetic parameters for the overall cure process at each heating rate, while the Kissinger equation estimates activation energy for specific peaks (Wang *et al*. 2006).

The patterns of activation energy against the degree of cure of the curing process can be evaluated by model-free kinetics of Vyazovkin method. Wang *et al*. (2005) reported this method as the most appropriate for gaining insight on the cure mechanisms of commercial PF resoles. The method has been described previously (Vyazovkin 2001; Wang *et al*. 2005) and summarized as follows. In the Vyazovkin method, n scans are performed at different heating programs, $T_i(t)$. The activation energy at a specific degree of cure is obtained by minimizing the function $\varphi(E_\alpha)$:

$$\varphi(E_\alpha) = \sum_{i=1}^{n} \sum_{\substack{j=1 \\ (j \neq i)}}^{n} \frac{I[E_\alpha, T_i(t_\alpha)]}{I[E_\alpha, T_j(t_\alpha)]} \tag{39}$$

In Eq. (39) the temperature integral, I, is defined as:

$$I[E_\alpha, T(t_\alpha)] = \int_{t_{\alpha-\Delta\alpha}}^{t_\alpha} \exp\left(\frac{-E_\alpha}{RT(t)}\right) dt \tag{40}$$

Eq. (40) can be solved numerically by integrating the experimental data within small time intervals $\Delta\alpha$. The 'I' values are then substituted into $\varphi(E_\alpha)$, and this function is minimized by Brent's method (Brent 1973) leading to E_α. The procedure is repeated for distinct values of α. A new parameter $C_v(\alpha)$ can be created that complements E_α in fully describing the cure kinetics:

$$C_v(\alpha) = \int_0^\alpha \frac{d\alpha}{Af(\alpha)} = \frac{1}{\beta}\int_{T_0}^{T} \exp\left(\frac{-E_\alpha}{RT}\right) dT \tag{41}$$

For model-free predictions under isothermal temperature T_{iso} from Vyazovkin parameters E_α and $C_v(\alpha)$, the equations are:

$$\Delta t_\alpha = \frac{C_v(\alpha) - C_v(\alpha - \Delta\alpha)}{\exp\left(\frac{-E_\alpha}{RT_{iso}}\right)} \tag{42}$$

$$t_\alpha = t_{\alpha-\Delta\alpha} + \Delta t_\alpha \tag{43}$$

Model-free kinetics does not assume any definite form of the reaction model and allows for variations in activation energy as the reaction progresses.

RESULTS AND DISCUSSION

DSC of moist wood

The thermogram of wood with a 25% MC consists of a flat baseline, whereas wood with a moisture content of 125%, i.e. above the fiber saturation point, exhibits an endotherm between 0 and 50 ˚C that is ascribed to ice melting (Figure 5.1). The cure exotherms of PF resin is generally observed at higher temperature windows (He and Yan, 2005). Consequently, in the wood/PF mixtures used in these studies with a moisture content from 24% to 220%, the thermal events arising from moist wood will likely not overlap with the resin cure.

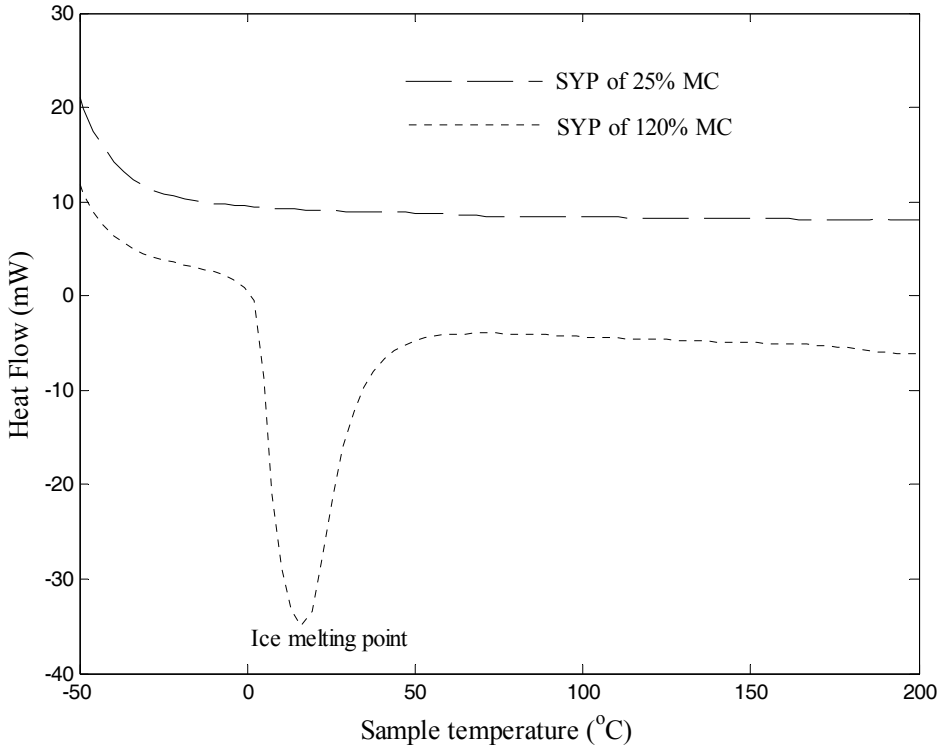

Figure 5.1 Baselines of southern yellow pine (SYP) at two moisture contents scanned at 10 ^{o}C/min in a high pressure crucible.

Comparison among different SYP contents

The mixture with 20% SYP exhibited a similar thermogram as the PF alone, with the first and third peaks depressed and the intermediate peak 2 increased (Figure 5.2). With southern yellow pine contents at or above 35%, the first peak disappeared and the third peak gradually vanished into a shoulder. Regardless of wood content, all three peaks, when present, occur at the same temperature and have a similar activation energy (Table 5.1). Apparently, time to cure completion is also unaffected by the wood content (Figure 5.2) which has practical implications in terms of utilizing the

cure characteristics of neat resin for panel hot-pressing cycle determination. This suggests that the overall kinetics of the main cure reactions is marginally affected by the presence of wood.

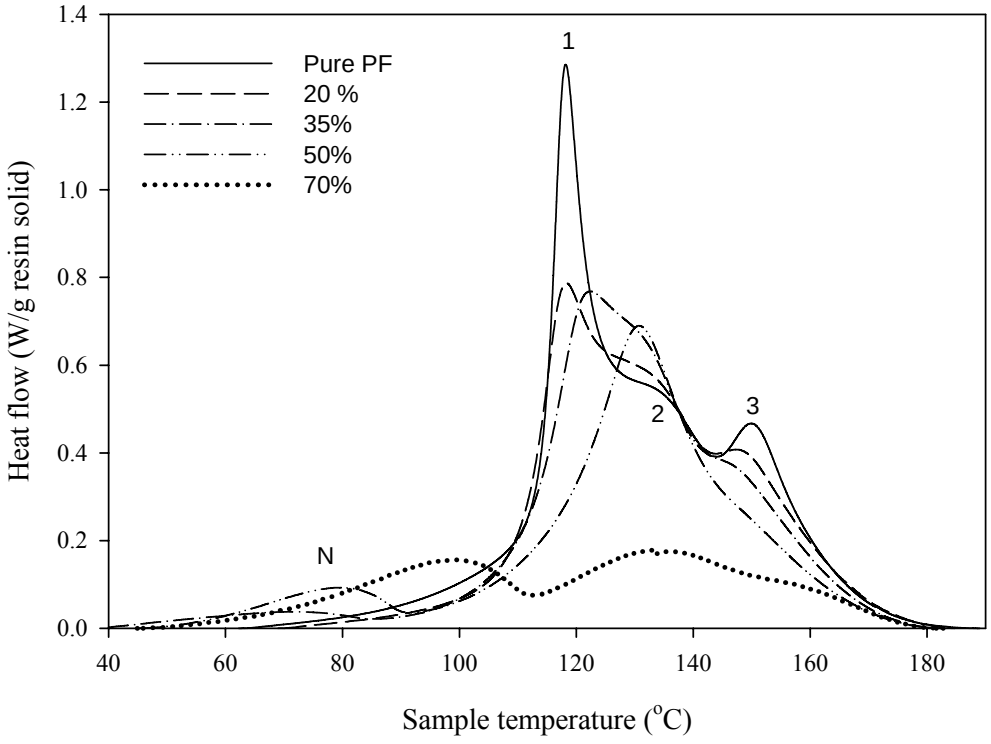

Figure 5.2 DSC thermograms of PF/southern yellow pine at various contents.

Interestingly, at 35% wood content, a new peak (labeled N peak) appears at lower temperature, between 60 and 100°C, and the heat of reaction associated with this peak increases with increasing wood content, from 5 % of the total heat of cure at 35% wood content to 15% for a 70% wood content mixture. The activation energy for the new peak is around 50 kJ/mol, approximately half that of the other peaks (Table 5.1). While the origin and reaction underlying the new peak, labeled N peak, cannot

be defined with certainty based on these data, a range of reactions can be proposed. First, as the appearance of the new peak is concommittant with the disappearance of peak 1, similar reactions may underlie both peaks and be simply catalyzed by SYP. In fact, He and Riedl (2004) and he and Yan (2005) observed this new peak as a shoulder in his thermogram of a 50/50 weight % mixture of spruce and PF, which they assigned to a catalyzed substitution reaction in the PF resin.

Table 5.1 Summary of DSC features at different southern yellow pine contents.

C (%)	New Peak		Peak 1		Peak 2		Peak 3		ΔH* (J/g)	$\frac{\Delta H_{mix.}}{\Delta H_{pure}}$
	T_N (^oC)	E_N (kJ/mol)	T_1 (^oC)	E_1 (kJ/mol)	T_2 (^oC)	E_2 (kJ/mol)	T_3 (^oC)	E_3 (kJ/mol)		
0			118	99	130	85	149	98	363	1.00
20			118	97	130	80	147	95	344	0.91
35	74	42			123	82	145	93	316	0.86
50	81	51			131	85			283	0.78
70	99	48			132	85			190	0.52

C: wood content level, based on the total resin; T& E: peak temperature at 5 ^oC/min and the corresponding activation energy by the Kissinger equation, R^2>0.99; ΔH: reaction heat normalized to resin solid, average of all heating rates.

Similarly, this new peak may also represent PF condensation reactions. If this is the case, the activation energy for PF cure reactions is extensively depressed, from 99 to 50 kJ/mol by the presence of wood reaction, supporting previous reports of wood catalytic effects (Pizzi *et al*. 1994; He and Riedl 2004). The new exotherm may also

originate from a new reaction, such as wood-resin covalent bonds as hypothesized early on (Chow 1969). Indeed, Chow (1969) proposed that the activation energy for wood-resin covalent bond formation is one half that required to form a resin-resin bond, which would agree with our measurements of activation energies. With increasing wood content, the greater availability of hydroxyl groups from wood would allow greater proportions of wood-resin bonds versus resin self-condensation which is consistent with the thermograms. Finely ground wood flour provides a large surface area, upon which the PF species may adsorb facilitating their polymerization.

Interestingly, the resin heat of cure also decreases with increasing wood content (see Table 5.1), indicating in accordance with previous findings (He and Riedl 2004) that wood limits the state of full cure for PF resins. A lower state of full cure for PF resins in the presence of wood has previously been ascribed to wood imparting physical separation and lower mobility to PF species by wood absorbing water in resin, hence reducing their ability for self-condensation (He and Riedl 2004). Wood-resin reactions have also been proposed to release one fourth the heat released by PF self-condensation (Jones 1946; Chow 1969).

The catalytic effect of wood is also evident when evaluating conversion as a function of temperature during a heating scan (Figure 5.3). With increasing wood content, cure develops faster at the low degree of cure (Figure 5.3), whereas at $\alpha>0.7$ there is no difference in PF conversion with temperature between neat resin and wood/PF mixtures.

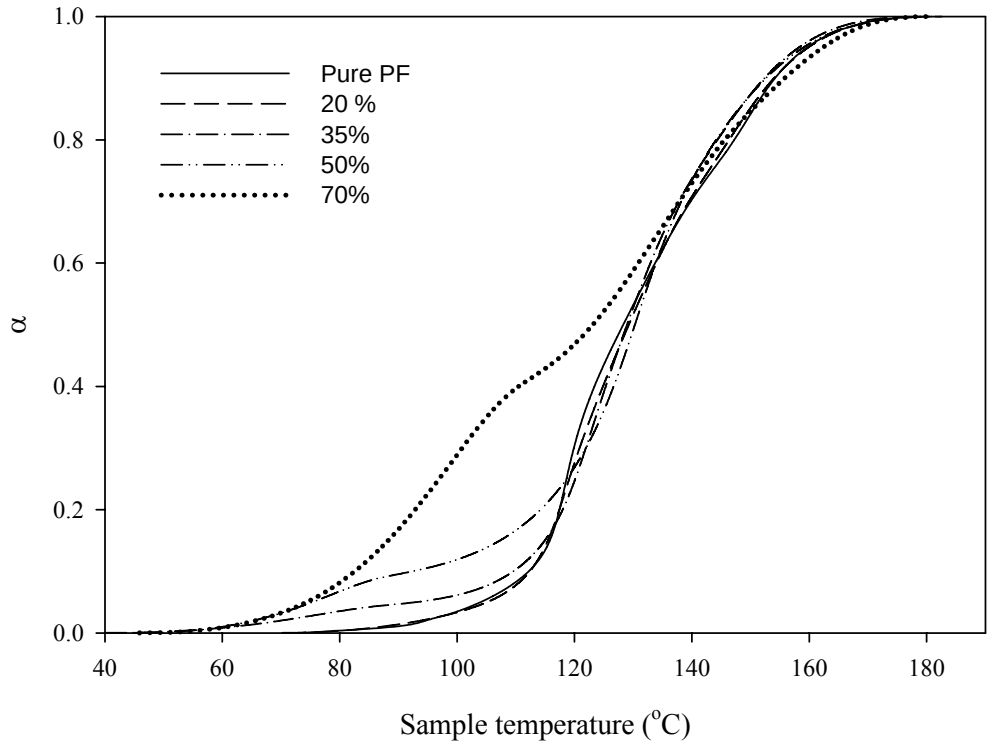

Figure 5.3 Experimental cure development of PF/southern yellow pine at various wood contents.

Table 5.2 Kinetic parameters by the nth order Borchadt-Daniels method for southern yellow pine mixtures.

C (%)	Ln A (1/s)	E (kJ/mol)	n	R^2
0	24	99	1.13	0.93
20	24	100	1.11	0.93
35	13	66	0.85	0.88
50	11	56	0.83	0.87
70	9	49	0.83	0.83

C: wood content level; A: preexponential factor; E: activation energy; n: reaction order; R^2: coefficient of determination.

Next, we turn to evaluating the information provided by the various cure kinetic models for wood/PF mixtures. With the Kissinger equation, the individual peaks are evaluated, and the presence of wood does not significantly change the activation energy of the main cure exotherms of PF resin. The Kissinger approach also allows measurement of the activation energy of the new peak, at approximately half that of the other PF reactions (Table 5.1). The ability to monitor individual exotherms is valuable when a mechanistic understanding of the cure chemistry is desired. On the other hand, the n^{th}-BD method gives a single activation energy for the overall cure process (Wang *et al*. 2006). With nth BD, a decrease in activation energy with increasing wood content from 99kJ/mol to 49 kJ/mol (Figure 5.2**)** is measured, clearly showing wood's catalytic effect, while providing no insight on the mechanistic

origins for this effect. It is noted that the preexponential factor A **(**Table 5.2**)** declines, and if this is interpreted in terms of the probability of collision of reactive species, this is consistent with the lower mobility and lower accessibility of reactive species with increasing wood content.

If a mechanistic understanding of the reactions is desired, then model free kinetics and the Vyazovkin method (Vyazovkin 1997) in particular are likely best suited for understanding the *in situ* PF resins cure (Wang *et al*. 2005). Figure 5.4 compares the activation energy changes as a function of conversion for the neat PF

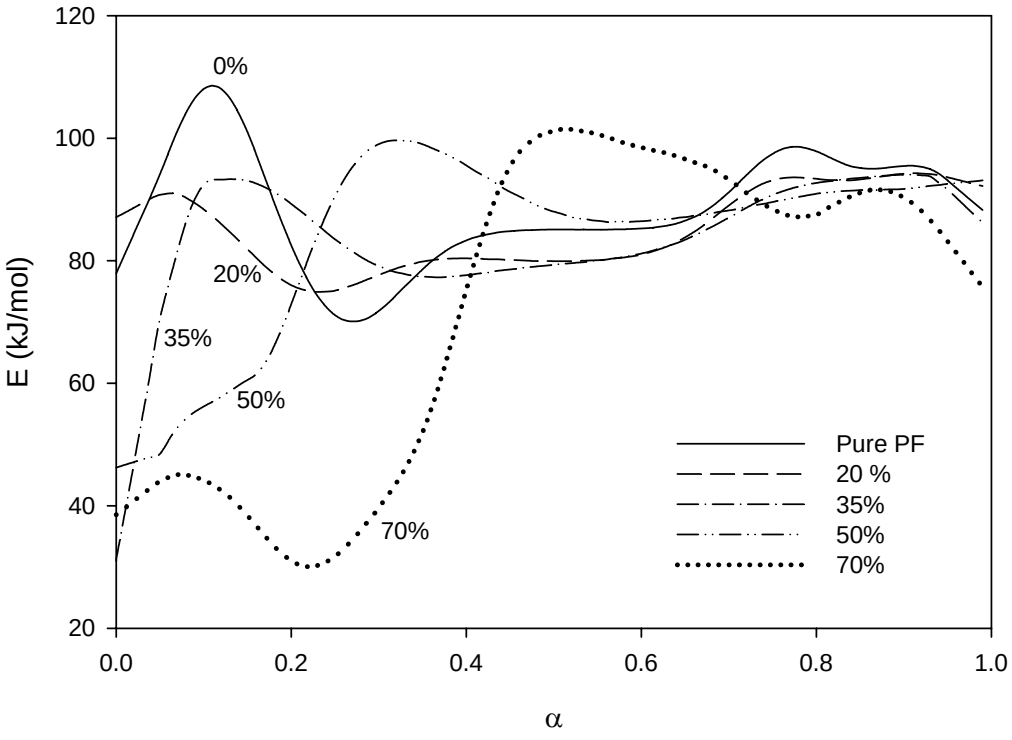

Figure 5.4 Activation energy changing patterns of PF/southern yellow pine mixtures at various wood contents by Vyazovkin method.

and the SYP/PF mixtures. The activation energy of the PF/wood mixtures follows

similar patterns to that of pure PF, albeit in the mixture, the activation energy peaks reach lower values and they are delayed at high wood content. At a conversion between 0 to 0.2, the activation energies are significantly depressed with increasing wood content. This confirms that wood catalytic effect occurs mainly at low conversions. At a higher degree of cure, however, the activation energy for all the wood/PF mixtures follow a similar trend to that of the neat PF, and the activation energy measured in all PF/ wood mixtures merge to a same value. Using the KAS algorithm, He & Riedl (2004) also reported a slower increase in activation energy for wood/PF mixture below 10% degree of cure and similar Ea at higher degrees of cure. As previously observed for neat PF resins (Wang *et al.*2005), the Vyazovkin method is more sensitive to changes in mechanisms than the KAS method, and in the case of wood/PF mixtures, differences in Ea are more marked with the Vyazovkin method. In any case, wood influence at low conversions from the Ea curves is consistent with the results from Kissinger equation, which established the influence of wood on the low temperature/ low conversion exotherm only (Table 5.1).

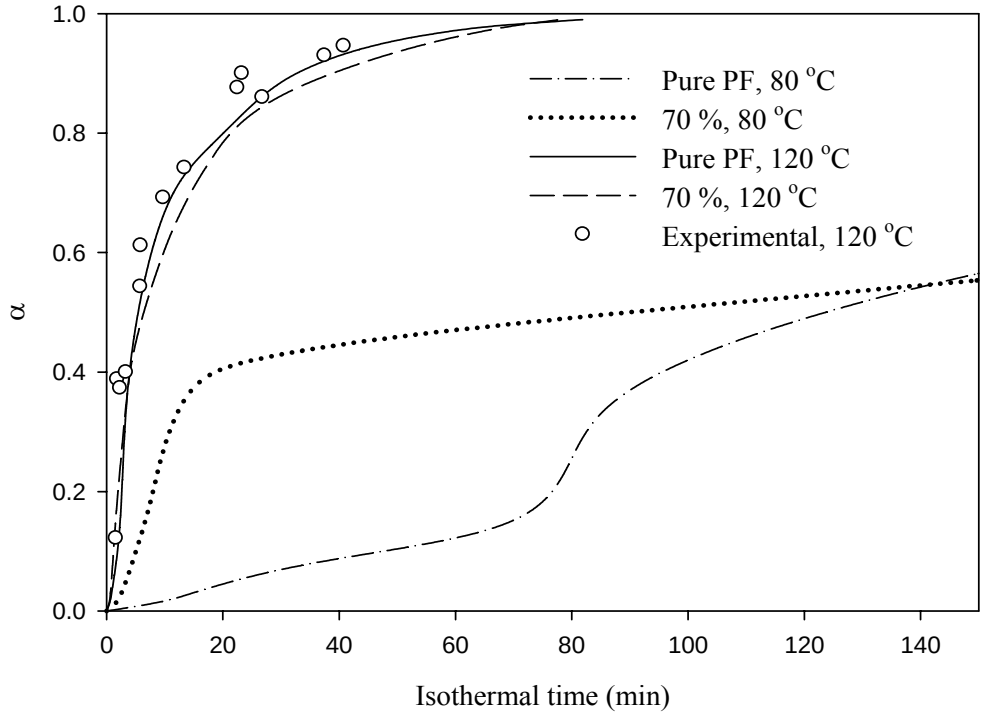

Figure 5.5 Experimental cure development of pure PF at 120 °C and model-free predictions at 120 °C and 80 °C by Vyazovkin method for pure PF and 70% PF/southern yellow pine.

Using the kinetic parameters obtained from the Vyazovkin method, the cure development of neat PF resins and wood/PF mixtures with 70% wood content have been predicted under isothermal cure conditions at 80°C and at 120 °C (Figure 5.5). Furthermore, experimental cure data for the neat resin at 120°C are plotted to demonstrate the validity of the Vyazovkin method (Wang *et al*. 2005). It is clear that at the lower cure temperature (80°C) , which is close to that of the new peak exotherm, wood influences the cure of PF resins; whereas at 120°C the wood has little impact of the cure of PF resin (Figure 5.5). Again, this is consistent with wood's influence on PF

cure, and is more prominent at low conversion and low temperature.

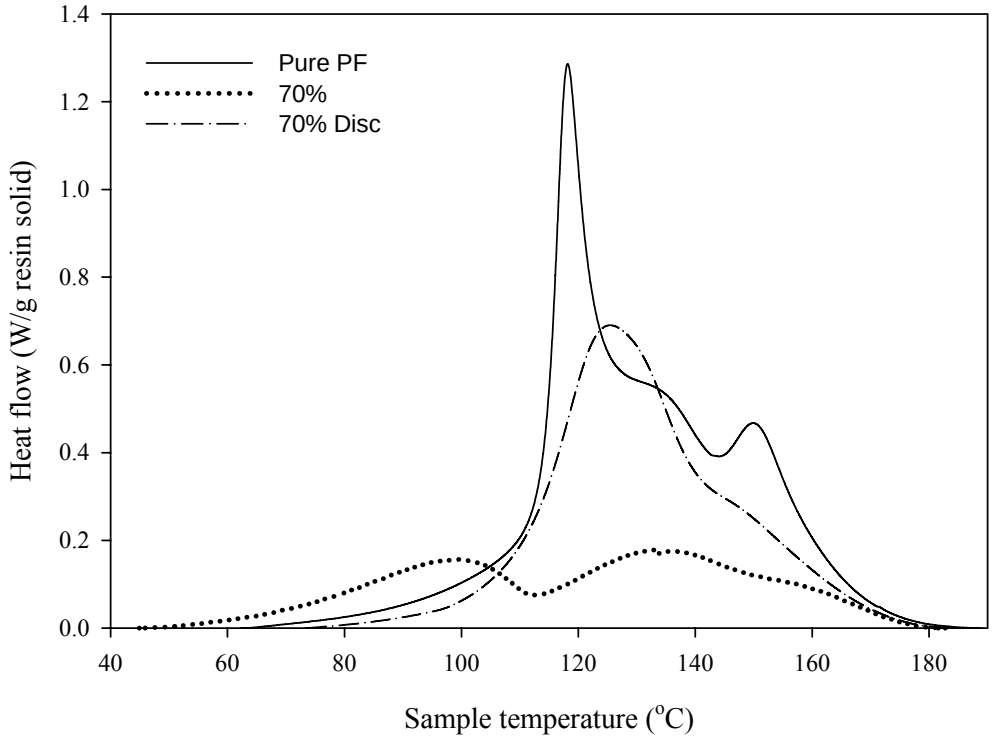

Figure 5.6 Comparison of DSC thermograms for wood particle size.

It is worthwhile to mention that PF resin is usually applied on the wood surface, and thus does not have as much contact with wood as it would in the form of powder. Similar wood content at 70% level on a small disc surface shows that wood effect on curing development is small, at a level of only about 20% wood content (Figure 5.6). To further investigate the impact of wood on PF cure and cure kinetics, the influence of wood constituents on PF cure was examined at a mixture level of 35 weight % next.

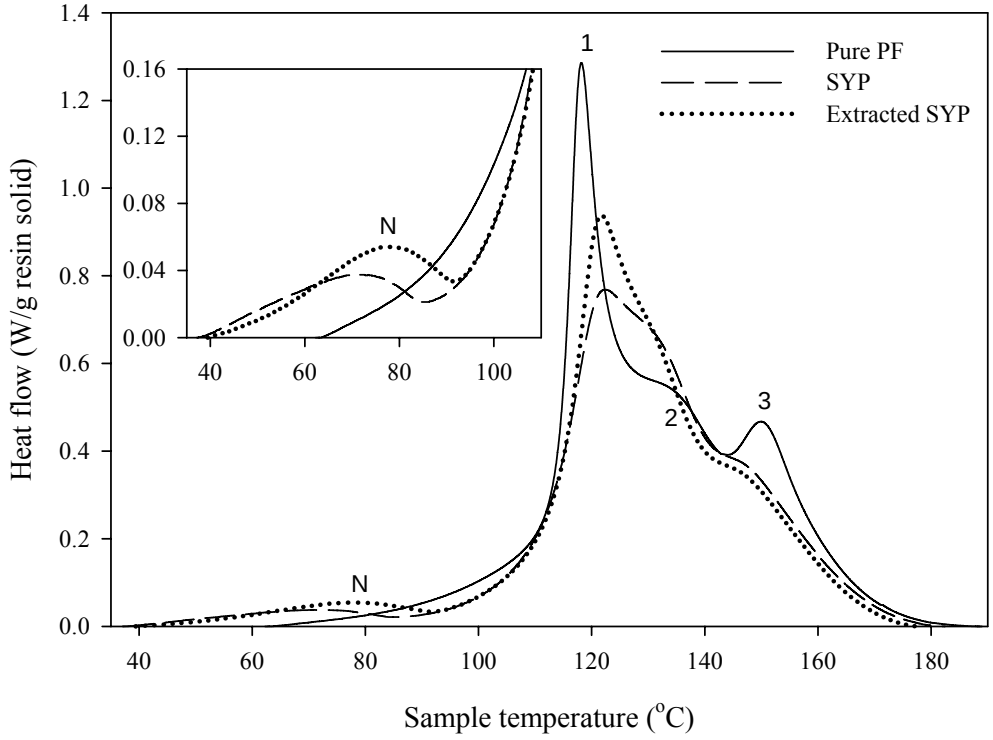

Figure 5.7 DSC thermograms of southern yellow pine (SYP) and extracted SYP/PF mixtures at 35% wood content.

Comparison among wood constituents and species

The presence of SYP and extracted SYP decreased onset cure temperatures and prompted a small peak (N peak in Figure 5.7) in a low temperature, with around 5% of total area under the new peaks (Figure 5.7**)**. The DSC curves for SYP and extracted SYP were similar, with peak temperatures differing slightly. The one-way ANOVA results and Tukey multiple comparison tests indicated no significant

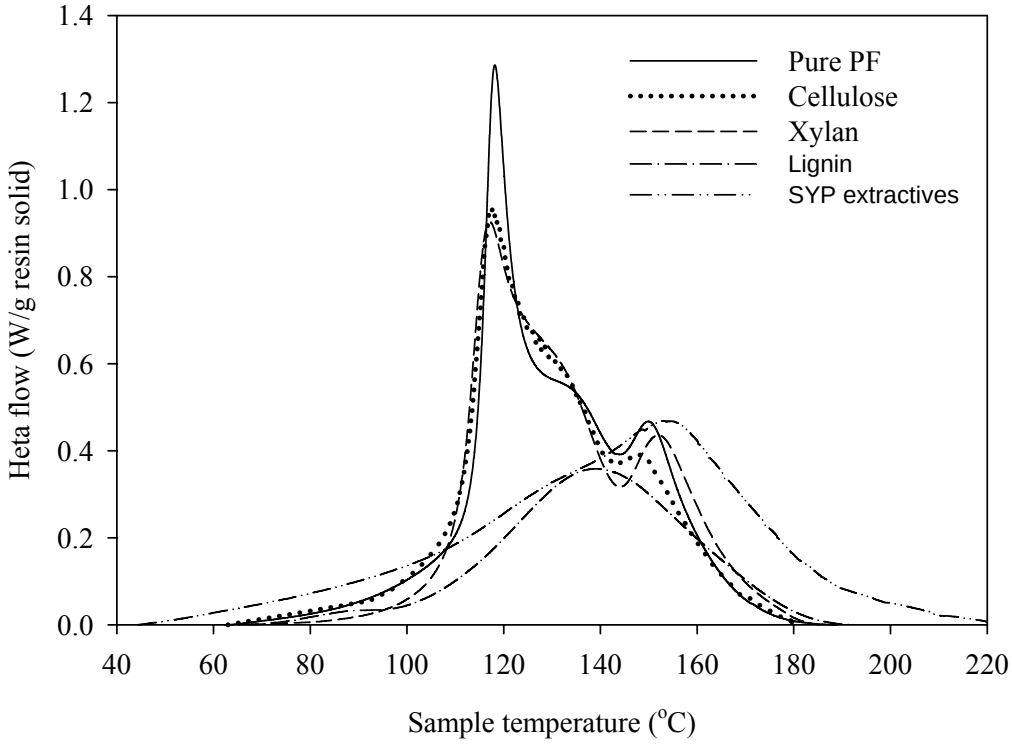

Figure 5.8 Comparison of DSC thermograms for cellulose, xylan, lignin, and SYP extractives mixtures at 35% substrate content at a linear heating rate of 5 °C/min.

difference for all three peak temperatures at 2, 5, 10, and 20˚C/min. There was also no significant different in the heat of reactions between SYP and extracted SYP. However, the area under the new small peak for the extracted SYP/PF mixture was larger than that for SYP mixture. This indicates that extraction enhanced catalytic effects. DSC thermograms of cellulose/PF and xylan/PF mixtures followed similar trends as PF alone (Figure 5.8), whereas lignin and SYP extractives changed the DSC traces (Figure 5.8). SYP extractives decreased the onset cure temperature and extended the end of the cure to a higher temperature. The cure development for the lignin mixture

follows a distinct pathway from the pure resin. Lignin has a similar onset cure temperature compared with pure PF resin, but the cessation temperature extended to a higher temperature (Figure 5.8). Like SYP and extracted SYP, a small new peak appears at a low temperature. This suggests that lignin was one of the contributors to the early catalytic effect of wood.

There is a small but significant difference with ANOVA analysis at $\alpha = 0.05$ for the heat of reaction between cellulose/PF, xylan/PF mixtures and PF alone (Table 5.3). The reduction of reaction heat may be due to a physical separation effect, which accounts for a 3% loss in heat of reaction as compared with pure PF. ANOVA analysis shows that the PF/lignin mixture released significantly less heat in reaction than any other mixtures. The extent of reduction of reaction heat cannot only be ascribed to physical separation; it may be due to interactions between the resin and lignin. The ANOVA analysis shows that there were no significant differences in the heat of reaction between SYP extractives and pure resin. The reduction in heat reaction due to physical separation by SYP extractives was compensated by reactions between PF and extractives so that the total heat of the reaction did not change. It was also envisioned that this compensation effect might come from decreased pH value due to addition of acidic extractives, which may increase the reactivity of functional groups of PF resins (He and Yan 2005). There is around 14% less heat of reaction for SYP and extracted SYP as compared with pure resin. It is assumed that around 11% reaction heat reduction was due to wood-resin interaction, since around 3% reduction can be ascribed to physical separation as indicated by the lack of catalytic paper cellulose and

xylan.

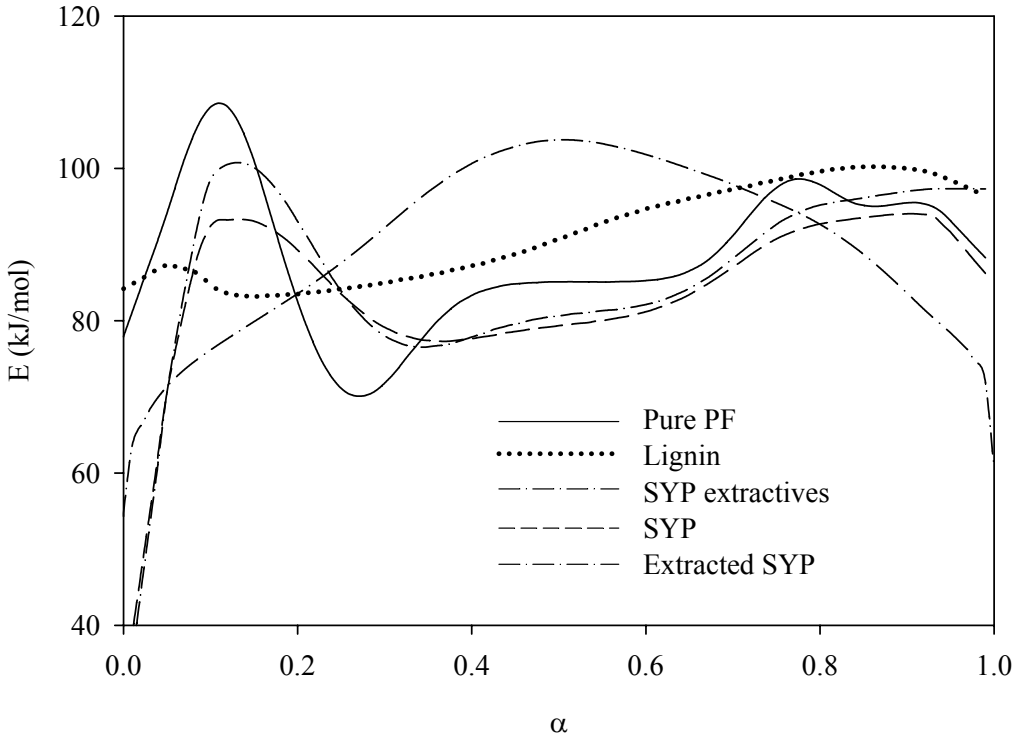

Figure 5.9 Comparison of activation energies with theVyazovkin method for southern yellow pine (SYP), extracted SYP, SYP extractives, and lignin/PF mixtures at 35% substrate content.

Table 5.3 DSC local peak temperatures (T) at 5 ^{o}C/min, activation energies (E) of the peaks by the Kissinger equation, heat of reaction (ΔH) and ratio of reaction heat to that of pure PF resin at 35% wood contents.

Mixture	New Peak		Peak 1		Peak 2		Peak 3		ΔH	$\frac{\Delta H_{mix.}}{\Delta H_{pure}}$
	T_N (˚C)	E_N (kJ/mol)	T_1 (˚C)	E_1 (kJ/mol)	T_2 (˚C)	E_2 (kJ/mol)	T_3 (˚C)	E_3 (kJ/mol)	(J/g)	
SYP	74	42			123	82	145	93	316	0.86
Extracted SYP	78	50			122	86	145	92	315	0.86
Pure resin			118	99	130	85	149	98	363	1
Cellulose			117	97	131	90	148	100	355	0.97
Xylan			117	95	131	87	152	94	353	0.97
Lignin					139	75			201	0.55
SYP Extractives					153	121			387	1.06

SYP: southern yellow pine; $R^2 \geq 0.99$ for activation energy

Table **5.3** lists the peak temperatures and corresponding activation energies calculated with the Kissinger equation for various mixtures. Cellulose and xylan do not change the peak temperature and activation energy as compared with pure PF resin. SYP and extracted SYP prompted a new peak with activation energy half of that disappeared peak 1, whereas the activation energy of main exotherms does not change significantly as compared with pure PF. Lignin decreases the activation energy, while

SYP extractives increases the activation energy. The activation energies by nth-BD are summarized in Table 5.4, supporting the thesis that wood, lignin, and extractives decreased the activation energy and catalyzed the PF curing. The model-free activation energy changing patterns are depicted as in Figure 5.9. The activation energy of cellulose and xylan mixtures follows a similar changing pattern with that of pure PF, while the model-free activation energy of SYP, extracted SYP, lignin and SYP extractives follows different patterns (Figure 5.9). These observations corroborate the thesis that cellulose and xylan contribute little to the catalytic effects of wood on PF curing, but that lignin and extractives is responsible for wood catalytic effects.

Table 5.4 Comparison of kinetic parameters by the nth order Borchadt-Daniels method for various wood/PF mixtures at 35% wood contents.

Mixture	Ln A (1/s)	E (kJ/mol)	n	R^2
SYP	13	66	0.85	0.88
Extracted SYP	14	67	0.81	0.87
Pure PF	24	99	1.13	0.93
Cellulose	23	97	1.12	0.94
Xylan	23	98	1.09	0.90
Lignin	18	82	0.99	0.94
SYP Extractives	14	71	0.82	0.91

SYP: southern yellow pine; A: preexponential factor;
E: activation energy; n: reaction order; R^2: coefficient of determination.

CONCLUSION

DSC analysis showed that the curing behavior of the PF resin did not change significantly when the wood content was below 20%. When the wood content was over 35%, wood catalyzed one reaction and moved it to the lower temperature. The cure behavior differed significantly from that of pure resin in terms of the curve shape; however, it appeared that wood substrates' effects on each individual reaction were different. An activation energy analysis for specific peaks demonstrated that the activation energy of one peak did not change with the addition of wood; thus, the cure rate could be controlled by this reaction and the cure process reached completion at the same end temperature as PF alone for various wood/PF mixtures. If conversion above 70% is of particular interest for practical application, the kinetic parameters obtained from pure resin can be used for prediction of PF/wood mixture. The wood effects were mainly in low temperature, yet when the mixtures were suddenly subjected to a high isothermal temperature, the overall effects of wood addition on cure behavior would be minor. When kinetic parameters from various mixtures by Vyazovkin method were used to predict isothermal cure behaviors, they all obtained similar predictions. The activation energy by nth-BD method decreased with wood addition and with increasing wood content.

Further investigation with the Vyazovkin method indicated that activation energy decreased only at lower conversion, and followed similar trends with PF alone at higher conversion. Moreover, the effects of wood on the curing behavior of the resins among the wood and its extracted counterparts were similar. Additionally, the

paper cellulose and hemicelluloses did not change the cure behavior of PF resin at the current studied content level, but the heat of reaction was reduced due to physical separation of PF resin molecules, while lignin and SYP extractives changed the cure development significantly. A small peak appeared in the thermograms of wood/PF and lignin/PF mixtures, supporting the idea that lignin may be the main contributor of the catalytic effect of PF curing.

REFERENCES

ASTM E2041-03 Standard Method for Estimating Kinetic Parameters by Differential Scanning Calorimeter Using the Borchardt and Daniels Method.

Barry, A. O.; Peng, W.; Riedl. B. The effect of lignin content on the cure properties of phenol formaldehyde resin as determined by differential scanning calorimetry. *Holzforschung (1993), 47*(3): 247-252.

Brent, R. P. Algorithms for minimization without derivatives. Englewood Cliff, N.J., Prentice-Hall, 1973.

Chow, S.-Z. A kinetic study of the polymerization of phenol-formaldehyde resin in the presence of cellulosic materials. *Wood Science (1969), 1*(4), 215-221.

Detlefsen W. D. In: M. Chaudhury, A.V. Pocius (Eds.), Surfaces, chemistry and applications. Elsevier: Amsterdan, (2002) pp. 869-945.

He, G., &B. Riedl (2004). Curing kinetics of phenol formaldehyde resin and wood-resin interactions in the presence of wood substrates. *Wood Science Technology 38*(1): 1432-5225.

He, G.; Yan, N. Effect of wood on the curing behavior of commercial phenolic resin systems. *Journal of Applied Polymer Science (2005), 95*(2): 185-192.

Jones, T. T. Some preliminary investigations of the phenol-formaldehyde reaction. Transaction, *Journal of Society of Chemical Industry, London (1946)*, *65*, 264-275.

Kissinger, H. E. Reaction kinetics in differential thermal analysis. *Analytical*

Chemistry (1957), 29, 1702-1706.

Kottes-Andrews, B.A.; Reinhardt, R. M.; Frick, J. G. Jr.; Bertoniere N. R. In Formaldehyde Release from Wood Products, American Chemical Society Symposium Series No. 316, (1986), Washington, DC.

Laborie, M.-P. G.; Frazier, C. E. ^{13}C CP/MAS NMR study of a wood/phenol-formaldehyde resin bondline. *Journal of Materials Science (2006), 41*(18), 6001-6005.

Mizumachi, H.; Morita, H. Activation energy of the curing reaction of phenolic resin in the presence of woods. *Wood Science (1975), 7* (3): 256-260.

Pizzi, A., Mtsweni, B.; Parsons, W. Wood-induced catalytic activation of PF adhesives. Auto-polymerization vs. PF/wood covalent bonding. *Journal of Applied Polymer Science (1994), 52* (13), 1847-56.

Prime R. B. Thermosets, In: Turi E. A., (Ed.). Thermal characterization of polymeric materials. New York: Academic Press (1997), 435–569.

Wang, J.; Laborie, M.-P. G.; Wolcott, M. P. Comparison of model-free kinetic methods for modeling the cure kinetics of commercial phenol–formaldehyde resins. *Thermochimica Acta (2005), 439*: 68–73.

Wang, J.; Laborie, M.-P. G.; Wolcott, M. P. Comparison of model-fitting kinetic methods for modeling the cure kinetics of commercial phenol–formaldehyde resins. *Journal of Applied Polymer Science (2006), accepted*.

Vyazovkin, S. Modification of the integral isoconversional method to account for variation in the activation energy. *Journal of Computational Chemistry (2001)*, *22* (2), 178-183.

Vyazovkin, S.; Sbirrazzuoli, N. Isoconversional kinetic analysis of thermally stimulated processes in polymers. *Macromolecular Rapid Communications (2006)*, 27(18), 1515-1532.

Chapter 6 Dynamic Mechanical Analyses of Phenol-formaldehyde Bonded Wood Joints

ABSTRACT

Modeling and optimizing of wood-based composite manufacture is playing a larger role in the design of processes and manufacturing equipment. In these models, internal temperature and moisture conditions are predicted with an aim towards predicting when polymeric cure is sufficient to avoid delamination. However, most cure kinetics models are focused on predicting the chemical state of the resin rather than the resulting mechanical properties. The objective of this research is to examine the feasibility of obtaining kinetic cure data using dynamic mechanical analysis (DMA). Dynamic three-point bending tests were conducted on a sandwich specimen of two wood adherends bonded with an adhesive layer. The specimen was cured using various isothermal and linear heating regimes. In addition, two commercial PF resins of different molecular weights distributions (labeled as PF-high and -low respectively) were evaluated under different experimental conditions influencing moisture loss. The results showed that the coefficient of variation for maximum storage modulus (E'_{max}) was smallest among all possible dynamic parameters and subsequently used to evaluate cure. Theoretically, the E' ratio, defined as, $R = E'_{max} / E'_{min}$ should be good parameter to evaluate bond development because it eliminates the variation in adherend modulus. However, this parameter was found to be sensitive to variables such as adhesive thickness and changes in the adherend modulus due to moisture loss

and thermal softening. The PF-low joints achieved a significantly higher E'_{max} and R as well as a lower tan δ after curing than the PF-high joints suggesting superior interphase development. The shear modulus and flexural storage modulus of the adhesive were calculated by an analytical solution. The values are in general agreement with the results obtained by parallel-plate rheometry. Overall, the sandwich beam was deemed to be simple in both sample preparation and measurement procedure for obtaining PF resin cure transitions and modulus development.

Key words: Dynamical mechanical analysis (DMA); phenol formaldehyde resins; shear modulus; storage modulus.

INTRODUCTION

The curing of thermoset resins is most typically characterized using differential scanning calorimetry (DSC) where the measurement of the energy release rate provides information for modeling the reaction kinetics. However, DSC does not provide information about the structural changes at the molecular level leading towards mechanical property development. In contrast, dynamic mechanical analysis (DMA) offers a quantitative view of the adhesion mechanics from which the glass transition, gelation, and vitrification points may be inferred (Prime 1997).

Thermosetting resins used as adhesives are usually in a fluid state at ambient temperatures. Different approaches have been used to obtain the solid specimens

suitable for DMA. First, resin samples may be cured beyond gelation prior to the DMA testing. Then the cure development and characteristic transitions of the partially cured materials can be measured (Prime 1997). However, to fully characterize the resin cure, from the fluid to solid states, necessitates the use of a support. For phenol formaldehyde (PF) resins, both an impregnated, multifilament glass braid (Steiner & Warren 1981) and a glass cloth (Kim and Nieh 1991, Follensbee *et al*. 1993)) have been investigated. A glass cloth impregnated with the PF resol was used to evaluate the effects of pre-treatment and *in situ* cure conditions on cure development (Follensbee *et al*. 1993). These supports are inert to the PF resins (Follensbee *et al*. 1993) and successfully provided information regarding the cure development for the neat resins. However, it is well established that for PF resins, cure kinetics are influenced by the presence of wood (Chow 1969, Pizzi *et al*. 1994, Wang *et al*. 2007). In addition, the adhesive/glass cloth interface is very different from the interphase formed between PF and wood (Ebewele 1995). Therefore, it is important to characterize PF cure *in situ* when seeking a realistic view of adhesive bond development. Towards this end, impregnated poplar strips (Laborie 2002) and sandwich specimens, composed of two wood strips separated by an adhesive layer (Garcia and Pizzi1998; He and Yan 2005a) have been used to study the PF cure development. A sandwich structure was favored in that the compliant adhesive layer was subjected to the maximum shear force within the specimen and thus enhancing any phase transitions (Carlier *et al*. 2001). More importantly, the sandwich geometry more closely resembles the practical application of the adhesives when compared to

impregnated specimens. As compared with a fiber glass support, wood is a hygroscopic and viscoelastic material that can display significant variation in storage modulus (E') resulting from moisture loss and thermal softening during the DMA scans that may reach 200 °C. This condition presents a challenge to interpreting the resulting DMA spectra (Follensbee *et al*. 1993).

The difference in the storage modulus (*ΔE'*) before and after cure has been used as a criterion to evaluate the effects of resin synthesis parameters (He and Yan 2005a), bio-scavengers (Kim *et al*. 2006), and catalysts (Onica *et al*. 1998) on the rigidity of PF/wood strip sandwich joints. He and Yan (2005b) realized that *ΔE'* was affected by the wood substrate and recommended that ΔE' should be normalized by minimum E'. Onica *et al*. (1998) recommended using the difference between maximum E' and that at 200 °C ($E'_{\max} - E'_{200}$) for evaluating the softening and degradation of wood-adhesive joints.

It is also worthwhile to mention that the DMA signal may be dominated by the substrate, rather the resin layer depending on the ratio of the adherend (h) to adhesive (t) thicknesses. When h/t is high, the sensitivity of the beam stiffness to the presence of adhesive layer is low. Therefore, some researchers (Starkweather & Giri 1982) have recommended a thick adhesive layer to enhance the behavior of the resin when polymer properties, not interphase behavior, are of interest. The characteristic properties associated with pure polymers may not be observed with a sandwich structure. It is important to remember that the DMA spectra should only be interpreted as the behavior of the total joint rather than that of the polymeric resin alone (Onica *et*

al. 1998).

Considerable interest exists in measuring the *in situ* shear properties of an adhesive when it is used in a bonded joint. Such measurements allow one to assess the state of the adhesive as a function of time and temperature. For example, during hot-pressing of wood-based composites, the wood-adhesive system experiences the thermodynamic and viscoelastic process of consolidation. The pressing time should be minimized to reduce energy use and production time while avoiding defects such as delamination during press opening. The *in situ* shear or flexural modulus of adhesive during cure is one of basic material parameters needed to construct a useful hot-pressing model. Adams and Weinstein (1975) provided an analytical expression to calculate the shear modulus of the adhesive in a sandwich beam. In this solution, the adherends were assumed to be thin enough that the induced axial stress can be approximated as constant along the cross section. Moussiaux *et al*. (1987) provided another analytical solution to deduce the shear modulus for similar geometry. This analysis assumed that the adhesive is constrained to a thin layer at the core of a thick, bonded structure. He *et al.* (2001) confirmed Adams and Weinstein's solution using a finite element analysis and concluded that it provided a better estimate of shear modulus than the more simplistic Moussiaux's solution. The analytical results produced significantly different values of shear modulus compared to those obtained from rheometry of neat resins evaluated in the glassy region. However, the results were in good agreements in rubbery region (He *et al*. 2001). Miyagi *et al*. (1999) found that the behavior of sandwich beam was liner viscoelastic. Consequently,

extension of the method to viscoelastic characterization of the adhesive might be possible.

OBJECTIVES

Understanding cure kinetics and property development in wood/adhesive systems is important for evaluating adhesive performance, formulating new resins, and optimizing process parameters. DMA is a commonly used analytical technique for evaluating cure development of polymer systems but has not been standardized in wood adhesion research. Therefore, the objectives of this research are to:

1. Explore improved techniques for directly evaluating wood-adhesive systems
2. Investigate the potential to use an analytical expression of sandwich specimens to estimate the i*n situ* shear modulus development of the adhesive layer during a curing process.

EXPERIMENTAL

PF resins

Two PF resole resins, tailored as adhesives for oriented strand boards, were obtained from Georgia-Pacific Company and then frozen for storage at -20°C until use. The low molecular weight resin (PF-low) had a weight-average molecular weight (M_w) of 621 g/mol and a polydispersity (M_w/M_n) of 1.41. The high molecular weight resin (PF-high) displayed an M_w = 6576 g/mol and M_w/M_n =1.72. The resin solid

contents were 54.5% and 45.0% for PF-low and PF-high respectively. In addition, elemental analysis showed the presence of 3.9 and 3.7 wt % nitrogen for PF-low and PF-high respectively, indicating the presence of urea in both systems.

Specimen preparations

Planed basswood strips (Midwest Products, Inc.) with nominal dimensions of 50x12x1 mm were oven-dried at 103 °C and stored in a desiccator over anhydrous calcium sulfate until use. Sandwich-type specimens (Figure 6.1) were produced using a layer of PF resin between two wood strips. Care was taken to match the grain, thickness, and weight of the adherend pairs within the specimen to maintain a balanced composite design. The bonding surfaces were lightly hand sanded along the grain with 220-grit sandpaper and cleaned with a paper towel immediately prior to resin application. The resin was uniformly applied to the prepared surface of both wood strips using a small airbrush (BADGER Model 350). The amount of resin solid applied to each surface was set at ca. 50 g/m^2, which equates to ca. 12% of dried wood mass.

Maintaining a consistent resin content was deemed important to repeated cure analysis. He & Yan (2005b) demonstrated that the degree of resin loading can influence the cure development. They concluded that this influenced occurred primarily through water absorption and evaporation during the DMA test. Therefore, other measures to maintain moisture content during the tests were investigated. These include (1) short open and closed assembly times in producing the specimens and (2)

foil wrapping of the specimens for the DMA analysis.

DMA and rheology

DMA measurements were conducted on the sandwich specimens in three point bending mode using either a Tritec 2000 instrument (Triton Technology) (span 25 mm) or a Rhemetric RSA II DMA (span 48 mm). The frequency was fixed at 1 Hz. Strain sweep tests have been conducted to establish the linear viscoelastic ranges at working temperature. Oscillation displacement amplitude of 0.03 mm was thus chosen for Tritec DMA and a strain of 10^{-4} for RSA II DMA. DMA was performed isothermally at 90, 100, 110, 115, 120, and 130 °C. In each test, the DMA oven was preheated to predetermined isothermal temperature, and then the specimen was installed quickly and held at the cure temperature until both modulus and damping approached a constant value signifying the completion of detectable cure. The specimen then cooled down to room temperature, and re-scan at 2 °C/min. In addition, ramp experiments were performed at heating rates of 2, 3, 4, and 5 °C/min from room temperature to 250 °C. Low heating rates were selected to make sure that the effect of thermal lag was minimal.

Rheological experiments of the uncured samples were conducted on a Rhemetric RDA III rheometer using the 25 mm parallel plates. A strain of 1% and linear heating rate at 3 °C/min from 25 to 200 °C was used.

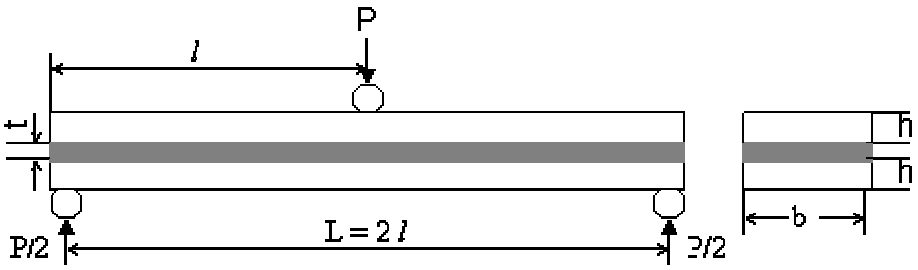

Figure 6.1 The three point bending sandwich beam, the gray adhesive layer between two wood adherends.

RESULTS AND DISCUTION

In situ shear modulus development of adhesives

An idealized sandwich specimen geometry for the three-point bending test is shown in Figure 6.1. Under the forced oscillation test used by most DMA instruments, the load (P) and mid-span deflection (Δ) of the beam are out of phase by some angle δ. The storage component of the sandwich beam stiffness is given as $C' = P'/\Delta$ where $P' = P\cos\delta$. The beam stiffness can be related to the material properties and geometric variables of the adherends and adhesive using an analytical solution analog to the static mechanic solution as following (Adams and Weinstein 1975). In this solution, we consider the dynamic stiffness properties (K) for the components and total laminate:

$K = E'_a I_a + 2E'_f I_f$; $K_T = E'_a I_a + 2E'_f I_{fa}$

These beam stiffness equations consider the storage modulus (*E'*) and moment of inertia values (*I*) of both the adhesive and adherend as represented by subscripts *a* and *f*; respectively. Separate components, the *I* for the adhesive and adherend layers can be computed as $I_a = \frac{bt^3}{12}$ and $I_f = \frac{bh^3}{12}$; respectively. Likewise, the stiffness of total bonded assembly may be computed using the fictitious variable:

$I_{fa} = \frac{bh^3}{12} + \frac{bh(t+h)^2}{4}$. From this basis, the experimentally determined values for *C'* may be related to shear storage modulus of the adhesive (*G'a*) through the following three equations:

$$C' = \frac{P'}{\Delta} = \frac{6K_T}{l^3(1+M)} \tag{44}$$

$$\gamma^2 = G_a' \left(\frac{2K + (t+h)^2 E_f' bh}{K E_f' ht} \right) \tag{45}$$

$$M = \frac{3(K_T - K)}{l^3 K \gamma^2} \left(l - \frac{\tanh \gamma l}{\gamma} \right) \tag{46}$$

Where: γ and M represents variables used to combined terms and simplify the expression without specific physical meaning. The units for γ are the reciprocal of length while M is dimensionless. Further, M will be bound by $0 \leq M \leq 3$ depending on the shear modulus of the adhesive layer as will be discussed later. Note that these equations assume that the adhesive layer is isotropic when relating the adhesive E and G using $E_a' = 2(1+\nu_a)G_a'$, where ν_a represents the Poisson's ratio of adhesive.

Equations (44) through (46) provide a means to compute the *G'a* from the experimentally determined *C'*. Modern DMA instruments such as the Tritec 2000 and Rheometric RSA II allow storage stiffness C' to be directly output as an option. The

change in C' during curing process was shown in Figure 6.2 for a typical test at a linear heating rate. In addition, a number of material properties must be assumed. In our case, a constant adhesive Poisson's ratio of ν_a= 0.35 and wood flexural storage modulus E_f = 9000 MPa at 12% MC (Wood handbook) were used. For any specific specimen, the geometric variables (*L*, *b*, *h*, and *t*) are measured. With these known variables, K and K_T can then be computed. Finally, $G_a^{'}$ is solved using a reverse interpolation process implemented to avoid iterations. First, an assumed vector of $\overline{G}_a'$ was created (e.g. $\overline{G}_a'$ = [1, 100, 200,…, 10^8] Pa). Then, the correspond vectors $\bar{\gamma}$, $\overline{M}$, and $\overline{C}'$ were computed by sequential substitution into Eq. (45), (46), and (44), thereby, producing a one to one mapping between values of $G_a^{'}$ and C'. Finally, the corresponding $G_a^{'}$ value for each measured C' from a scan was determined using the interpolation function within Matlab and the previously established $\overline{G}_a'$ and $\overline{C}'$ vectors. The calculated $G_a^{'}$ values for a representative specimen are shown in Figure 6.2. Note that $G_a^{'}$ follows the same trend as C' but has a slight difference in the slope at the beginning and final stages.

The calculated value for $G_a^{'}$ for this specific test changes from 0.01 to 11 MPa during curing process for a foil-wrapping wood joint bonded with PF-high resin. This range is in general agreement with experimental data collected with a parallel-plate rheometer using the same linear heating rate, however differences exist (Figure 6.3). Before the onset of the curing process, both techniques determined that $G_a^{'}$ decreased with temperature. However, the decrease in $G_a^{'}$ determined with DMA was much more pronounced than that determined using the rheometer. Recall that the

beam solutions assume that the adherend modulus is constant throughout the test. The softening that occurs in the wood substrate is, therefore, combined with the resin softening. In contrast, the rheometer showed difficulty in determining a consistent value for $G_a^{'}$ for temperatures following vitrification. The latter difficulty is consistent with observations by others (Mekernd 1998) Both Laza *et al*. (2002), and Peng and Riedl (1994) also reported a similar range of $G_a^{'}$ for a PF resin using paralle-plate rheology. In addition, Dean *et al*. (2005) has showed that the $G_a^{'}$ changes from 10^{-6} to 1 MPa for epoxy resins during curing at 150 °C (lager than its fully cured T_g). These reported values are of the same order with the calculated storage shear modulus of PF resin here and lend credibility to the results.

Figure 6.4 depicts a comparison of the $G_a^{'}$ development calculated from wood joints bonded with PF-low and PF-high resin and cured at an isothermal temperature of 120 °C. The $G_a^{'}$ of the PF-low resin develops more slowly and reached a higher value than that of the PF-high bonded wood joint. The bulk shear modulus of the fully cured PF resin was reported to be 209.9 MPa at room temperature (Lee and Wu 2003), which is an order of magnitude higher than that calculated here by DMA. The discrepancy might be explained by the fact that the DMA measures the *in situ* shear modulus under the effects of the elevated temperature and somewhere near or in the rubbery state. Using torsion tests on fully cured expoxy resin, Dean *et al*. 2005 found that the shear modulus decreased from 1800 to 5 MPa while passing through the glass to rubbery transition. He *et al*. (2001) found that the shear modulus calculated with the Adams and Weinstein's Eq. (44) was in agreement with the bulk shear modulus

obtained using torsion when the resin is in rubber state. However, the negligible contribution of the adhesive layer to the beam stiffness in the glass state (i.e. dC'/dG_a' is very small) places doubt on the calculation (He *et al*. 2001).

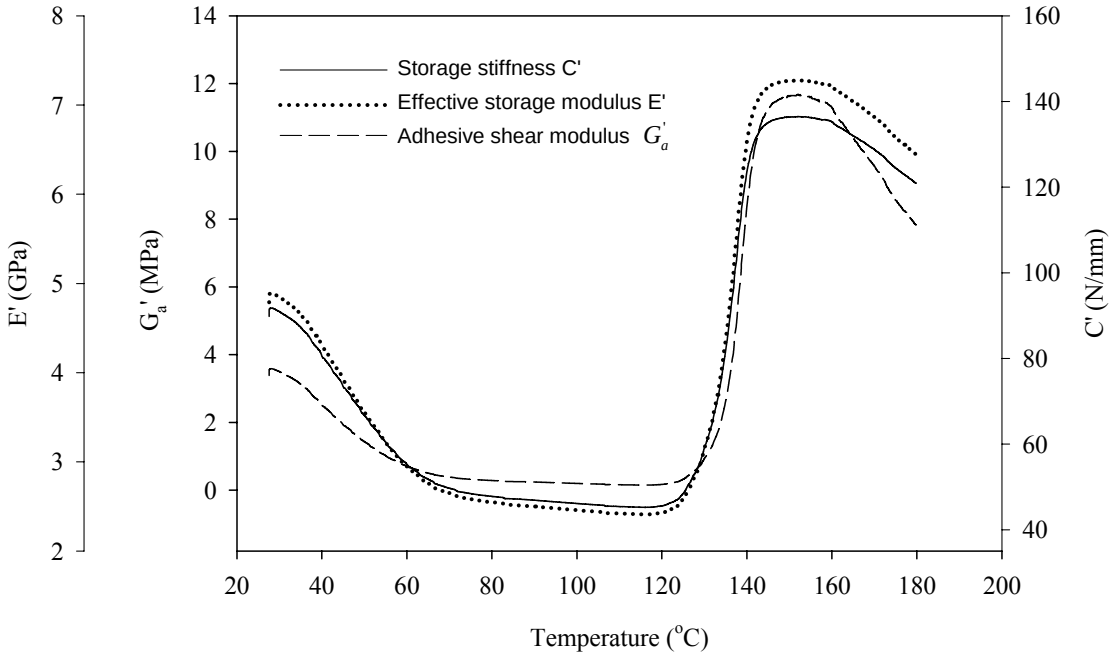

Figure 6.2 A typical of DMA output. Effective storage modulus (E') and storage stiffness (C') changes with temperature during curing at 3 °C/min for a foil wrapped PF-high bonded wood joint. Shear modulus of the adhesive layer (G_a') was calculated with an analytical solution from C'.

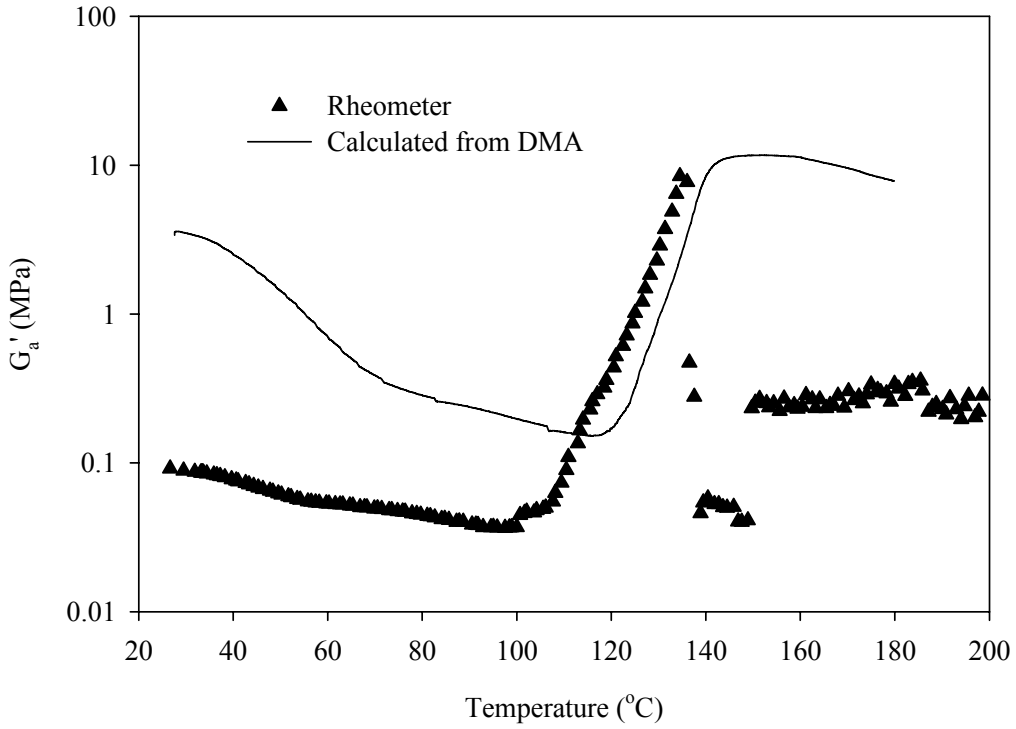

Figure 6.3 Comparison of shear storage modulus ($G_a^{'}$) calculated from DMA and experimental data from a rheometer at 3 °C /min.

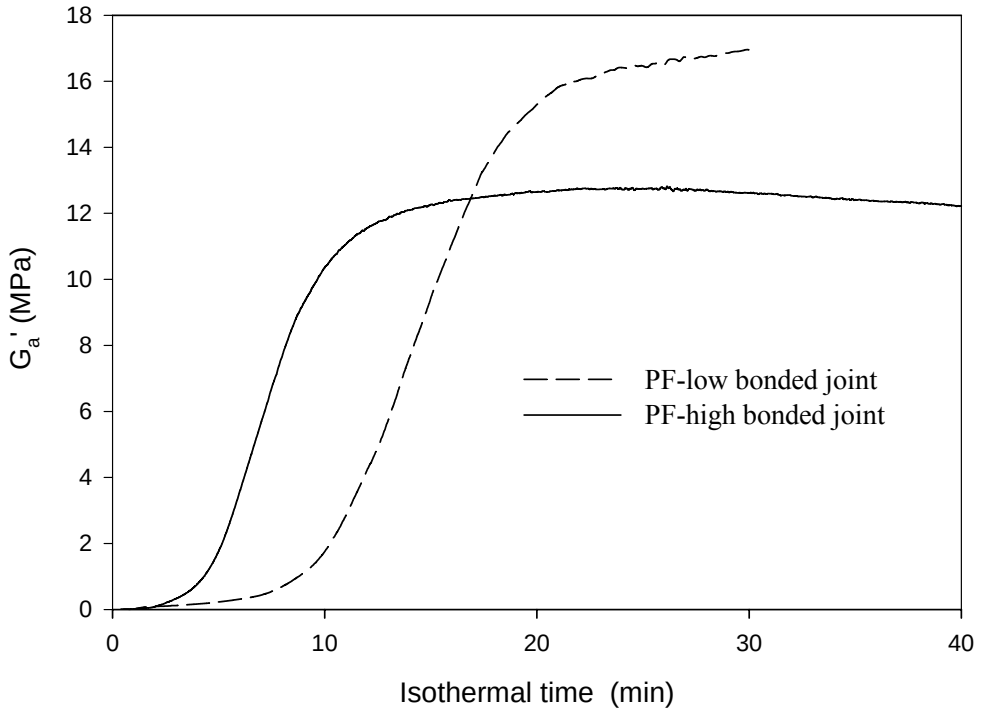

Figure 6.4 Comparison of calculated $G_a^{'}$ for PF-low and PF-high bonded wood joints at isothermal temperature 120 °C.

Theoretical limits of the ratio $R = E'_{\max} / E'_{\min}$ of PF bonded joints

The accuracy of shear modulus calculation depends on the accuracy of estimating material properties and the sensitivity of the analysis to geometric variables. For instance, the wood modulus is affected by changes in moisture content and temperature during thermal scanning. In addition, the Poisson ratio of the PF resin is expected to change during curing process where it experiences the sol, gelation, and vitrification stages. Finally, there are uncertainties in measuring the adhesive because the layer undergoes severe physical and morphological changes. Hence, the calculated

shear modulus as mentioned above is merely an estimate of the interfacial shear modulus in the specimen.

During the curing process, the shear modulus changes from a minimum to a maximum as it passes from a sol to vitrified state. Let us investigate the two extreme cases of the resin in the lowest and highest shear modulus states. When the resin softens to a minimum viscosity before curing, the sandwich beam behaves as three individual beams bending about their own neutral axes, i.e. $G_a^{'}$ approaches zero. In this case, the variable M in Eq. (44) approaches 3 if thickness of the adhesive layer is small (Figure 6.5). This point with minimum shear modulus is referred with subscript 0. Hence, Eq. (44) can be simplified as following:

$$C_0^{'} = \frac{6(E_{a0}^{'} I_a + 2E_{f0}^{'} I_{fa})}{4l^3} \tag{47}$$

In contrast, when the shear modulus of the fully cured approaches a large value (i.e. comparable to that of the adherend) then M approaches zero (Figure 6.5) and the shear deformation of the bonded layer becomes negligible. The point of minimum shear deformaton is referenced with a subscript ∞. In this case, Eq. (44) can be simplified as following:

$$C_\infty^{'} = \frac{6(E_{a\infty}^{'} I_a + 2E_{f\infty}^{'} I_{fa})}{l^3} \tag{48}$$

Now, when h/t is high and $E_f^{'} I_f >> E_a^{'} I_a$, then $I_{fa} \approx bh^3 / 4$, i.e. assuming that the adhesive layer is in a state of pure shear and the contribution of adhesive bending to the total beam stiffness is negligible. Hence, Eqs. (47) and (48) become:

$$E_{f0}^{'} = \frac{P_0^{'} L^3}{48\Delta_0 \frac{2bh^3}{12}} = \frac{P_0^{'} L^3}{48\Delta_0 2I_f} \tag{49}$$

$$E_{f\infty}^{'} = \frac{P_\infty^{'} L^3}{48\Delta_\infty \frac{8bh^3}{12}} = \frac{P_\infty^{'} L^3}{48\Delta_\infty 8I_f} \tag{50}$$

Note that Eq. (49) indicates that when the adhesive shear modulus is very low and the h/t is large, the sandwich beam can be treated as two separate homogenous beams bending about their own axes. Consequently, the total flexural rigidity of sandwich beam can be reasonably approximated by the sum of flexural rigidities for the two adherends. Note also that Eq. (50) indicates that when the adhesive modulus is comparable to that of the adherend, the total flexural rigidity of the beam converges to the pure bending rigidity of the beam treating two adherends as a homogeneous beam, since the shear deformation of the bonded layer becomes negligible.

For metals and other composites whose modulus is not influenced by moisture and temperature, $E_{f0}^{'} = E_{f\infty}^{'}$. That is saying that the flexural storage modulus should not change during the curing process. However, DMA uses the simple beam theory treating the three-layer sandwich structure as a solid homogeneous beam without including the contribution of the shear deformation in the adhesive. The result is an

effective or nominal flexural modulus $E_0^{'}$ when the shear modulus of the adhesive is in minimum:

$$E_0^{'} = \frac{P_0 L^3}{48\Delta_0 \frac{8bh^3}{12}} \tag{51}$$

Comparing Eqs (49) and (51) we can deduce that the calculated effective shear modulus of the sandwich beam when the resin is at its lowest shear modulus is one fourth of its cured state ($E_0^{'} = E_{f0}^{'} / 4 = E_{f\infty}^{'} / 4$). This finding leads to the theoretical conclusion that the ratio of the un-cured to cured modulus ($R = E'_{t=0} / E'_{t=\infty}$) would be the most effective parameter to monitor for cure because this variable would eliminate variability in the adherend properties. However, this assumption is only valid if the storage modulus of the adherends does not change during curing process.

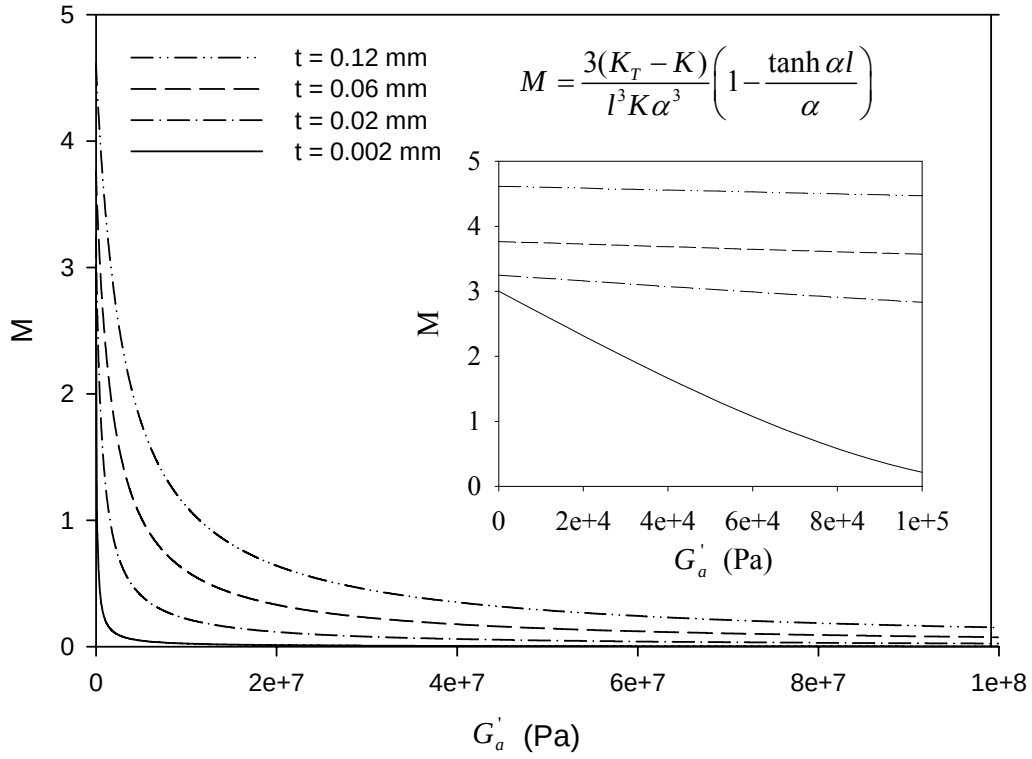

Figure 6.5 The effects of thickness of the adhesive layer on the item M.

Optimizating DMA derived parameters for directly evaluating a wood-adhesive systems

In Figure 6.6**a**, two sandwich cure scan are depicted to show the ideal case where R ≈ 4 for both a PF-high and –low resin system. For cases where the bond formation is deficient, 1 < R < 4. Experimentally determined values for R of 129 specimens in three categories (PF-low, PF-high and foil wrapped PF-high bonded wood joints) are shown in Figure 6.6c. For these specimens 72 percent fell into the range of 2.5 < R < 4, for 11 percent samples, R < 2.5, and for the remaining 17 percent R > 4.

We speculate that some specimens may produce an $R > 4$ because the assumption that adherend properties remain constant throughout the test is violated. To investigate this hypothesis, a sample of overlapping wood adherends conditioned to 12% MC and lacking in PF-resin was scanned with the results shown in Figure 6.6**a**. Note that the modulus increased for temperatures less than 120°C and then decreased somewhat for higher temperatures. It is likely that moisture evaporation resulted in the initial stiffening while thermal softening prevailed after the wood had dried. Whatever the exact mechanism, it is clear that the adherend stiffness changes during the test and that it results in a higher value at completion. Assuming that the wood completely dries during the test, the ration of the modulus in the dry and wet states could reach 1.5. Following this reasoning, the flexural rigidity in the cured state could be $8E_{fd}I_f$ and compared to $2E_{fw}I_f$ before curing; resulting in an $R \leq 6$ ($8E_{fd}/2E_{fw} = 6$). It is likely that even with specimens where $R < 4$ the results may be biased by a portion of modulus increment resulting from moisture loss and not simply adhesion effects.

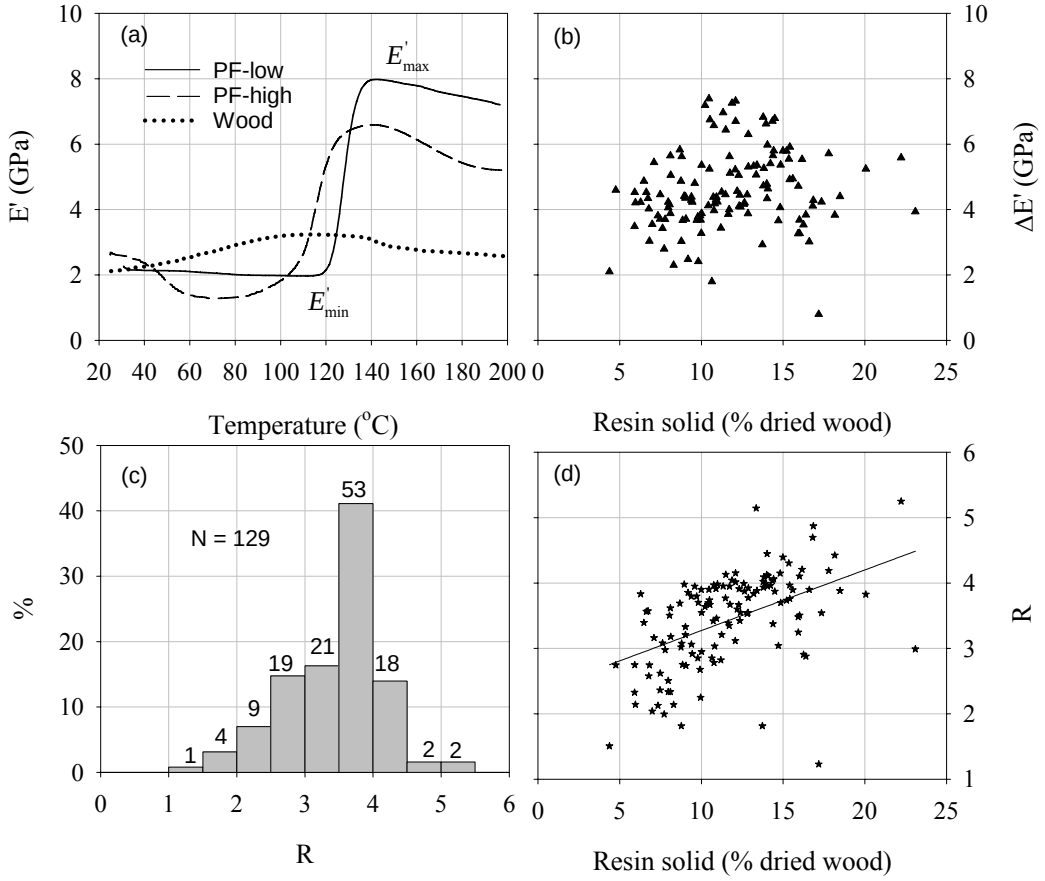

Figure 6.6 Summary of effective storage modulus (E') development with all three kinds of samples together. (a) Typical E' development for PF-low and PF-high bonded wood joints and double pieces of wood at MC of 12%, (b) $\Delta E' = E'_{max} - E'_{min}$ versus resin loads, (c) the histogram of $R = E'_{max} / E'_{min}$, and (d) R versus resin loads.

In bonded wood products, mechanical testing of the cured glueline is used to determine the quality of adhesive cure and the effectiveness of the wood-adhesive interaction. Since DMA can record thermal and viscoelastic properties simultaneously during the curing process, it has advantages to provide not only cure kinetics but also

mechanical performance of the entire adhesive joint. In Table 6.1**,** the average E'_{max}, E'_{min}, $\Delta E'$, and R values for specimens cured at heating rates from 2 to 5 °C /min and isothermal temperatures 90-130 °C are presented. In each category, the coefficient of variation (CV) for resin load is larger than those for mechanical properties, which suggests that E' is relatively insensitive to the resin load. Among the derived E' parameters, the CV is largest for E'_{min}. However, variations of resin loads and preparations parameters (e.g. open and close assembling time before the DMA test) were observed to produce a relatively larger CV for E'_{min}. Lower resin load and longer assembling time seem to result in a larger value of E'_{min}. R and ΔE' inherited this variation although the variations appears less than that of E'_{min}. The CV for the ratio R was slightly smaller than that for ΔE'. The CV reduced to a maximum extent for E'_{max} and it indicated that E'_{max} was not as sensitive to resin load and preparations as other parameters. DMA was used as an analytical tool for evaluating the effectiveness of formulations or the performance of wood-adhesive systems (Garcia and Pizzi1998; He and Yan 2005a). In these cases, one parameter is prefered for directly evaluating the joint performance, it could be E'_{max}. In addition, the E'_{max} and loss factor tan δ reflect the final product performance, substantiating their use for evaluating product quality. In contrast, the other parameters are mainly related to the process and might be used for optimizing the cure process. There was no doubt that the modulus of the bonded wood joints determined by DMA was related to the modulus of wood substrate. If the effects of wood species on adhesive performance need to be evaluated, the ratio R is likely to be a good choice since the parameter

corrected on wood modulus and has a theoretical value approaching 4 if sandwich structure is used.

Comparison of PF-high and PF-low performance

The results of an analysis of variance (ANOVA) demonstrated a significant difference ($\alpha = 0.05$) among the means of E'_{max} for the two resins evaluated. The PF-Low bonded wood joints resulted in a higher E'_{max} and lower damping coefficient tan δ than those produced with the PF-High resin. Two types of DMA (Tritec 2000 and Rheometrics RSA II) were used and similar conclusions were obtained (Table 6.1). Conducting a second scan of the cured specimens further confirmed that PF-low bonded joints possessed a higher E' and lower damping tan δ than PF-high bonded joints, whereas the joints with both resins displayed a lower E' and higher tan δ as compared with the solid wood (Figure 6.7). There was no significant difference among levels of resin load for the PF-high or PF-low bonded wood joints. However, the average thickness of adhesive layer for PF-low bonded wood joints is 0.02 mm while it is 0.06 mm for PF-high bonded wood joints. This observation suggests that PF-low resin penetrates significantly into the wood structrue as compared with PF-high. Laborie *et al*. (2006) has hypothesized that low molecular weight PF can penetrate into cell wall to possibly form interpenetrating network with lignin and increase intermolecular cooperativity and relaxation time. This concept is in agreement with the higher E' and lower damping for the PF-low found in this research. It was also observed during the application of resin by the air brush where the PF-Low

was easily air-atomized and uniformly formed a layer on the wood surface as compared with PF-high. It appears that the high molecular weight of the PF-High detracted from good wetting and distribution on the wood surface as compared with PF-Low. It was noted that PF-Low bonded wood joints maintained a minimum E' plateau longer than PF-high either in linear or isothermal heating rate, which was beneficial for wetting the wood surface and forming good interphase. Wrapping with aluminum foil also increased slightly the E' and tan δ since wrapping film did not integrate with wood perfectly.

Table 6.1 Summary of average E'_{max} and E'_{min} as well as their ratio R and difference $\Delta E' = E'_{max} - E'_{min}$ under isothermal and ramp heating regimes with coefficient of variation in parenthesis.

		Resin Load (%)	E'_{max} (GPa)	E'_{min} (GPa)	R	ΔE' (GPa)	Min. Tan δ
Triton 2000	PF-high Foil Iso	9.50 (32)	7.04 (10)	2.07 (15)	3.43 (11)	4.96 (12)	0.051 (14)
	PF-high Iso	12.95 (23)	5.32 (21)	1.40 (24)	3.85 (13)	3.93 (22)	0.037 (11)
	PF-low Iso	12.11 (16)	8.65 (12)	2.29 (12)	3.82 (7)	6.38 (13)	0.025 (15)
	PF-high Foil ramp	9.36 (33)	6.38 (13)	2.55 (21)	2.55 (13)	3.83 (13)	0.057 (15)
	PF-high ramp	13.28 (33)	5.64 (13)	2.05 (44)	3.13 (31)	3.59 (26)	0.041 (17)
	PF-low ramp	14.18 (16)	7.58 (8)	1.95 (11)	3.92 (7)	5.64 (8)	0.030 (11)
RSA II	PF-high ramp	9.35 (22)	5.43 (15)	1.55 (19)	3.56 (11)	3.88 (16)	0.046 (27)
	PF-low ramp	9.32 (32)	6.47 (7)	1.84 (23)	3.61 (14)	4.63 (15)	0.034 (14)

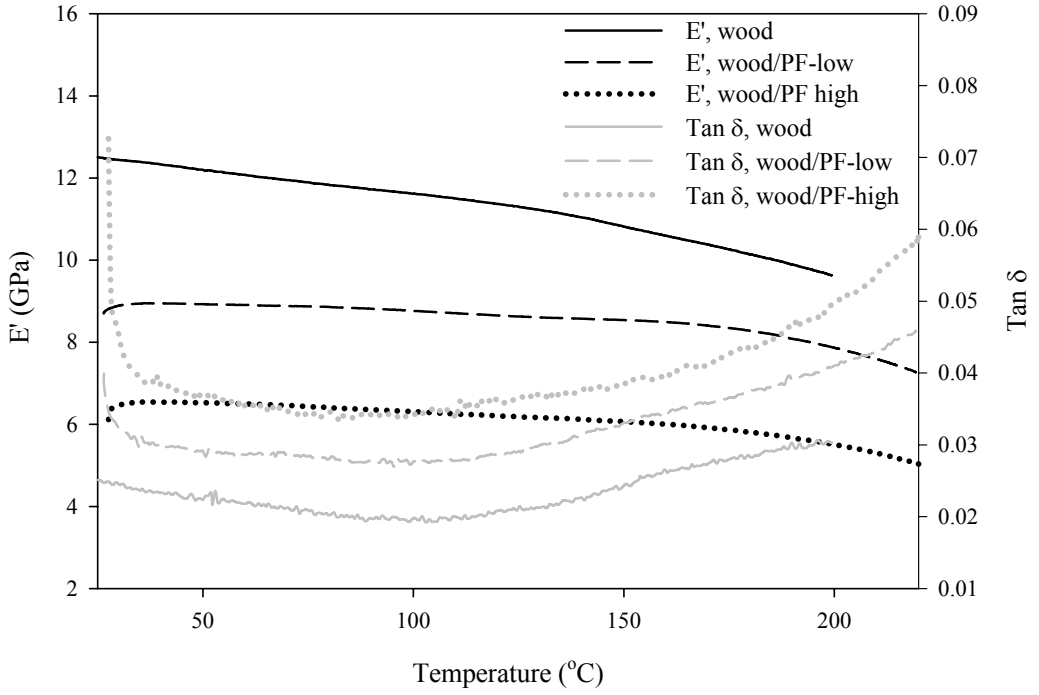

Figure 6.7 Comparison of E' and tan δ changing with temperature for cured PF bonded wood joints at 2 °C /min. Wood was scanned at oven-dried.

CONCLUSION

The experiment involved measuring the bending stiffness of the sandwich beam using DMA under linear and isothermal heating regimes, and combining an analytical solution to determine the *in situ* shear modulus of the adhesive. The *in situ* shear modulus of the PF resins changed from 0.01 to around 16 MPa during curing process and was typical of the rubber range for polymers. The measured value was in general agreement with results independently produced by parallel-plate rheometry. In

practice, the DMA test was much easier to execute than the rheology test for PF resols since water vaporization induced a large shrinkage and non-uniform curing under the parallel plate, especially in later stage of curing process. Although the combined use of a sandwich specimen and an analytical solution to measure shear modulus development during curing of an adhesive layer is simple for both sample preparation and measurement procedure, the sensitivity of the technique is unknown. Further research should be conducted to explore the effects of experimental variables on the calculation of shear modulus.

During a DMA test of a wood-PF sandwich beam, the effective modulus E' was calculated by the instrument under assumption of a homogeneous beam throughout the curing process. Therefore the ratio of the maximum to minimum E' (R) approaches a value of 4 in two extreme cases when the shear modulus is negligible before curing and is comparable to the adherends after curing. Experimentally, a large portion of measured values for R was near 4. The fact that the modulus of wood adherend increased from moisture lost during the test accounted for the large values of R in excess of 4. The difficulty of accurately maintaining or measuring sample dimensions during curing process further affected accuracy of determining R. Despite these uncertainties, the ratio, R, can be used as a parameter to direct evaluation of wood adhesive system performance. Further, variation for the maximum E' was smallest among all possible parameters derived from DMA E' curves. Hence, this parameter was deemed best for direct evaluation of wood-adhesive systems as compared with ΔE' since minimum E' was a parameter of cure process and subjected

to a variety of source of variations. It was noted that maximum E' was highly related to the modulus of the wood substrate. Hence, for evaluating the effects of wood species on wood-adhesive system, the ratio of maximum to minimum was recommended which had a theoretical value of 4.

DMA curves showed that the PF-low bonded wood joints cured slower and achieved a higher maximum E' and a lower magnitude of tan δ than those of PF-high bonded wood joints. With similar resin load and small applied force, the PF-low formed a very thin bond layer as compared with PF-high, suggesting a good interphase responding for good stiffness and low viscoelasticity for cured PF-low wood joints.

REFERENCES

Adams, R. D.; Weinstein, A. S. Flexural stiffness of sandwich beams. *Journal of Engineering Materials and Technology (1975), 97*(3), 264-270.

Carlier, V.; Sclavons, M.; Legras, R. Supported dynamic mechanical thermal analysis : an easy, powerful and very sensitive technique to assess thermal properties of polymer, coating and even nanocoating. *Polymer (2001), 42*(12), 5327-5335.

Chow, S.-Z. A kinetic study of the polymerization of phenol-formaldehyde resin in the presence of cellulosic materials. *Wood Science (1969), 1*(4), 215-221.

Dean, D.; Walker, R.; Theodore, M.; Hampton, E.; Nyairo, E.; Chemorheology and properties of epoxy/layered silicate nanocomposites. *Polymer (2006)*, Article in press, www.elsevier.com/locate/polymer

Ebewele, R. O. Differential scanning calorimetry and dynamic mechanical analysis of amine-modified urea-formaldehyde adhesives. *Journal of Applied Polymer Science (1995), 58*(10), 1689-1700.

Follensbee, R. A.; Koutsky, J. A.; Christiansen, A. W.; Myers, G. E.; Geimer, R. L. Development of dynamic mechanical methods to characterize the cure state of phenolic resole resins. *Journal of Applied Polymer Science (1993), 47*(8), 1481-1496.

Garcia, R.; Pizzi, A. Crosslinked and entanglement networks in thermomechanical analysis of polycondensation resins. *Journal of Applied Polymer Science (1998), 70*(6), 1111-1119.

He, J.; Chiang, M. Y. M.; Hunston, D. L. Assessment of sandwich beam in three-point bending for measuring adhesive shear modulus. *Journal of Engineering Materials and Technology (2001), 123*(7), 322-328.

He, G.; Yan, N. Influence of the synthesis conditions on the curing behavior of phenol-urea-formaldehyde resol resins. Journal of Applied Polymer Science (2005a), 95(6), 1368-1375.

He, G.; Yan, N. Effect of wood species and molecular weight of phenolic resins on curing behavior and bonding development. *Holzforschung (2005b), 59*(6), 635-640.

Kim, M. G.; Nieh, W. L.-S.; Meacham, R. M. Study on the curing of phenol - formaldehyde resol resins by dynamic mechanical analysis. *Industrial & Engineering Chemistry Research (1991), 30*(4), 798-803.

Kim, S.; Kim, H.-J.; Kim, H.-S.; Lee, H. H. Effect of bio-scavengers on the curing behavior and bonding properties of melamine-formaldehyde resins. *Macromolecular Materials and Engineering (2006), 291*(9), 1027-1034.

Laborie, M.-P. G. Investigation of the morphology of the wood/phenol-formaldehyde adhesive interphase. Doctoral dissertation, Virginia Polytechnic Institute and State University, (2002), Blacksburg, VA.

Laborie, Marie-Pierre G.; Salmen, Lennart; Frazier, Charles E. A morphological study of the wood /phenol-formaldehyde adhesive interphase. *Journal of Adhesion Science and Technology (2006), 20*(8), 729-741.

Laza, J. M.; Vilas, J. L.; Rodriguez, M.; Garay, M. T.; Mijangos, F.; Leon, L. M. Analysis of the Crosslinking Process of a Phenolic Resin by Thermal Scanning Rheometry. Journal of Applied Polymer Science (2002), 83, 57–65.

Lee, J. N.; Wu, Q. Continuum modeling of engineering constants of oriented strandboard. *Wood and Fiber Science (2003), 35*(1), 24-40.

Miyagi, Z.; Zaghi, S.; Hunston, D.; Brinson, H. The sandwich bending specimen for characterizing adhesive properties. *Proceedings of the Annual Meeting of the Adhesion Society (1999),* 22nd, 119-121

Moussiaux, E., Brinson, H. F.; Cardon, A. H., Bending of a bonded beam as a test

method for adhesive properties. In Mechanical behavior of adhesive joints, A. H. Cardon and G. Verchery, Eds. (Pluralis, Paris, 1987), pp. 3-25.

Onica, L.; Bucur, V.; Ansell, M. P.; Pizzi, A.; Deglise, X.; Merlin, A. Dynamic thermomechanical analysis as a control technique for thermoset bonding of wood joints. *International Journal of Adhesion and Adhesives (1998), 18*(2), 89-94.

Peng, W.; Riedl, B. The chemorheology of phenol-formaldehyde thermoset resin and mixtures of the resin with lignin fillers. *Polymer (1994), 35*(6), 1280-1286.

Pizzi, A.; Mtsweni, B.; Parsons, W. Wood-induced catalytic activation of PF adhesives. Auto-polymerization vs. PF/wood covalent bonding. *Journal of Applied Polymer Science (1994), 52*(13), 1847-1856

Prime, R. B. Thermosets. In: Turi E.A, editor. Thermal characterization of polymeric materials. New York: Academic Press, (1997), 435–569.

Starkweather, H. W., Jr.; Giri, M. R. Use of a dynamic mechanical analyzer to study supported polymers. *Journal of Applied Polymer Science (1982), 27*(4), 1243-1248.

Steiner P.R.; Warren, S. R. Rheology of Wood-Adhesive Cure by Torsional Braid Analysis, *Holzforschung (1981), 35* (6) 273-278.

Wang, J.; Laborie, M.-P. G.; Wolcott, M. P. Comparison of model-free kinetic methods for modeling the cure kinetics of commercial phenol-formaldehyde resins. *Thermochimica Acta (2005), 439*(1-2), 68-73.

Wang, J.; Laborie, M.-P. G.; Wolcott, M. P. Comparison of model-fitting kinetic methods for modeling the cure kinetics of commercial phenol-formaldehyde resins. *Journal of Applied Polymer Science (2006),* accepted.

Wang, J.; Laborie, M.-P. G.; Wolcott, M. P. Influence of wood on the cure kinetics of phenol-formaldehyde resins. Chapter 5, 2007.

Chapter 7 Model-fitting Kinetic Analysis of Phenol-formaldehyde Bonded Wood Joints

ABSTRACT

Cure development of phenol-formaldehyde (PF) resins has been extensively modeled based on chemical advancement. However, it is *in situ* mechanical development of wood-adhesive systems that is most relevant with process optimization such as hot-pressing of wood-based panels. The objective of this research is to examine the feasibility of applying common model-fitting kinetic analysis to describe cure development based on storage modulus development recorded with dynamic mechanical analysis (DMA). Dynamic three-point bending tests were conducted on a sandwich specimens composed of two wood adherends bonded with an adhesive layer. Two commercial PF resins of different molecular weights distributions (labeled as PF-high and -low respectively) were used as adhesive. In addition, PF-high bonded wood joints were also wrapped by aluminum foil to investigate the effect of moisture loss. The specimen curing process was monitored using various isothermal and linear heating regimes. The results showed that the PF-low joints cured more slowly than the PF-high joints. The foil-wrapped PF-high joints displayed slower curing process than the unwrapped joints and rendered two peaks in the tan δ curves. These peaks were attributed to gelation and vitrification with an activation energy of 40 and 48 kJ/mol; respectively. The activation energy from three model-fitting models of autocatalytic, Prout-Tompkins,

and Avrami-Erofeev was in agreement with that from vitrification. Overall, model-fitting kinetic analyses were effective to describe the mechanical development of wood-adhesive systems.

Key words: Dynamical mechanical analysis (DMA); kinetic models; phenol formaldehyde resins; gelation; vitrification; activation energy.

INTRODUCTION

Cure development of phenol-formaldehyde resins has been extensively modeled based on chemical advancement in their neat state or in wood-resin blends (He and Yan 2005a; Wang *et al*. 2006, 2007a). These kinds of investigations most commonly utilize differential scanning calorimetry (DSC) to monitor the chemical advancement and are important for understanding PF resin formulations and wood-resin interactions. However, it is *in situ* mechanical development of wood-adhesive systems that is most relevant with process optimization such as hot-pressing of wood-based panels. Wang *et al*. (2007b) demonstrated that a wood-adhesive sandwich beam evaluated in dynamic three-point bending provided a basis to probe the *in situ* shear and flexural modulus development during curing process. From an empirical viewpoint, kinetics may represent the rate of development for physical, mechanical or electrical properties. In this sense, the mechanical development during curing can also be modeled in a similar way with chemical advancement determined using DSC. However, a difference may exist in the defined degree of cure because physical properties development is not necessarily linearly

related to chemical advancement. The qualitative extent of curing extent of adhesives was conveniently determined by their glass transition tempearture comparison of the DMA first scanning and re-scanning (Chi & Hui 2001). The areas under tan δ cure (Christiansen *et al*. 1993; Wang *et al*. 1995) and the magnitude of tan δ (Connolly *et al*. 2002) were also used as indication of qualitative cure extent. The quantitative mechanical degree of cure (β) is commonly defined as a fraction of E' spanning from zero to unity (Vazquez *et al*. 2005). The commonly used n^{th} order and autocatalytic models have been applied to the cure of polyurethanes/lignin mixtures (Toffey and Glasser 1997). Activation energy determined using DMA data is often lower than that determined by DSC and rheometry (Malkin *et al*. 2005). Time and temperature at the peak of tan δ is commonly used as a point value to access the reaction rate while comparing various formulations (Kim & Nieh 1991) and synthesis conditions (He and Yan 2005a).

Studying the cure of epoxy resins with torsional braids, Gillham (1979) found two peaks distinguished in the tan δ curve. The first peak was defined as gelation point and the second as vitrification. However, in most cases, only one peak appears on the tan δ curves and it has been interpreted either vitrification (Kim & Nieh1991) or gelation (Toffey and Glasser 1997). When only one peak is present, some researchers interpret the onset of increase in E' as gelation (He and Yan 2005b) while others define the point where E' levels as vitrification (Lopez *et al*. 2002).

For PF resins, some researchers find two peaks in the tan δ curve (Garcia and Pizzi 1998, Laborie 2002) while others only find a single peak (Kim & Nieh 1991;

Onica *et al*. 1998). Based on gelation and vitrification point at various isothermal temperatures, Time-Temperature-Transformation (TTT) diagrams can be constructed to characterize the curing behavior of thermosetting resins and composites (Simon and Gillham 1992). The TTT diagram can provide necessary information for process parameter optimization. For example, extended dwell time before gelation when the viscosity of the resin during curing process is a minimum allows good wetting of the wood fibers and consequently provides a good adhesion of the wood fibers in the final product. Garcia and Pizzi (1999) and Laborie (2002) have constructed partial TTT cure diagrams for the PF-wood bonded joint and PF impregnated strips respectively. In summary, the data recorded with DMA enriches a lot of information about resin cure development.

OBJECTIVES

Understanding cure kinetics and strength development in wood/adhesive systems is important for evaluating adhesive performance, formulating new resins, and optimizing process parameters. DMA is a commonly used analytical technique for evaluating cure development of polymer systems but has not been standardized in wood adhesion research. To date, all cure kinetic analyses are exclusively used for modeling DSC data (Wang *et al*. 2006). In this perspective, the objectives of this research are to:

3. Investigate the effectiveness of DMA in characterizing the gelation and vitrification events for PF resins,

4. Validate the application of model-fitting kinetics to DMA data.

EXPERIMENTAL

PF resins

Two PF resole resins, tailored as adhesives for oriented strand boards, were obtained Georgia-Pacific Company, frozen and stored at -20°C until use. The low molecular weight resin (PF-low) had a weight-average molecular weight (M_w) of 621 g/mol and a polydispersity (M_w/M_n) of 1.41. The high molecular wieght resin (PF-hi) displayed an M_w = 6576 g/mol and M_w/M_n =1.72. The resin solid contents were 54.5% and 45.0% for PF-low and PF-high respectively. In addition, elemental analysis showed the presence of 3.9 and 3.7 wt % nitrogen for PF-low and PF-high respectively, indicating the presence of urea in both systems.

Specimen preparations

Planed basswood strips (Midwest Products, Inc.) with nominal dimensions of 50x12x1 mm were oven-dried at 103 °C and stored in a desiccator over anhydrous calcium sulfate until use. Sandwich-type DMA specimens were produced from a layer of PF resin between two pieces of wood strips. Care was taken to match the grain, thickness, and weight of the two wood strips within the specimen to maintain a balanced composite design. The bonding surfaces were lightly hand sanded along the grain with 220-grit sandpaper and cleaned with a paper towel immediately prior to resin application. The resin was uniformly applied to the prepared surface of both wood strips using a small airbrush (BADGER Model 350). The amount of resin solid

applied to each surface was set at ca. 50 g/m^2, which equates to ca. 12% of dried wood mass.

Maintaining a consistent resin content was deemed important for obtaining reproducible repeated cure analysis. He & Yan (2005b) demonstrated that the degree of resin loading can influence the cure development. They concluded that this influenced occurred primarily through water absorption and evaporation during the DMA test. Therefore, other measures to maintain moisture content during the tests were investigated. These include (1) short open and closed assembly times in producing the specimens and (2) foil wrapping of the specimens for the DMA analysis. The latter technique was only used while evaluating the cure kinetics to compare to DSC data.

DMA

DMA measurements were conducted on the sandwich specimens in three point bending mode (span 25 mm) using a Tritec 2000 instrument (Triton Technology). Scans were conducted using a fixed of 1 Hz under various isothermal conditions from 70 to 180 ^{o}C and thermal ramps from 2 to 5 °C/min. Low heating rates were selected to make sure that the effect of thermal lag was minimal. When conducting isothermal tests, the DMA oven was preheated to the predetermined isothermal temperature, upon which time the specimen was quickly installed. After the scan began, the oven was maintained at the cure temperature until both the *E'* and *tan* δ approached a constant value signifying the completion of detectable cure. The specimen was then

cooled to room temperature, and re-scan at 2 °C/min. Strain sweep tests were conducted to establish the linear viscoelastic ranges at each working temperature. Typical strain settings ranged from 1-2•10^{-4}.

RESULTS AND DISCUSSION

Characterization of cure development

The representative changes for *E'* and *tan* δ with temperature is represented in Figure 7.1a for a typical aluminum foil-wrapped PF-high bonded wood joint cured at 2 °C/min. Three distinct zones were observed from *E'* curve: thermal softening of un-cured wood-resin system, resin curing, and thermal softening of cured wood-resin system. Upon application of the liquid PF resin to the dry wood surface, water is absorbed by the wood causing the adhesive layer to become semi-solid at room temperature. In this state, the adhesive can transfer partial shear forces between two pieces of wood. With increasing temperature, the resin gradually softens and the *E'* decreases reaching a minimum *E'* plateau. This event appears on *tan* δ curve as the first peak centered at *ca.* 50 to 70 °C (Figure 7.1a). At this point, the *E'* reaches a minimum plateau corresponding to a competitive relationship between the resin softening and curing during the heating process. With the subsequent increase in *E'*, the resin cure began to outpace the softening. For convenience, this point ($E'_{\min}$) is defined here as the onset of the mechanical cure ($\beta = 0$). Shortly after E'_{min}, a second peak is evident in *tan* δ (Figure 7.1a). This second peak is taken to be the gelation

point, where the cross-links progressed to form an "infinitely" network (Gillham 1979; Toffey and Glasser 1997). When only a single peak is evident in the *tan* δ curve, gelation was similarly defined by temperature corresponding to the onset of increase in *E'* (He and Yan 2005b). Finally, the third peak in the *tan* δ curve was defined as the vitrification point, *i.e.* the attainment of a glass state where the glass transition temperature of the forming polymer exceeded or was equal to the oven cure temperature (Gillham 1979; Toffey and Glasser 1997). At higher temperatures *E'* began to decrease slightly due to thermal softening of the cured resin and the attained maximum, E'_{max}, may represent progressive degradation of wood substrate or differential expansion between resin and wood (Onicaa *et al*. 1998).

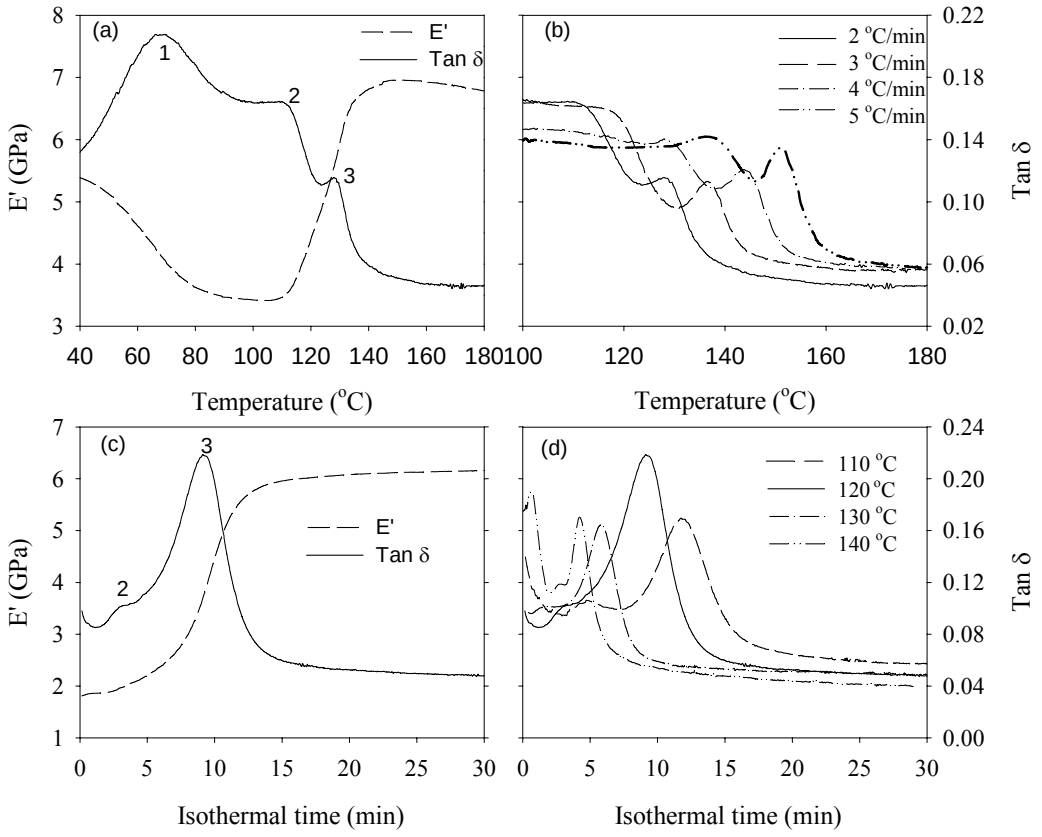

Figure 7.1 The DMA cure profiles of the aluminum foil-wrapped PF-high bonded wood joints: a) storage modulus development *(E')* and three peaks in *tan δ* showing glass transition temperature of the uncured and dehydrated PF resin (Peak 1), gelation (Peak 2), and vitrification (Peak 3) events at 2 °C /min; b) gelation and vitrification temperature dependence on heating rates; c) modulus development and gelation (small shoulder 2) and vitrification (Peak 3) in *tan δ* curve at 120 °C; d) tan δ at different isothermal temperatures.

Typical plots of the *E'* and *tan δ* of the PF bonded wood joints as a function of the time during isothermal cure were presented in Figure 7.1c & d. The *E'* curve displayed a sigmoidal shape while the *tan δ* exhibited a peak followed by a decrease

toward an asymptotic limit. Similar behavior may be observed as a function of decreasing temperature, and therefore increasing relaxation time, for a non-reacting system (Dillman & Seferis 1989). Polymer viscoelasticity or damping as quantified by the *tan* δ, is around from 0.1 to 1 or more while *tan* δ is 10^{-3} or less for structural metals such as steel, brass, and aluminum (Lakes and Quackenbush 1996). During the cure process, the magnitude of *tan* δ passed through a range typical of the rubbery state before vitrification and decreased to a minimum of around 0.05 after vitrification,, which is typical of cured polymers. The vitrification is an analog to the rubber to glass transition of the forming amorphous polymer. Under isothermal cure, the time required to reach full cure can be easily determined and can be subsequently used as a tool to establish an optimal pressing time during wood composites manufacturing. At 120 °C, it required around 20 min to complete the cure for foil-wrapped PF-high bonded joints. This state was confirmed by re-scanning the cured sample where no secondary curing has been detected.

Gelation and vitrification temperatures at different ramp rates are summarized in Table 7.1 for foil-wrapped PF-high bonded wood joints and vitrification times under isothermal cure regimes are summarized in Table 7.2. The gelation point under isothermal temperature appears only as a small shoulder (Figure 7.1c) and is unable to be reproducibly quantified in some samples. It was assumed that the sudden temperature increase from room temperature might account for this problem because gelation could occur while the instrument established equilibrium. For un-wrapped samples, the gelation peak was not evident both under linear heating and isothermal

regimes. Typical *tan δ* traces for PF-low bonded wood joints are shown in Figure 7.2. It was assumed that rapid moisture loss in the un-wrapped samples was responsible for unrecorded gelation peaks. Hence, only vitrification temperatures were summarized in Table 7.1under linear heating rates for un-wrapped wood joints and vitrification times in Table 7.2 under isothermal temperature.

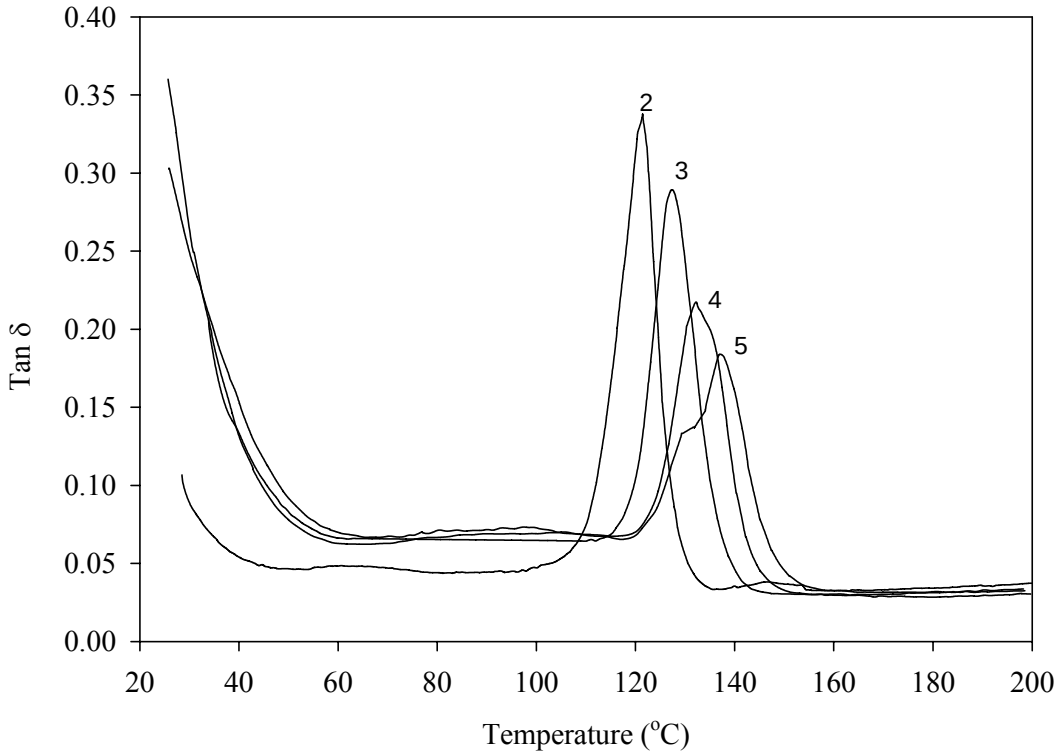

Figure 7.2 DMA tan δ traces for PF-low bonded wood joints at different heating rates designated on the curves. Only vitrification has been recorded at all heating rates.

Table 7.1 Characteristic temperature (°C) at different heating rates and activation energy E_a by the Kissinger equation.

Heating rate (^oC/min)		2	3	4	5	E_a (kJ/mol)
PF-high Al	Gelation	112.3	120.2	128.6	137.7	40.4
	Vitrification	128.5	137.4	146.8	151.4	48.0
PF-high	Vitrification	114.5	123.2	127.5	132.2	61.8
PF-low	Vitrification	121.4	127.5	132.6	137.0	72.4

CV is less than 1.4% for temperature, R^2 >0.99 for activation energy, E_a

Table 7.2 Vitrification time (min) and activation energy E_a at different isothermal cure temperatures as determined using the peak time method.

Resin Type	**Vitrification Times (min)**					E_a (kJ/mol)
	Isothermal Cure Temp (^oC)					
	90	100	110	120	130	
PF-high Al	30.3	16.0	11.0	9.6	5.8	44.6
PF-high	19.1	10.0	8.0	5.2	4.6	42.2
PF-low	30.9	23.1	14.9	10.4	5.8	46.6

CV is less than 5.8%, R^2 >0.99 for E_a

Activation energy of gelation and vitrification

Under the isothermal cure regimes, the time required to reach the peak *tan* δ (t_{ipeak}) at the resident temperature (T_i) was used to calculate the activation energy (E_a). A linear regression of $ln(t_{ipeak})$ and $1/T_i$ across the isothermal temperatures yielded activation energy, i.e.

$$E_a = \frac{8.314 d(\ln t_{peak})}{d(1/T)} \tag{52}$$

Under cure regimes using constant heating rates (φ_i), the T_{ipeak} is defined as the temperature associated with the peak *tan* δ. A linear regression of $\ln\left(\varphi_i / T_{ipeak}^2\right)$ versus $1/T_{ipeak}$ across several heating rates yields the activation energy with the Kissinger Eq. (53)

$$E_a = \frac{8.314 d[-\ln(\varphi / T_{peak}^2)]}{d(1/T_{peak})} \tag{53}$$

The respective activation energy is then assigned to either the gelation or vitrification processes depending on which the peak is selected. Computed values for each are summarized in Table 7.1and Table 7.2.

Sample preparation effects on Tan δ

In practice, the time between sample preparation and DMA testing varied from sample to sample. As mentioned above, the curing event of vitrification is consistently evident and gelation point does not appear in the *tan* δ curve for the un-wrapped wood joints. The prominence and temperature of the peak 1 (Figure 7.1) varied with open and closed assembling time during the sample preparations. Figure 7.3 shows the

effects of closed assembly time at different temperature on this peak for the PF-low bonded wood joints. With a minimal closed assembly time, the peak appears at 20 °C. With increasing closed assembly time or pre-conditioning temperature, the temperature of peak 1 increases. DSC scanning has shown that the PF-low resin begins cure at around 70 °C (Wang *et al*. 2005). This behavior appears consistent with the findings using DMA here. When the sample was pre-conditioned at 70 °C for 8 hours, it appears to undergo substantial pre-cure. Accordingly, the first peak disappears and the intensity of the vitrification peak decreases (Figure 7.3). For PF-high bonded wood joints, the peak 1 appears at around 40-70 °C, which is consistent with its higher molecular weight.

When using a glass fiber braid for characterizing the polyurethane cure process, Toffey and Glasser (1997) defined this first peak as the glass transition temperature of uncured resins. Due to the fact that the peak temperature changes with water content in our research, it is reasonable to assume this peak may, in fact, be a glass transition temperature of the uncured PF resins. With DSC, Park and Wang (2005) reported that the glass transition temperature of an un-cured powder OSB resin was *ca*. 50 °C. This is consistent with Menard (1999) who defined the initial peak as the softening point of the un-cured resin, especially when the resin in its dehydrated state. However, we note that the melting point of phenol and hydroxymethelated phenol is in this same region (Merck 2001). Finally, it is also worthwhile to mention that the glass transition temperature of plasticized lignin is located in this temperature region (Kelly *et al*. 1987). In summary, Peak 1 is likely to be a glass transition of

un-cured PF resin but other explanations might be possible. Regardless of the cause of this peak, the specimen preparation substantially influences its appearance and temperature while the effects on the further curing events appear negligible.

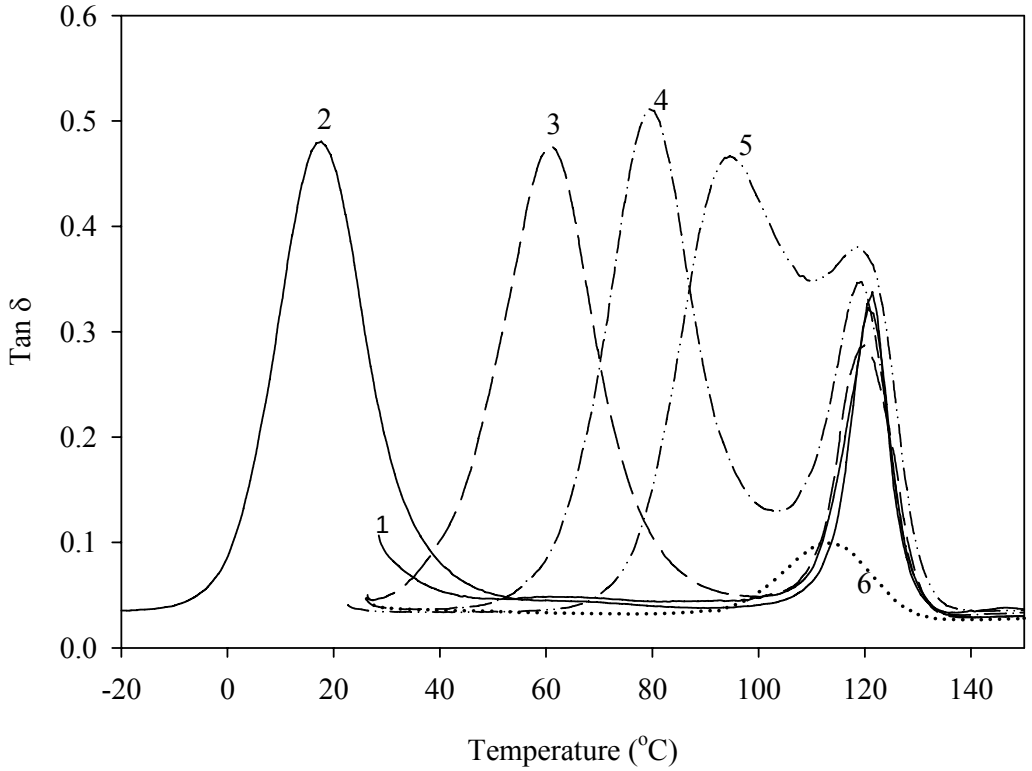

Figure 7.3 The effect of preparations on cure development of PF-low bonded wood joints scanned at 2 °C/min: 1. DMA scan beginning at room temperature immediately followed sample preparation; 2. DMA scanning immediately followed sample preparation from low temperature; 3. closed assembly at 30 °C for16 hours; 4. closed assembly at 50 °C for 16 hours; 5. closed assembly at 60 °C for 16 hours; 6. closed assembly at 70 °C for 8 hour.

Mechanical cure development

Using DMA, the degree of mechanical cure (β) can be defined (Vazquez *et al*. 2005) as

$$\beta = \frac{E^{'}(t) - E^{'}_{\min}}{E^{'}_{\max} - E^{'}_{\min}} \tag{54}$$

where *E'(t)* is the storage modulus at time *t*. The effects of foil-wrapping on the mechanical cure development of PF-high bonded wood joints cured under linear heating and isothermal regimes are shown in Figure 7.4 and Figure 7.5; respectively. Assuming that the primary influence of the foil-wrap is to limit moisture loss in the specimen, the cure development appears to be determined by at least two processes: moisture loss and resin crosslinking. Therefore, it is the superposition of these two processes that dictate mechanical cure development, especially during early stages for un-wrapped samples. Under linear heating regimes, the foil-wrapping reduces delays the beginning of cure as well as the peak temperature. The long inital tail in the storage modulus curves of un-wrapped PF-high bonded samples likely results from both moisture loss and resin curing (Figure 7.4). It is assumed that the abrupt inflection represents a shift to a process dominated by resin curing. Under isothermal temperature, moisture loss promoted a fast initial mechanical cure as compared with foil-wrapped PF-high bonded joints. However, these specimens experienced a plateau in the rising *E'* which was likely associated with the shifting mechanisms.

In Figure 7.6, it is shown that under the linear heating regime the un-wrapped

PF-high bonded wood joints begin curing at a lower temperature than PF-low bonded joints. These specimens were also observed to cure faster at the same isothermal temperature. It seems that the effect of moisture loss on cure development of PF-high bonded joints is larger than that on PF-low bonded joints. However, we note that the interaction between water and the PF-high resin is weaker than that between water and PF-low since PF-high is more advanced and has less hydroxyl groups available. Thus the moisture in the PF-high bonded adhesive layer is less restricted and may evaporated at lower temperature and faster than in the PF-low bonded adhesive layer. This potential moisture influence simply adds to the demonstrated increased cure rate of the PF-high resin when comparted to the PF-low (Wang *et al*. 2005). Despite the difference in initial cure rate between the PF-high and PF-low bonded joints, they appear to reach full mechanical cure at same temperature under linear heating regime. This observation is also consistent with the results characterized by DSC (Wang *et al*. 2007). In summary, PF-low bonded wood joints cured more slowly than PF-high bonded joints, while foil-wrapped samples of PF-high bonded joints reduced the cure rate to the similar extent comparable to that of PF-low bonded joints.

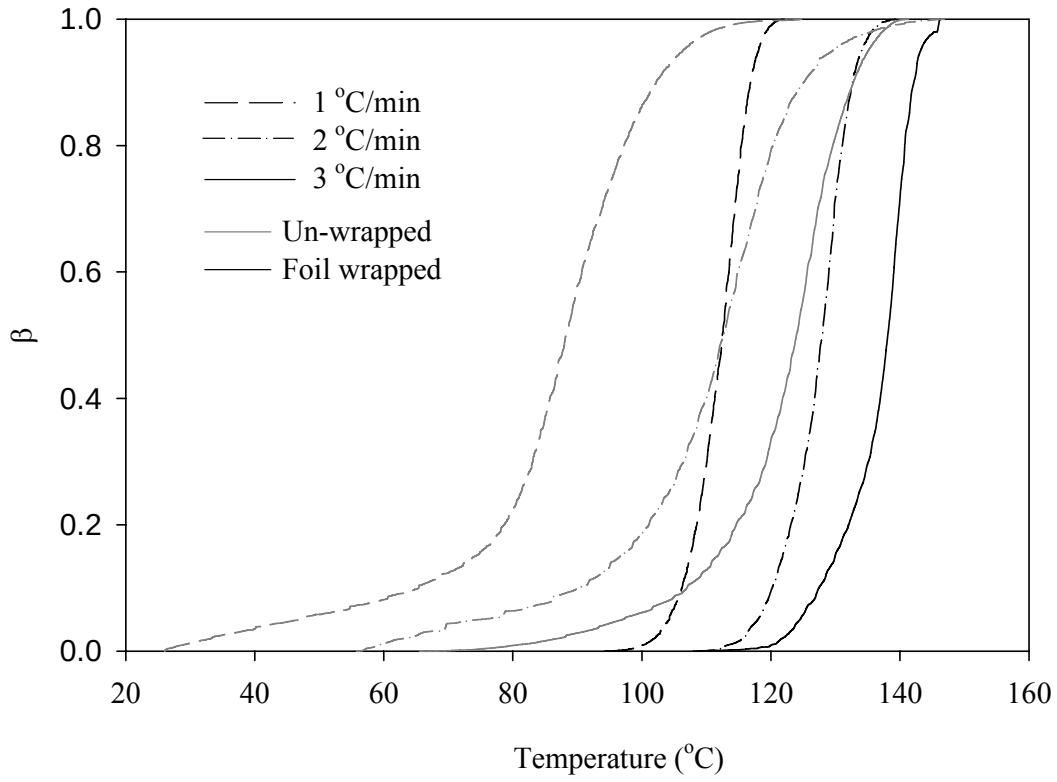

Figure 7.4 The effects of foil-wrapping on the mechanical cure development at linear heating rate for the PF-high bonded wood joints.

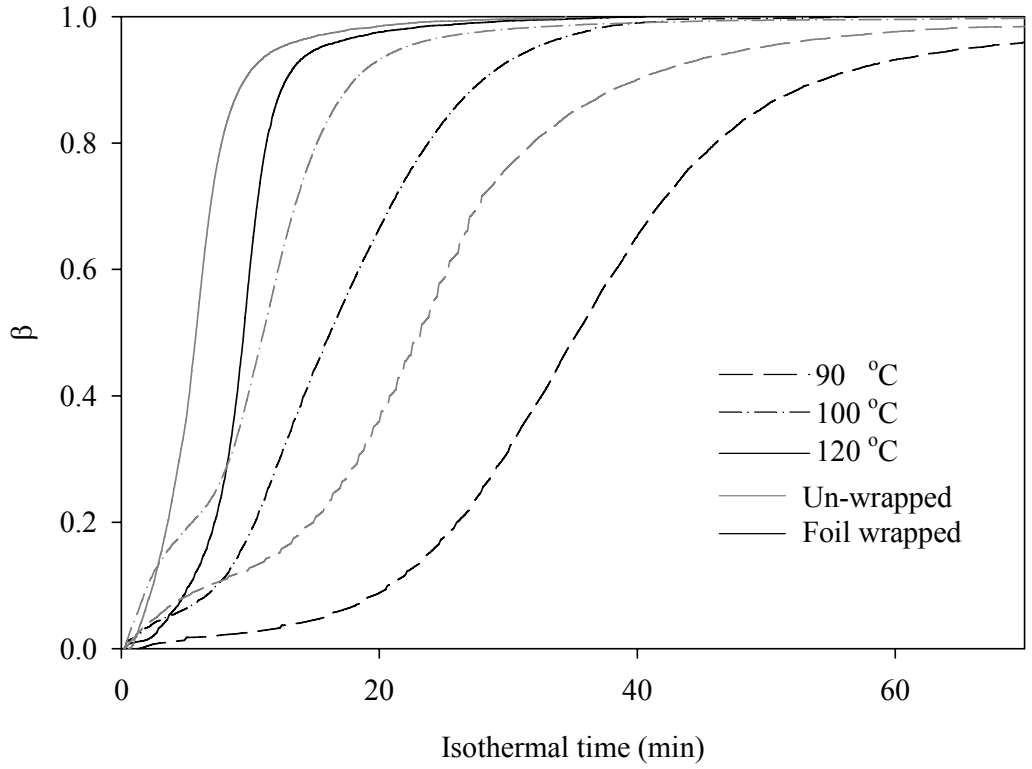

Figure 7.5 The effects of foil-wrapping on the mechanical cure development under isothermal regime for the PF-high bonded wood joints.

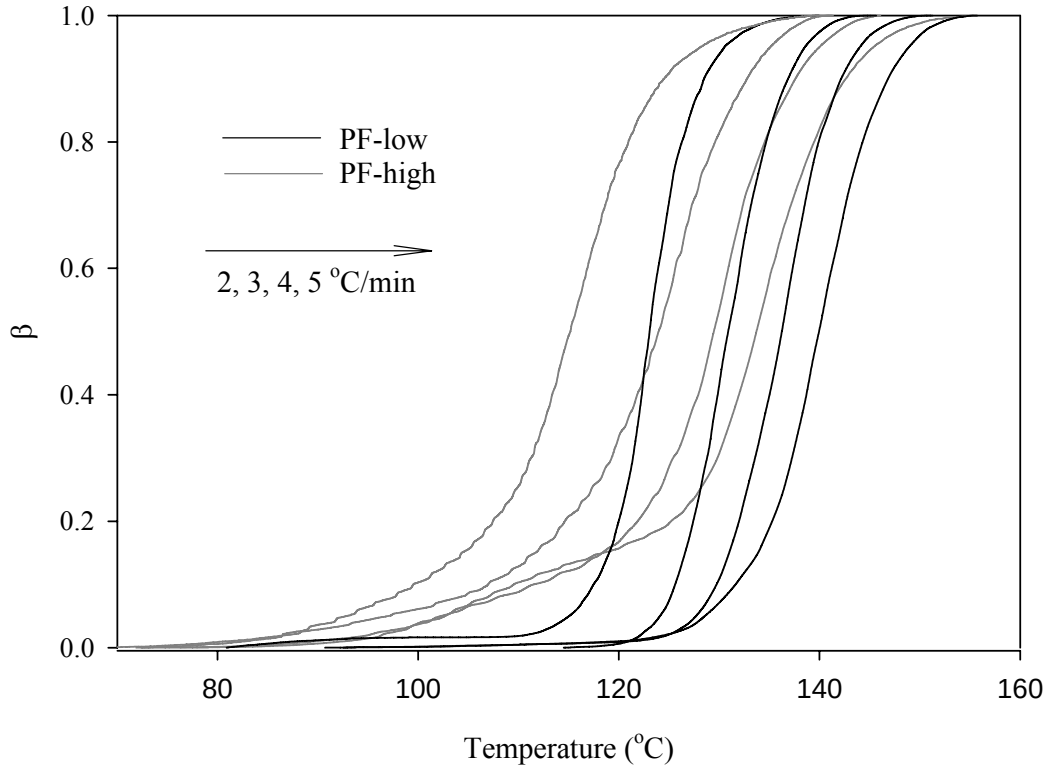

Figure 7.6 Comparison of the mechanical cure development at linear heating rate between the PF-high and PF-low bonded wood joints.

Model-fitting kinetics

It was observed that the *E'* development under a isothermal cure regime followed a sigmoidal shape as illustrated in Figure 7.7 for a PF-low bonded wood joint. The autocatalytic (Eq. (55)), Prout-Tompkins (Eq. (56)), and Avrami-Erofeev (Eq. (57)) were used to fit the curve at each isothermal temperature (Galwey & Brown 1998).

$$\frac{d\beta}{dt} = k\beta^m(1-\beta)^n \tag{55}$$

$$\frac{d\beta}{dt} = k\beta(1-\beta) \tag{56}$$

$$\frac{d\beta}{dt} = kn(1-\beta)\left[-\ln(1-\beta)\right]^{(n-1)/n} \tag{57}$$

where $d\beta/dt$ is rate of mechanical cure; k is rate constant; m and n are model constants, or reaction order. The data from the isothermal experiments were analyzed to yield values for the rate constant k_i at each temperature T_i (subscript i refers to different isothermal temperature). The rate constants, k_i, were found to increase with temperature. Using a linear regression on the relationship between $ln\ k_i$ versus $1/T_i$ (Arrhenius plot) yielded values for E_a/R and lnA (ASTM E2070).

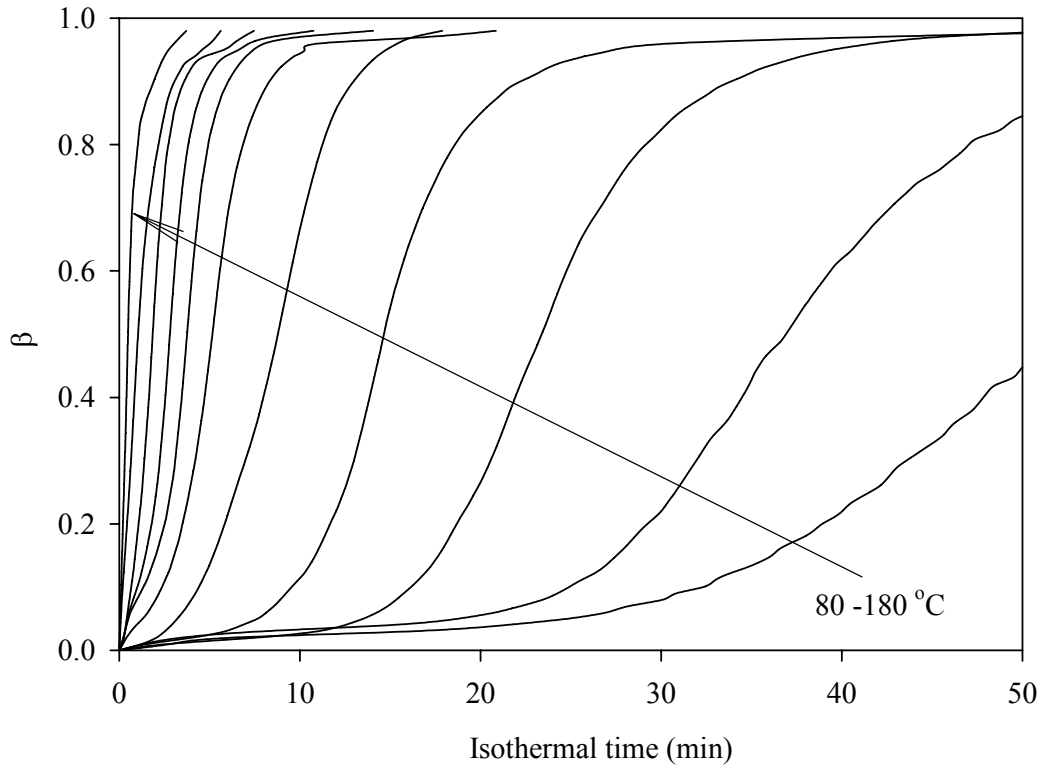

Figure 7.7 An example of cure development under isothermal temperatures for PF-low bonded wood joints.

The advantage of the Prout-Tompkins and Avrami-Erofeev models over the general autocatalytic model is that it can obtain explicit equations for the degree of cure at specific cure times (Eqs (58) and (59)). Therefore, Eqs (58) and (59) can be used to directly fit the experimental data under isothermal cure regimes.

$$\beta = \frac{1}{1+\exp\left(k(t-t_0)\right)} \tag{58}$$

$$\beta = 1-\exp\left(-(kt)^n\right) \tag{59}$$

In addition, Eq. (58) can be rewritten into Eq. (60) for describing mechanical cure development under a linear heating regime.

$$\beta = \frac{1}{1+\exp\left(\frac{T_0-T}{k_T}\right)} \tag{60}$$

where T is temperature in Celsius degree; T_0 and k_T was two fitting constants. The variables required to conduct an isothermal kinetic analyses include β, t,and $d\beta/dt$ under isothermal conditions, and β, T, and $d\beta/dt$ under a linear heating regime. These data are then tested for fitting accuracy to three models. For the autocatalytic model,

multiple linear regression analyses were used to extract necessary constants. For the Prout-Tomkins and Avrami-Erofeev models, a non-linear regression with Levenberg-Marquardt algorithm was used to extract constants using the explicit equation forms found in Eqs. (58) and (59). For each individual temperature program, all three models fit the data very well with R^2 >0.99.

For PF-low bonded wood joints, not all extracted constants for rate equations (Eqs. (55)-(57)) are independent of temperature. The autocatalytic model parameter, *n*, did not show any consistent pattern and was treated as a constant with an average value of *n* = 1.34 and a standard deviation of 0.18; *m* displays a bell-shape relationship with isothermal temperature (Figure 7.8) and was fitted with a three parameter Gaussian function (61) with $R^2 = 0.99$.

$$m = 1.27 \exp\left(-0.5 \left(\frac{T - 108.8}{24.6} \right)^2 \right) \tag{61}$$

where T is temperature in Celsius degree. As shown in Figure 7.8, *m* approaches zero at high temperature, where the rate of storage modulus development appears to follow an nth order model, indicating some mechanisms change. A high isothermal temperature may be beyond the glass transition temperature of fully cured resins.

The Avrami-Erofeev model constant *n* (Figure 7.9) provides information similar to that of the autocatalytic model parameter, *m*. With low value of *n*, the storage modulus development follows nth order. Like *m*, the Avrami-Erofeev constant *n* also can be fitted with a three parameter Gaussian functions (62) with R^2 =0.95.

$$n = 0.79 + 3.3\exp\left(-0.5\left(\frac{T-106.8}{33.7}\right)^2\right) \quad (62)$$

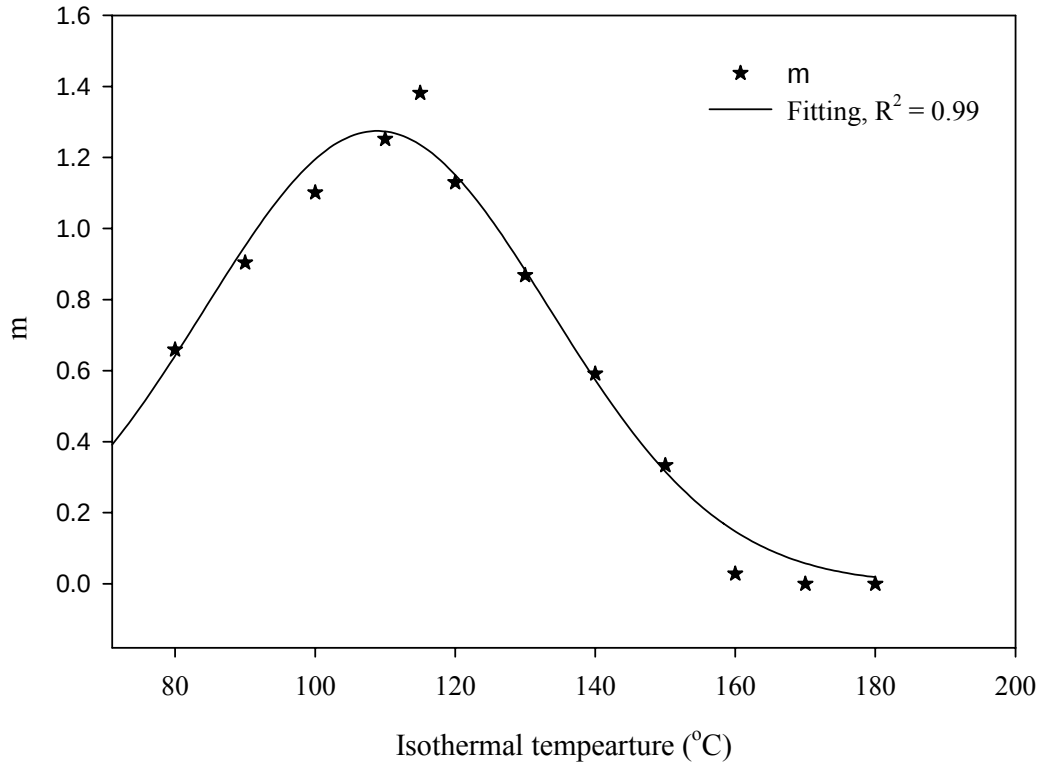

Figure 7.8 Kinetic parameter m of autocatalytic model changes with isothermal temperature for the PF-low bonded wood joints.

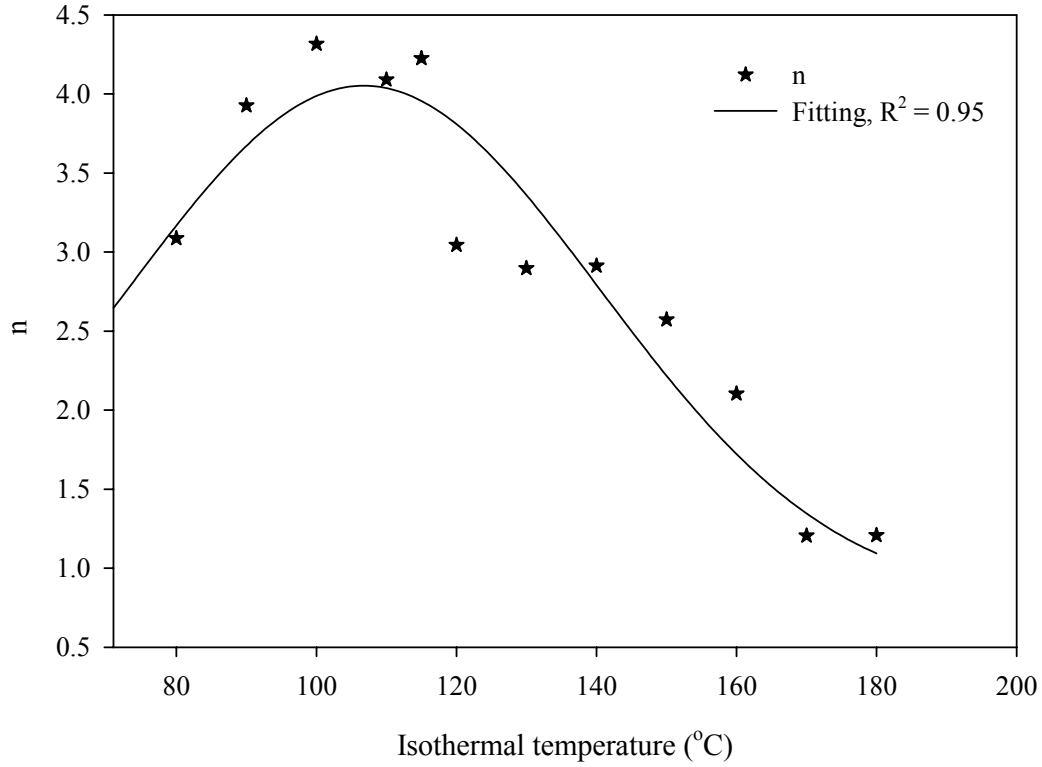

Figure 7.9 Kinetic parameter n of Avrami-Erofeev model changes with isothermal temperature for PF-low bonded wood joints.

The Prout-Tompkins constant t_0 decreases exponentially with temperature, and can be fit linearly with the $\ln(t_0)$ and temperature (63) with $R^2 = 0.99$.

$$\ln(t_0) = -0.0447T + 19.812 \tag{63}$$

The three models and extracted constants under the isothermal regime for the PF-low bonded wood joints are summarized in Table 7.3. As an example, the constants of the Prout-Tomkins model for the PF-low, PF-high, and foil-wrapped PF-high bonded

wood joints are summarized in Table 7.4 for both the isothermal and linear heating regimes. With these models and extracted parameters, the mechanical cure development can be readily described for both the isothermal and linear regimes.

Table 7.3 Summary of models and constants for PF-low bonded wood joints under isothermal temperature

Model	Predictor	Parameter
Autocatalytic	$d\alpha/dt = k\alpha^m(1-\alpha)^n$ $k = A\exp(-E/RT)$	$m = 1.27\exp\left(-0.5\left(\frac{T-381.95}{24.63}\right)^2\right)$ $n = 1.34(0.18)$ $E = 53.7$ (kJ/mol) $\ln(A) = 12.24$ (1/s)
Prout-Tomkins	$d\alpha/dt = k\alpha(1-\alpha)$ $k = A\exp(-E/RT)$ $\alpha = 1/(1+\exp(k(t_0-t)))$	$\ln(t_0) = -0.0447T + 19.812$ (min) $E = 53.3$ (kJ/mol) $\ln(A) = 11.68$ (1/s)
Avrami-Erofeev	$d\alpha/dt = kn(1-\alpha)(-\ln(1-\alpha))^{(n-1)/n}$ $k = A\exp(-E/RT)$ $\alpha = 1-\exp(-(kt)^n)$	$n = 0.79 + 3.26\exp\left(-0.5\left(\frac{T-379.91}{33.67}\right)^2\right)$ $E = 55.6$ (kJ/mol) $\ln(A) = 10.64$ (1/s)

All regression $R^2 > 0.95$; T: temperature in Celsius degree.

Table 7.4 Summary of parameters for Prout-Tomkins model under isothermal conditions.

	Parameters under isothermal $\beta = \frac{1}{1+\exp(k(t-t_0))}$ k=Aexp(-E/R(T+273))	Parameters under linear heating rate, ϕ $\beta = \frac{1}{1+\exp\left(\frac{T_0-T}{k_T}\right)}$
PF-low	$\ln(t_0) = -0.0447T + 19.812$ (min) $E = 53.3$ (kJ/mol) $\ln(A) = 11.68$ (1/s)	$T_0 = 5.59\varphi + 113.01$ $k_T = 2.73$ (0.23)
PF-high	$\ln(t_0) = -0.0366T + 16.182$ (min) $E = 49.6$ (kJ/mol) $\ln(A) = 10.59$ (1/s)	$T_0 = 6.24\varphi + 104.21$ $k_T = 5.64$ (0.27)
PF-high foil-wrapped	$\ln(t_0) = -0.0409T + 18.392$ (min) $E = 49.8$ (kJ/mol) $\ln(A) = 8.85$ (1/s)	$T_0 = 11.93\varphi + 101.76$ $k_T = 3.00$ (0.19)

All regression R^2>0.96; T: temperature in Celsius degree; φ: heating rate in °C/min

The activation energies obtained by these models were summarized on Table 7.5. The values listed as Peak time and Peak temperature were derived from vitrification peaks under the isothermal and linear heating regime (from Table 7.1 and Table 7.2), respectively, and listed here for comparison. The activation energies derived with the autocatalytic, Prout-Tompkins, Avrami-Erofeev, and Peak time methods utilized the isothermal data and were more similar than the Peak time method.

This approach utilizeds the Kissinger equation to analyze the linear heating data and is slightly larger than those obtained from isothermal data. An ANOVA analysis has indicated there is significant difference for activation energy between PF-low and PF-high, but no significant difference between PF-high and PF-high aluminum foil-wrapped. These activation energies from DMA mechanical cure development are smaller than those obtained from the DSC data for same neat resins (Wang *et al* 2006). The activation energy obtained for PF-high at ramp mode was at same order with that for PF/wood mixture at a wood content 35 percent obtained by DSC (Wang *et al*. 2007a). The activation energy in presence of wood has decreased.

Table 7.5 Summary of activation energy (kJ/mol) with different methods

	Auto-catalytic	Prout-Tomkins	Avrami-Erofeev	Peak time	Peak temp
PF-high Al	45.7	49.8	49.5	44.6	48.0
PF-high	51.6	49.6	44.3	42.2	61.8
PF-low	53.7	53.3	55.6	46.6	72.4

R^2 >0.99; Peak temp: calculated from vitrification temperature by Kissinger equation; all others are calculated from isothermal data.

CONCLUSION

The transition temperatures of the curing process and cure development could

be clearly assigned to storage modulus changes or to *tan* δ. The reproducibility among samples for recording curing process was good although the variations of sample preparations affected the glass transition temperature of un-cured wood-adhesive systems. Vitrification was probed in all samples, while gelation point was only detected for foil-wrapped wood joints under linear heating regime. It is assumed that moisture loss in un-wrapped joints muffled the gelation points. The activation energy of foil-wrapped PF-high joints for gelation and vitrification were 40 and 48 kJ/mol; repectively. DMA mechanical cure development showed that the PF-low bonded wood joints cured slower than PF-high bonded wood joints. Foil-wrapping retarded moisture loss and delayed mechanical degree of cure for PF-high bonded wood joints.

The model-fitting kinetics, which generates single value characteristic parameters, especially activation energy, represents an important established method of reporting and comparing kinetic data. Model-fitting kinetics of autocatalytic, Prout-Tompkins, and Avrami-Erofeev models was selected to model mechanical cure development since the E' development followed a sigmoid. The activation energies by three model-fitting models were closer to each other and in agreement with that from time events of vitrification with isothermal data. This is evidence that three models are comparable and capable to describing cure development. The activation energies obtained from ramp data by the Kissinger equation were a bit larger than those from isothermal data. Generally, the activation energy obtained from these methods under both linear heating and isothermal regime are around 50-70 kJ/mol. They were less than those obtained from neat resins by DSC (85-100 kJ/mol) (Wang *et al*. 2007) and

in agreement with those of PF/wood mixtures obtained by DSC (Wang *et al*. 2007b).

The results imply that the activation energy of cure processes decreased in the

presence of wood.

REFERENCES

ASTM E2070-03 Standard test method for kinetic parameters by differential scanning calorimetry using isothermal methods. West Conshohocken, PA, USA.

Chi, F. T.; Hui, K. H. An alternative method to the curing study of polymeric die attach adhesives using dynamic mechanical analysis. *Thermochimica Acta (2001), 367-368*, 169-175.

Christiansen, A. W.; Follensbee, R. A.; Geimer, R. L.; Koutsky, J. A.; Myers, G. E. Phenol-formaldehyde resin curing and bonding in steam-injection pressing. Part II. Differences between rates of chemical and mechanical responses to resin cure. *Holzforschung (1993), 47*(1), 76-82.

Connolly, C.; Fogg, D.; Fraser, F.; Natividad, R. Tan delta by DMA for measurement of cure state. Technical Papers - American Chemical Society, Rubber Division, Spring Technical Program, 161st, Savannah, GA, United States, Apr. 29-May 1, 2002 (2002), 794-805.

Dillman, S. H.; Seferis, J. C. Kinetic viscoelasticity for the dynamic mechanical properties of polymeric systems. *Journal of Macromolecular Science, Chemistry (1989), A26*(1), 227-47.

Galwey, A. K.; Brown, M. K. Kinetic background to thermal analysis and calorimetry. In M. E. Brown, ed. Handbook of thermal analysis and calorimetry. Vol. 1: Principles and practice. Elsevier Science B. V., 1998, p147-224.

Garcia, R.; Pizzi, A. Crosslinked and entanglement networks in thermomechanical analysis of polycondensation resins. *Journal of Applied Polymer Science (1998), 70*(6), 1111-1119.

Gillham, J. K. Formation and properties of network polymeric materials. *Polymer Engineering and Science (1979), 19*, 676-682.

He, G.; Yan, N. Effect of wood on the curing behavior of commercial phenolic resin

systems. *Journal of Applied Polymer Science (2005a), 95*(2): 185-192.

He, G.; Yan, N. Effect of wood species and molecular weight of phenolic resins on curing behavior and bonding development. *Holzforschung (2005b), 59*(6), 635-640.

Kelley, S. S.; Rials, T. G.; Glasser, W. G. Relaxation behavior of the amorphous components of wood. *Journal of Materials Science (1987), 22*(2), 617-624.

Kim, M. G.; Nieh, W. L.-S.; Meacham, R. M. Study on the curing of phenol - formaldehyde resol resins by dynamic mechanical analysis. *Industrial & Engineering Chemistry Research (1991), 30*(4), 798-803.

Laborie, M.-P. G. Investigation of the morphology of the wood/phenol-formaldehyde adhesive interphase. Doctoral dissertation, Virginia Polytechnic Institute and State University, (2002), Blacksburg, VA.

Lakes R.S.; Quackenbush, J. Viscoelastic behaviour in indium tin alloys over a wide range of frequency and time. *Philosophical Magazine Letters (1996), 74*, 227-232.

Lopez, J.; Ramirez, C.; Torres, A.; Abad, M. J.; Barral, L.; Cano, J.; Diez, F. J. Isothermal curing by dynamic mechanical analysis of three epoxy resin systems: gelation and vitrification. *Journal of Applied Polymer Science (2002), 83*(1), 78-85.

Malkin, A. Ya.; Gorbunova, I. Yu.; Kerber, M. L. Comparison of four methods for monitoring the kinetics of curing of a phenolic resin. *Polymer Engineering and Science (2004), Volume Date 2005, 45*(1), 95-102.

Menard, K. P. Dynamic Mechanical Analysis: a practical introduction to techniques and applications. (1999), Chapter 6, Published by CRC Press.

Merck & Co., Inc. The Merck Index, 13th Edition. (2001), Whitehouse Station, NJ, USA.

Onica, L.; Bucur, V.; Ansell, M. P.; Pizzi, A.; Deglise, X.; Merlin, A. Dynamic thermomechanical analysis as a control technique for thermoset bonding of wood joints. *International Journal of Adhesion and Adhesives (1998), 18*(2), 89-94.

Park, B.-D.; Wang, X.-M. Thermokinetic behavior of powdered phenol-formaldehyde (PPF) resins. *Thermochimica Acta (2005), 433*(1-2), 88-92.

Simon, S. L.; Gillham, J. K. Reaction kinetics and time-temperature-transformation cure diagrams for off-stoichiometric ratios of a high-glass-temperature epoxy/amine system. *Journal of Applied Polymer Science (1992), 46*(7), 1245-1270.

Toffey, A; Glasser, W. G. Cure characterization of polyurethanes with lignin and cellulose derivatives. *Holzforschung (1997), 51*(1), 71-78.

Vazquez, G.; Lopez-Suevos, F.; Gonzalez-Alvarez, J.; Antorrena, G. Curing process of phenol - urea - formaldehyde -tannin (PUFT) adhesives. Kinetic studies by DSC and DMA. *Journal of Thermal Analysis and Calorimetry (2005), 82*(1), 143-149.

Wang, J., Laborie, M.-P. G.; Wolcott, M. P. Comparison of model-free kinetic methods for modeling the cure kinetics of commercial phenol–formaldehyde resins. *Thermochimica Acta (2005), 439*: 68–73.

Wang, J.; Laborie, M.-P. G.; Wolcott, M. P. **C**omparison of model-fitting kinetic methods for modeling the cure kinetics of commercial phenol-formaldehyde resins. *Journal of Applied Polymer Science (2006),* accepted.

Wang, J.; Laborie, M.-P. G.; Wolcott, M. P. Influence of wood on the cure kinetics of phenol-formaldehyde resins. Chapter 5, 2007a.

Wang, J.; Wolcott, M. P.; Laborie, M.-P. G. Dynamic mechanical analyses of phenol-formaldehyde bonded wood joints, Chapter 6, 2007b.

Wang, X. M.; Riedl, B.; Christiansen, A. W.; Geimer, R. L. The effects of temperature and humidity on phenol-formaldehyde resin bonding. *Wood Science and Technology (1995), 29*(4), 253-66.

Chapter 8 Kinetic Analysis and Correlation of Mechanical and Chemical Cure Development for Phenol-formaldehyde Resin Bonded Wood Joints

ABSTRACT

The kinetics of phenol-formaldehyde (PF) resin cure governs both the duration of hot-pressing for wood-based composites and the properties of final panels. Chemical advancement of the forming polymer does not always produce a linear relation to mechanical development. The objective of this research is to relate the chemical and mechanical manifestation cure so that a cure model for hot-pressing can encompass information on both. Dynamic three-point bending tests were conducted on a foil-wrapped sandwich specimen of two wood adherends bonded with a PF adhesive layer using dynamic mechanical analysis (DMA). The specimen was cured using various isothermal and linear heating regimes. A small disc trimmed from the DMA specimen was scanned with differential scanning calorimetry (DSC) at the same linear heating rate as DMA. Assuming that the curing conditions in the foil-wrapped specimen were similar to that in the high pressure DSC pan, the relationship between chemical and mechanical degree of cure (i.e. α and β, respectively) was thus correlated by an equation analog to a two-parameter Weibull cumulative distribution function. From this relationship, it was found that the α at gelation was independent of the heating regime while the α at vitrification increased with cure temperature. The maximum rate, $d\beta/d\alpha$, was found to occur at the vitrification points. Model-free

kinetics was used to model mechanical cure development and an algorithm was obtained for describing the mechanical degree of cure during curing process.

Key words: Dynamical mechanical analysis (DMA); kinetic models; phenol formaldehyde resins; mechanical degree of cure; chemical degree of cure.

INTRODUCTION

Modeling and optimizing of wood-based composite manufacture is playing a larger role in design of processes and manufacturing equipment. In these models, internal temperature and moisture conditions are computed with an aim towards predicting when polymeric cure is sufficient to avoid delamination at the time of press opening. In order to incorporate cure kinetics into a comprehensive hot-pressing model for fully describing thermodynamic, adhesive, and rheological processes, it is necessary to find a suitable model for kinetics of cure development for the wood/phenol-formaldehyde (PF) bondline. PF resols are most commonly used adhesives in the manufacture of wood-based panels. Curing is intended to advance the PF molecules into a crosslinked network to achieve a high durability of the products; curing is also meant to develop physical and mechanical strength in the products. Most kinetics of PF resins are based on data from differential scanning calotrimrtry (DSC) (Wang *et al*. 2005, 2006). Heat evolution in DSC is typically assumed to be proportional to the formation of a chemical network during polymerization (Prime

1997), but how other mechanical and electrical properties relate to chemical bond formation remains unknown. The kinetics of chemical advancement of the adhesive layer is not necessarily linearly related with developing rate of mechanical properties.

It was observed that cure development derived from storage modulus E' (defined as mechanical cure) was not in agreement with that derived from reaction heat by DSC (defined as chemical cure) (Malkin *et al*. 2005). Dynamic mechanical analysis (DMA) detected that mechanical cure completes earlier than chemical cure under same cure conditions (Christiansen *et al*. 1993; Laborie 2002; Vazquez *et al*. 2005). However, Steiner and Warren (1981) reported that the dramatic stiffness increase in a torsional braid analysis was in agreement with the thermal event by DSC for an advanced plywood PF resin. Yet the relationship between the mechanical cure and chemical cure has not been expressed explicitly.

From an empirical point of view, kinetics may represent the rate of development of physical, mechanical or electrical properties. Therefore, mechanical cure kinetics can be modeled in a similar way that the chemical cure kinetics is determined using DSC. The difference is found in defining the degree of cure, β. The value for β is commonly defined as a fraction of E', with the minimum value set as zero and the maximum E' as unity (Vazquez *et al*. 2005). The commonly used nth order and autocatalytic models have been applied (Toffey and Glasser 1997) previously. There model-fitting approaches can describe a shape for a sigmoidal curve and have been used for kinetics of mechanical development using DMA data for PF resins (Wang *et al*. 2007).

OBJECTIVES

Understanding cure kinetics and mechanical property development in wood/adhesive systems is important for evaluating adhesive performance, formulating new resins, and optimizing process parameters. DMA is a commonly used analytical technique for evaluating cure development of polymer systems but has not been standardized in wood adhesion research. Most cure kinetics models are focused on either predicting the chemical state of the resin (Wang *et al*. 2005) or the mechanical properties (Wang *et al*. 2007). The relationship of the chemical and mechanical advancements remains unclear; however, both are needed to describe bondline development completely. To date, all model-free kinetics such as the Kissinger-Akhira-Sunnose (KAS), Friedman and Vyazovkin methods are exclusively used for modeling DSC data (Wang *et al*. 2005). In this perspective, the objectives of this research are to:

5. Explore improved techniques for directly evaluating wood-adhesive systems and the relationship between mechanical cure and chemical cure, and
6. Validate the application of model-free kinetics to DMA data.

EXPERIMENTAL

PF resin

A PF resole resin, tailored as an adhesive for the core layer of oriented strand boards, was obtained from Georgia-Pacific Company, frozen and stored at -20°C until use. The resin had a high molecular weight with an M_w = 6576 g/mol and M_w/M_n =1.72. The resin solid content was 45.0% with 3.7 wt % nitrogen, indicating the presence of urea in the resin (Wang *et al*. 2005).

Specimen preparations

Planed basswood strips (Midwest Products, Inc.) with nominal dimensions of 50x12x1 mm were oven-dried at 103 °C and stored in a desiccator over anhydrous calcium sulfate until use. Sandwich-type DMA specimens were produced from a layer of PF resin between two pieces of wood adherends. Care was taken to match the grain, thickness, and weight of the two wood adherends within the specimen to maintain a balanced composite design. The bonding surfaces were lightly hand sanded along the grain with 220-grit sandpaper and cleaned with a paper towel immediately prior to resin application. The resin was uniformly applied to the prepared surface of both wood adherends using a small airbrush (BADGER Model 350). The amount of resin solid applied to each surface was set at ca. 50 g/m^2, which equates to ca. 12% of dried wood mass.

Maintaining a consistent resin content was deemed important to repeated cure analysis. He & Yan (2005) demonstrated that the degree of resin loading can influence

the cure development. They concluded that this influence occurred primarily through water absorption and evaporation during the DMA test. Therefore, the specimens were wrapped with aluminum foil to maintain moisture content during the tests for the DMA analysis in order to evaluate the cure kinetics to compare to DSC data.

DMA

DMA measurements were conducted on the sandwich specimens in three-point bending mode at a span 25 mm with a Tritec 2000 analyzer (Triton Technology). The frequency was fixed at 1 Hz. Strain sweep tests have been conducted to establish the linear viscoelastic ranges at working temperature. Oscillation displacement amplitude of 0.03 mm was thus chosen. DMA was performed isothermally at 90, 100, 110, 120, 130, 140, and 160 °C with three replicates in each temperature. In each test, the DMA oven was preheated to predetermined isothermal temperature, and then the specimen was installed quickly and held at the cure temperature until both modulus and damping approached a constant value signifying the completion of detectable mechanical cure. In addition, ramp experiments were performed at heating rates of 2, 3, 4, and 5 °C/min from room temperature to 250 °C with three replicates in each heating rate. Low heating rates were selected to make sure that the effect of thermal lag was minimal.

DSC

To determine the relationship of cure development by DMA and DSC, a

Mettler-Toledo DSC 822e was used to scan a sample in a small disk shape (sandwiched a layer of resin between two pieces of wood), which could fit in a 30μl high pressure gold-plated crucible, trimmed from the DMA specimens immediately following DMA sample preparation for foil-wrapped PF bonded wood joints. Ramp temperature scans were conducted at 6 heating rates 2, 3, 4, 5, 10, and 15 °C/min from 25 to 240 °C. The chemical cure development was obtained under linear heating rates and isothermal chemical cure development was predicted with ramping data as described by Wang *et al*. (2005).

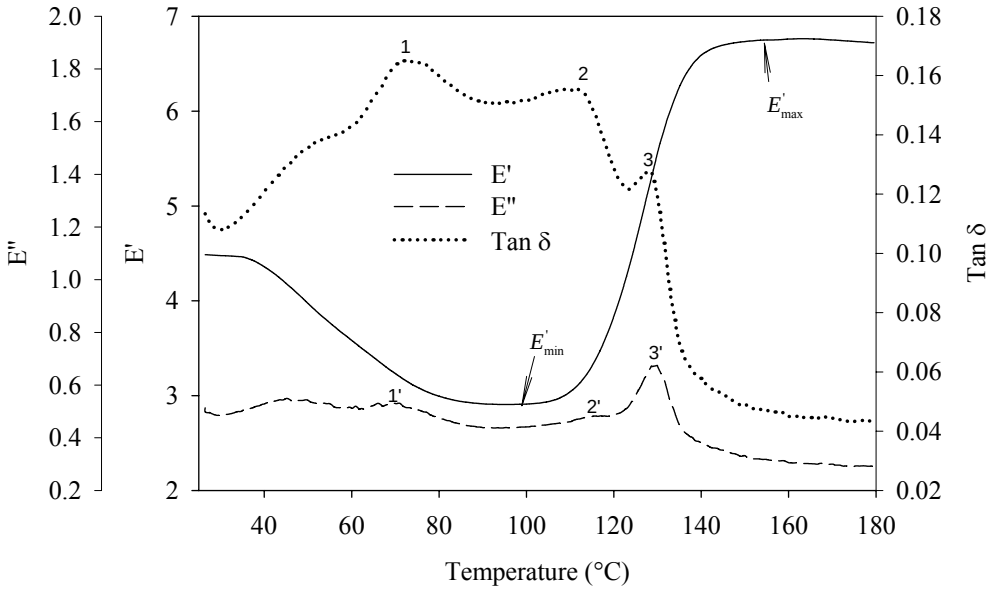

Figure 8.1 Typical DMA traces at 2 °C/min for flexural storage modulus E', loss modulus E", and loss factor tan δ. Numbers (1, 2, and 3 on tan δ; 1', 2' and 3' on E") indicate the glass transition temperature of uncured PF resin, cure transition of gelation and vitrification points; respectively.

RESULTS AND DISCUSSION

Relationship between mechanical cure and chemical cure

A typical DMA trace is shown in Figure 8.1 where the development of flexural storage modulus (*E'*), loss modulus (*E"*), and loss factor (tan δ) during temperature ramping are presented. The glass transition temperature of an un-cured dehydrated PF resin, gelation and vitrification points were assigned (Wang *et al*. 2007). Subsequently, the degree of mechanical cure can be defined as (Vazquez *et al*. 2005, Wang *et al*. 2007).

$$\beta = \frac{E^{'}(t) - E^{'}_{\min}}{E^{'}_{\max} - E^{'}_{\min}} \tag{64}$$

where: $E^{'}_{\min}$, $E^{'}_{\max}$, and $E^{'}(t)$ are the minimum, maximum E', and at the time t during cure processes; respectively. The normalized mechanical cure under linear and isothermal heating regimes are shown as in Figure 8.2(c) and (d); respectively.

It is generally assumed that the heat evolution by DSC is proportional to the molecular network formation, but the elastic modulus is only proportional to the molecular network density if the entire curing process proceeds in the rubbery state (Malkin *et al*. 2005). This assumption only holds for the PF-wood system when the curing temperature is always greater than the glass transition temperature of forming polymer. In order to investigate the relationship of mechanical degree of cure with chemical degree of cure, the chemical cure kinetics was obtained by DSC with small

discs taken from DMA samples. The evolution of α at linear heating rates (Figure 8.2a) was determined by the Mettler-Toledo DSC STARe software. Due to difficulty and accuracy problems of the isothermal DSC scans (Wang *et al*. 2005), the evolution at isothermal temperature (Figure 8.2b) was predicted according to the model-free Vyazovkin method (Wang *et al*. 2005). By comparing α to the prevailing time or temperature with the corresponding β (as shown by arrows in Figure 8.2), the relationship between chemical cure and mechanical cure was obtained in Figure 8.3. It was observed that the mechanical cure changed with chemical cure following a sigmoid.

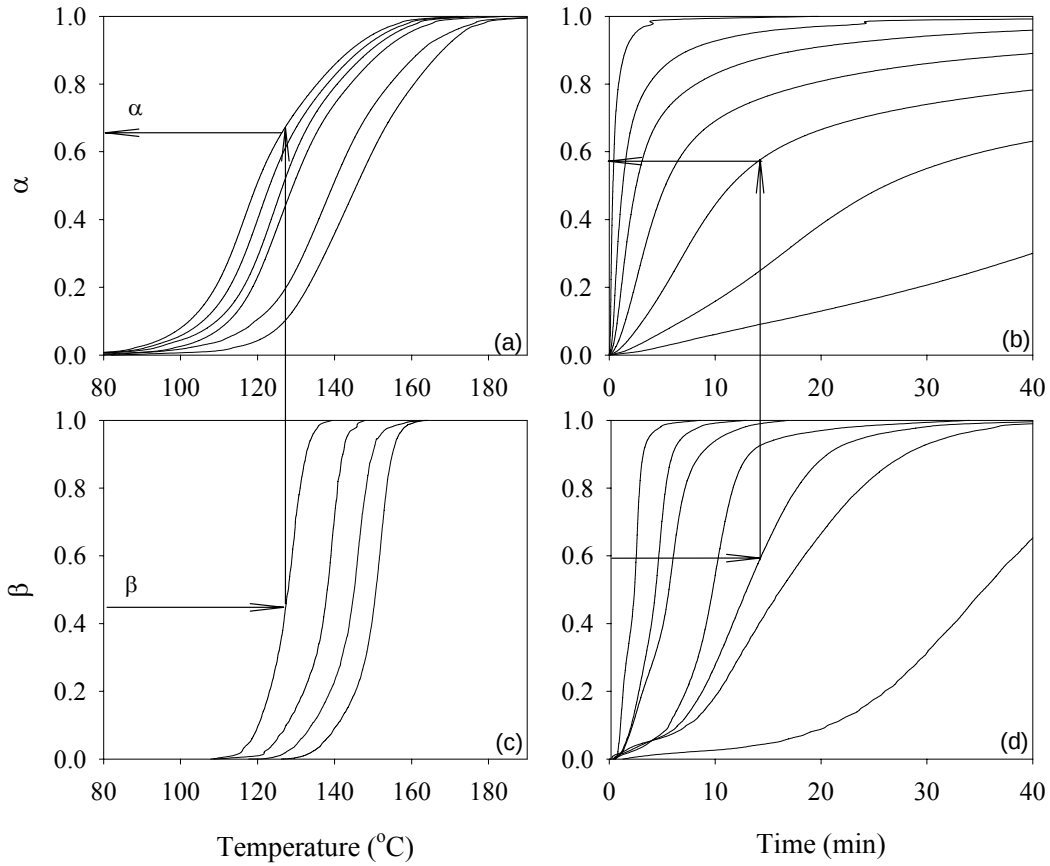

Figure 8.2 The evolution of degree of cure at different cure conditions: (a) Chemical cure by DSC at 2, 3, 4, 5, 10, and 15 °C/min from left to right, (b) Predicted chemical cure at isothermal temperature 90, 100, 110, 120, 130, 140, and 160 °C bottom up by Vyazovkin model-free kinetics from DSC ramp data in (a), (c) Mechanical cure by DMA at 2, 3, 4, and 5 °C/min from left to right for aluminum foil-wrapped PF bonded wood joints, and (d) Mechanical cure by DMA at 90, 100, 110, 120, 130, 140, and 160 °C bottom up for aluminum foil-wrapped PF bonded wood joints.

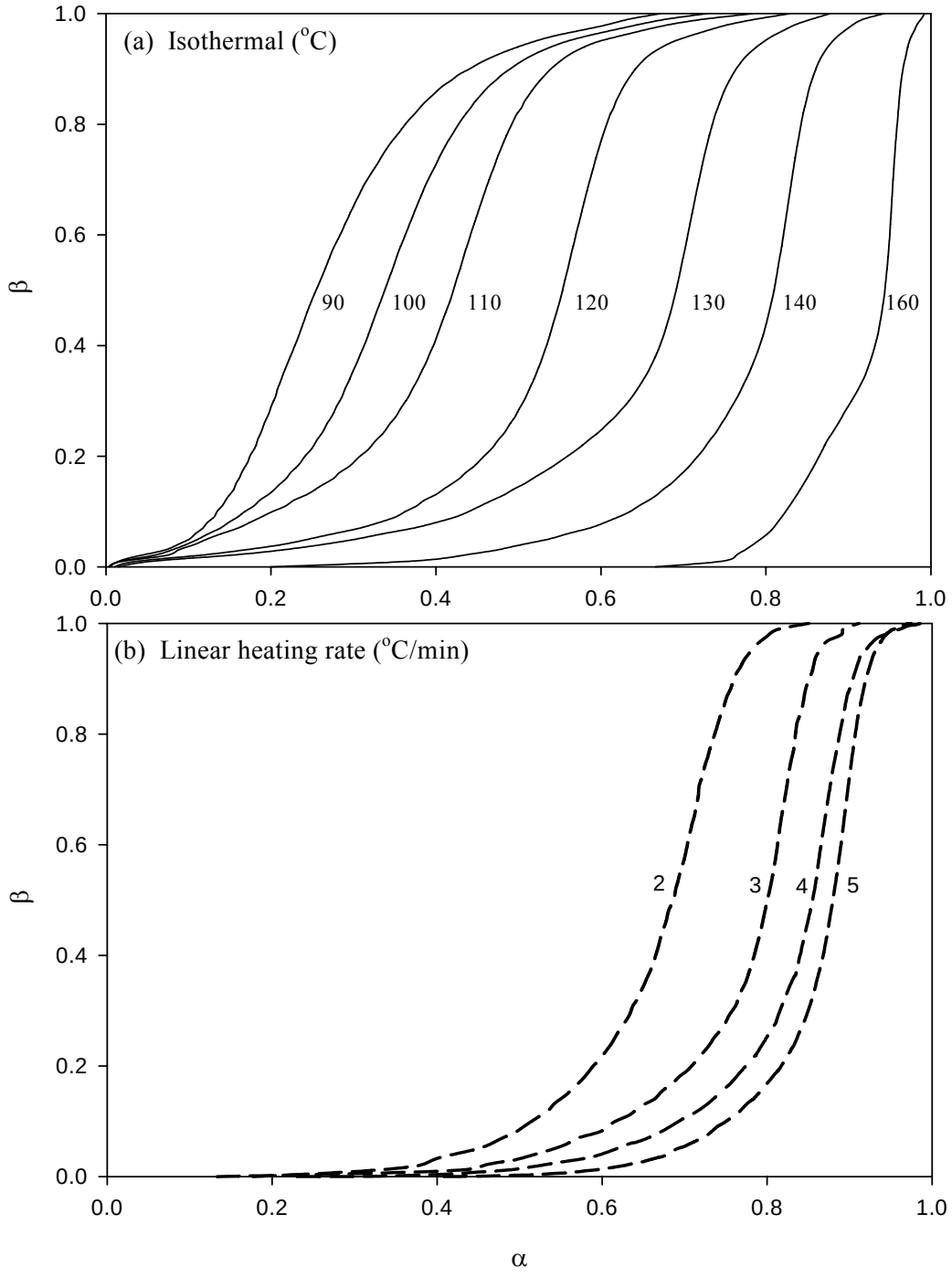

Figure 8.3 Relationship between mechanical cure (β) and chemical cure (α) from aluminum foil-wrapped PF bonded wood joints under isothermal temperature (a) and linear heating rate (b).

Under both isothermal and linear heating regimes, a comparison of mechanical cure with chemical cure includes: (1) a slow rate increasing or delay period of front tail; (2) a rapid increase in mechanical properties with medium to high levels of α; (3) a decreasing rate of mechanical property development leading to a cessation of mechanical cure. At low isothermal temperatures, the onset of mechanical cure was almost identical to the onset of chemical cure; however the sensitivity of mechanical cure development at the early stages of chemical cure was low. For these conditions, the cessation of mechanical cure occurred at a low chemical cure of around 0.6. With increasing isothermal temperature, the onset of mechanical cure was delayed until substantially high amounts of chemical cure accumulated. When the curing temperature was 160 °C, the mechanical cure did not start until the chemical degree of cure reaches 0.7 and the cessation of mechanical cure approached fully chemical cure. These observations indicate that the initial stages of chemical cure did not increase viscosity or shear modulus proportionally. When the curing temperature is high, the resin needs to attain substantial chemical cure to resist the softening effects of temperature. One might have expected that β depends only on the state of α and is independent of the time and cure regimes. The observations from the present study clearly indicated that although the β under the different cure conditions followed the same trend, the effect of cure temperature on the E' was clearly discernable. While the mechanical stiffness was influenced by chemical advancement, the cured materials are in a state of expansion and under the influence of temperature. Therefore, with an increasing heating rate or isothermal temperature, a higher degree of cure is required

to achieve an equivalent modulus observed at a lower temperature. Hence, the cure curve shifted to the higher degree of chemical cure as the cure temperature increased. The curing temperatures (peak temperature at tan δ peak) at heating rate 2 and 3 °C /min were ca. 128.5 and 137.0 °C (Wang *et al*. 2007). It is noted that relation of β–α curves developed from the ramp heating experiments at 2 and 3 °C /min were coincidently located in the same region as those from the isothermal temperatures of 130 and 140 °C (Figure 8.3). Similarly, the β-α curves under 4 and 5 °C /min heating ramps were located between the curves for 140 and 160 °C (Figure 8.3) since curing windows at these heating rates were around 150 °C.

In Figure 8.4, it is shown that the wood/PF system has a glass transition temperature around 145 °C by DSC. However, it is more appropriate to think of glass transition temperature as a region with an onset, a midpoint and an associated breadth. When the cure development was investigated in this region (130-160 °C), mechanical cure did not begin until substantial chemical cure occurred. However, regardless of the beginning, final mechanical and chemical cure occurred at similar points (Figure 8.3).

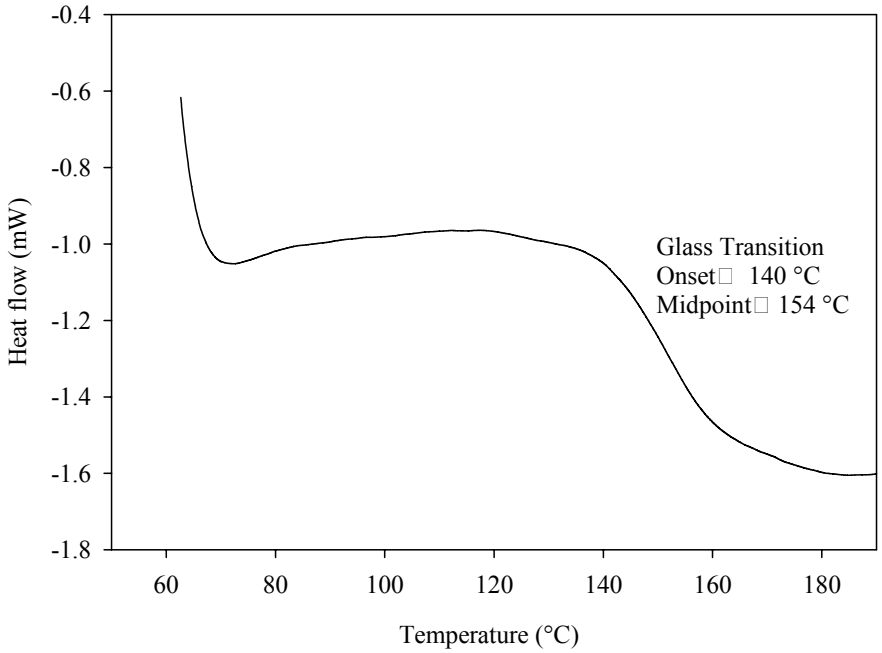

Figure 8.4 DSC thermgram at 10 °C/min showing glass transition temperature for a sample with two small pieces of basswood discs bonded by PF, trimmed from the DMA specimen after scanned from room temperature to 240 °C at 5 °C/min.

The β and α corresponding to the gelation and vitrification points were summarized in Table 8.1and Table 8.2. The gelation point defined by second peak on tan δ curve (Figure 8.1) was very close to the onset of mechanical cure as evidenced by small value for β. It has been reported that gelation occurs at a constant conversion, which is independent of cure regimes for a given thermosetting material (Prime 1997). In this study, the average value of α at gelation was ca. 0.51 and was relatively constant across heating rates (Table 8.1). There were other reports that gelation was not iso-conversional under different cure regimes suggesting the heterogeneity of the curing process, as shown by Han and Lem (1983), and Malkin *et al*. (2005). Gelation

was only recorded for the linear heating regime with aluminum foil-wrapped PF bonded wood joints because this event was not consistently evident in other samples. The value for α at the vitrification point increased with heating rate or isothermal temperature. That is, vitrification occurred at higher degrees of cure with increasing cure temperatures, which was in agreement with the report for an epoxy resin (Yu *et al*. 2006). Such a result was reasonable since at high temperature, the resin needed to reach a high degree of cure required to achieve a glass transition to exceed the cure temperature. For example, at 90 °C, the α of 0.22 rendered a glass transition temperature for the system beyond the 90 °C, while at 160 °C, the α of 0.95 are required to achieve a glass transition temperature of forming polymer to exceed the cure temperature for vitrification. In this sense, Table 8.2 also provides the relationship of α and the Tg, which was linear in the studied temperature region.

Table 8.1 Corresponding mechanical and chemical degree of cure at gelation and vitrification points under the linear heating regime for aluminum foil-wrapped PF bonded wood joints.

Ramp (^{o}C/min)		2	3	4	5
Gelation	β	0.04	0.04	0.03	0.04
	α	0.42	0.52	0.56	0.52
Vitrification	β	0.58	0.60	0.62	0.64
	α	0.70	0.81	0.87	0.89

Table 8.2 Corresponding mechanical and chemical degree of cure at the vitrification points under the isothermal heating regime for foil-wrapped PF bonded wood joints.

Iso Temp (^{o}C)	90	100	110	120	130	140	160
β	0.34	0.50	0.52	0.55	0.58	0.60	0.65
α	0.22	0.34	0.43	0.56	0.70	0.82	0.95

As mentioned above, the β-α curves are sigmoidal and can be fitted using the following two-parameter expression (Eq.(65)).

$\beta = 1 - \exp\left(-(k\alpha)^m\right)$	(65)
$\frac{d\beta}{d\alpha} = km\left(k\alpha\right)^{m-1}\exp\left(-(k\alpha)^m\right)$	(66)

where *k* and *m* are fitting parameters obtained with nonlinear regression. When investigating these parameters (Table 8.3**)** under different isothermal and linear heating regimes, it was noted that both were dependent on the isothermal cure temperature or heating rate (Figure 8.5). The sensitivity of β to changes in α, is defined by dβ/dα. This derivative is directly defined by the slope in plot of β versus α (Figure 8.3) and can be directly calculated from Eq. (66). Also note that when $(k\alpha)^m$ = (m-1)/m, dβ/dα reaches a maximum.

Experimental data of dβ/dα are presented in Figure 8.6 under isothermal heating regime and in Figure 8.7 under linear heating regime. By comparing the α defining the maximum of dβ/dα, it was found that the peak slope coincided with

vitrification; i.e. in the vicinity of the vitrification point, small changes in chemical advancement promoted a large mechanical increment. Mechanical properties are mainly related to molecule mobility and therefore, relaxation time.

It was concluded that mechanical cure changed with chemical cure following a sigmoid. Both the initial α and final curing stages contributed little to the state of mechanical cure. The chemical cure and mechanical cure are not equivalent and β changed with the curing regime at specific chemical degree of cure.

Table 8.3 Parameters for the relationship equation of mechanical and chemical cure

	Isothermal temperature (°C)							**Linear heating rate (**°C/min)			
	90	**100**	**110**	**120**	**130**	**140**	**160**	**2**	**3**	**4**	**5**
k	3.35	2.67	2.22	1.74	1.41	1.22	1.05	1.42	1.23	1.15	1.13
m	2.60	3.43	4.53	7.55	9.24	14.33	25.71	9.74	14.74	15.68	19.06

R^2>0.99 for all fitting parameters

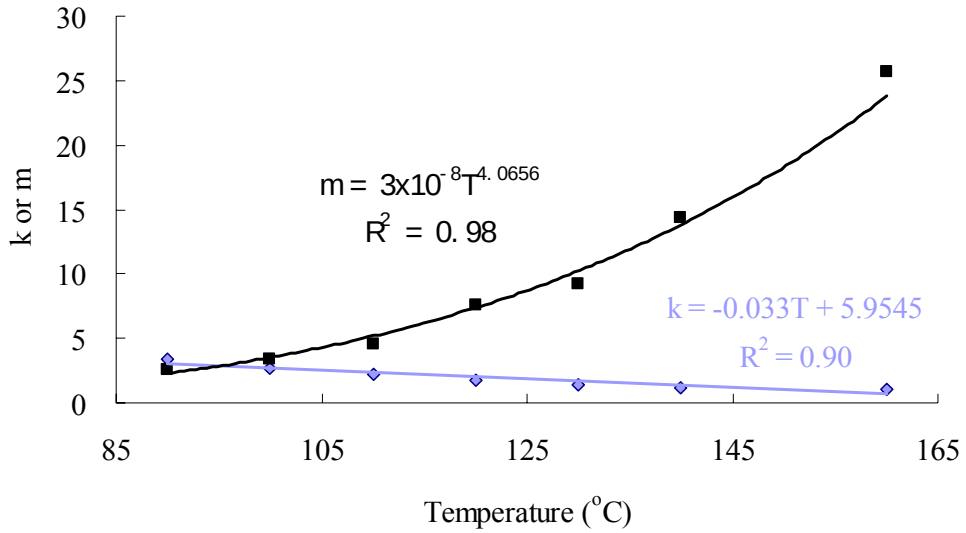

Figure 8.5 Temperature dependence of parameters for the relationship equation of the mechanical and chemical degree of cure under isothermal temperatures, T in Celsius degree.

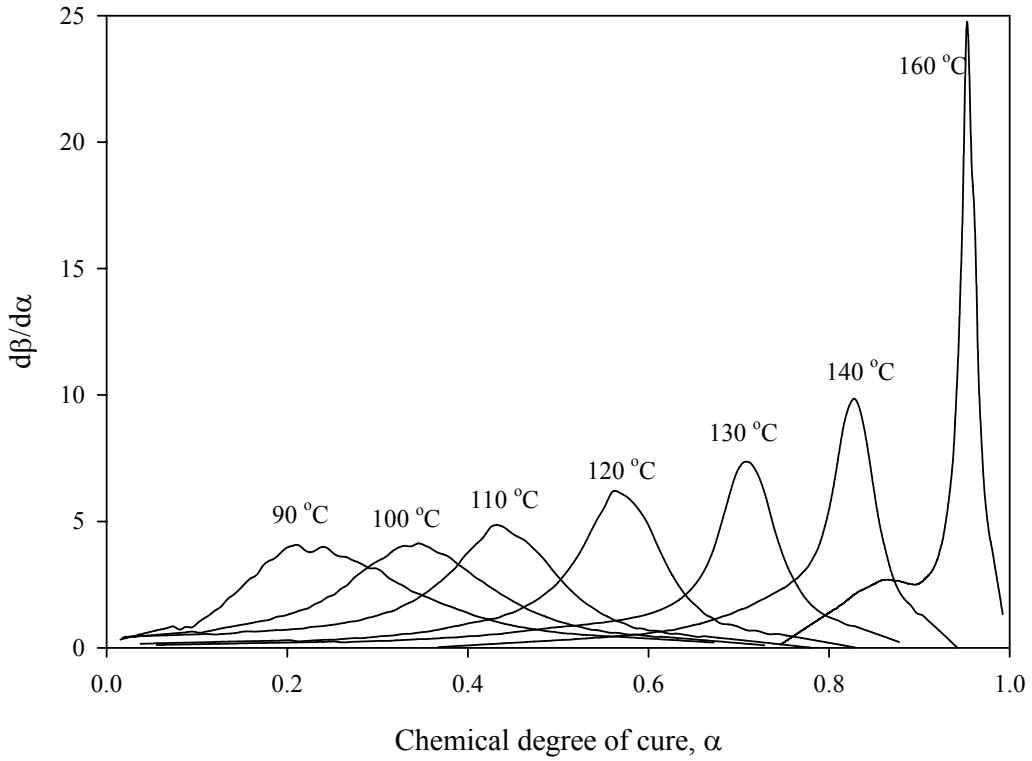

Figure 8.6 Sensitivity of mechanical property development to chemical advancement at designated isothermal temperature computed from experimental data.

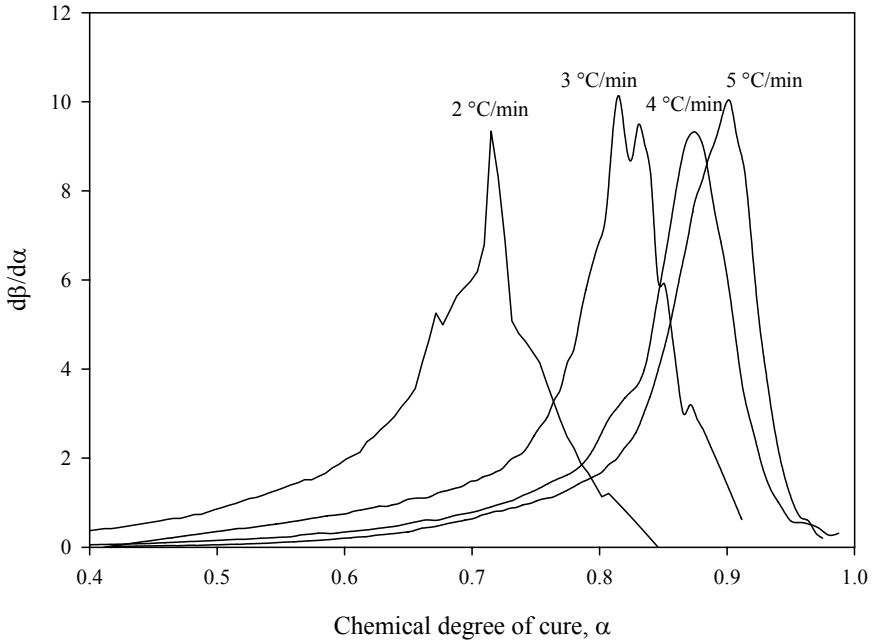

Figure 8.7 Sensitivity of mechanical property development to chemical advancement at designated linear heating rates.

Model-free kinetics of the mechanical cure development

The chemical cure kinetics for PF resin has been established by DSC (Wang *et al*. 2005; 2006). The relationship between chemical and mechanical degree of cure has been described by Eq.(65). In the following, model-free kinetics is used to describe the mechanical cure development by DMA. Using this approach, either α or β can be computer using a kinetics approach and then related to the other through Eq. (65). The basic assumption of the model-free methods is that activation energy is dependent on the development of the reaction. The MFK Friedman, Vyazovkin, KAS and time event algorithms can then be used to determine the activation energy

dependence on the advancing degree of cure. The basic kinetic model formulated for β is:

$$\frac{d\beta}{dt} = A\exp\left(-\frac{E}{RT}\right) f(\beta) \tag{67}$$

The direct use of Eq. (67) gave rise to the differential method of MFK Friedman ((68)) that could be applied to isothermal as well as to ramp data (Wang *et al*. 2005).

$$\ln\left(\frac{d\beta}{dt}\right)_{\beta i} = C_f(\beta) - \frac{E_\beta}{RT_{\beta i}} \tag{68}$$

where $C_f(\beta)$ and E_β are MFK Friedman complex parameter and activation energy; respectively (subscripts β and *i* refer to specific mechanical degree of cure and a series of heating regimes hereafter). For isothermal conditions, integration and rearrangement of Eq. (67) yields:

$$\ln(\Delta t_{\beta i}) = \ln\left(\frac{g(\beta)}{A_\beta}\right) + \frac{E_\beta}{RT_i} \tag{69}$$

where $g(\beta) = \int_0^\beta d\beta / f(\beta)$ is the integral form of the reaction model f(β) and $\Delta t_{\beta i}$ is the time required to reach a specified conversion, β, at an iso-temperature, T_i. Let $C_t(\beta) = \ln(g(\beta)/A_\beta)$, then E_β and $C_t(\beta)$ was evaluated from the slope and intercept of the plot $\ln\Delta t_{\beta i}$ against reciprocal of temperature $1/T_i$. This method was thereafter referred as the time-event model-free kinetics.

For ramp conditions, the model-free KAS method uses Eq. (70) (Wang *et al*. 2005).

$$\ln\left(\frac{\varphi_i}{T_{\beta i}^2}\right) = C_k(\beta) - \frac{E_\beta}{RT_{\beta i}} \tag{70}$$

Likewise, the model-free Vyazovkin method can be applied to isothermal and ramp data to obtain two set of parameters. In the Vyazovkin method, n scans are performed at different heating regimes $T_i(t)$. The activation energy at a specific degree of cure is obtained by minimizing the function $\varphi(E_\beta)$ (Wang *et al*. 2005):

$$\varphi(E_\beta) = \sum_{i=1}^{n} \sum_{\substack{j=1 \\ (j \neq i)}}^{n} \frac{I[E_\beta, T_i(t_\beta)]}{I[E_\beta, T_j(t_\beta)]} \tag{71}$$

In Eq. (71) the temperature integral, I, is defined as:

$$I[E_\beta, T(t_\beta)] = \int_{t_{\beta-\Delta\beta}}^{t_\beta} \exp\left(\frac{-E_\beta}{RT(t)}\right) dt \tag{72}$$

And

$$C_v(\beta) = \int_0^\alpha \frac{d\beta}{Af(\beta)} = \frac{1}{\varphi} \int_{T_0}^{T} \exp\left(\frac{-E_\beta}{RT}\right) dT \tag{73}$$

Figure 8.8a depicts the activation energy curves for PF bonded wood joints wrapped with foil. The parameters are calculated from isothermal data using the time-event and Vyazovkin methods; from ramp data by the KAS, Friedman and Vyazovkin methods. As Wang *et al*. (2005) demonstrated that the activation energy curves were overlapped by Friedman and Vyazovkin methods from DSC data, the activation energy curves were also overlapped by these two methods from DMA data. To simplify the graphs, the activation energy curves by the Friedman method are not plotted in Figure 8.8a. It was observed that the activation energy computed from ramp data by the KAS method nearly overlapped with that from isothermal data by time–event method. The most notable exceptions are at a low degree of cure. In this case, the activation energy obtained from both ramp and isothermal data with the Vyazovkin method followed a

similar pattern. Average activation energies are 52.6 and 49.4 kJ/mol from isothermal data by Vyazovkin and time event, and are 50.1, 47.8 and 52.2 kJ/mol from ramp data by Vyazovkin, Friedman and KAS methods; respectively. They are in general agreement with those obtained by model-fitting kinetic approaches (Wang *et al*. 2007). The MFK combined parameters C(β) are shown in Figure 8.8b. Their physical meanings are not obvious and can be used with activation energy to fully describe cure development.

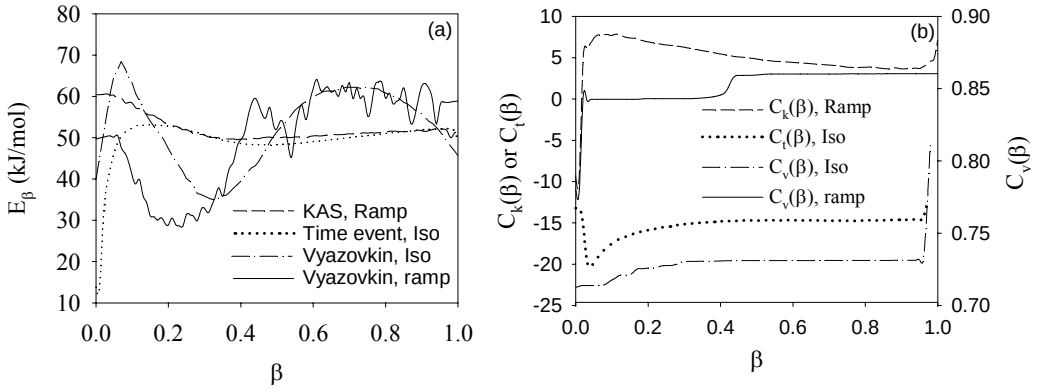

Figure 8.8 Activation energy dependence of mechanical cure (a) and combined parameters (b) obtained by KAS, time event, and Vyazovkin methods for aluminum foil-wrapped PF bonded wood joints.

The strength of model-free kinetics is in that providing an algorithm for predicting cure development across various temperature programs with only two vector parameters. C(β) and E_β obtained from the isothermal and ramp data were

utilized for assessing the MKF predictions on the mechanical cure development during ramp and isothermal cure of PF resins. Using the KAS parameters, $C_k(\beta)$ and E_β were extracted from ramp data to predict cure development both under ramp and isothermal temperature, and using Vyazovkin parameters from ramp data to predict cure development under isothermal conditions have been detailed elsewhere with DSC data (Wang *et al*. 2005). These algorithms also worked for DMA data. Figure 8.9 showed the experiment data at 1, 2, and 3 °C /min and KAS predictions; Figure 8.10 showed the experimental data at 120 °C and predictions by KAS, Friedman and Vyazovkin methods from ramp data. The parameters by Vyazovkin obtained from isothermal data can be used to predict cure behavior under isothermal temperature in the same manner as the Vyazovkin method from ramp data (Figure 8.11). With the MFK time-event method, substituting the parameters E_β and $C_t(\beta)$ into Eq. (69), the needed time to reach specific β can be obtained at specific isothermal temperature (Figure 8.11). Visually, all predictions were in agreement with the experiments.

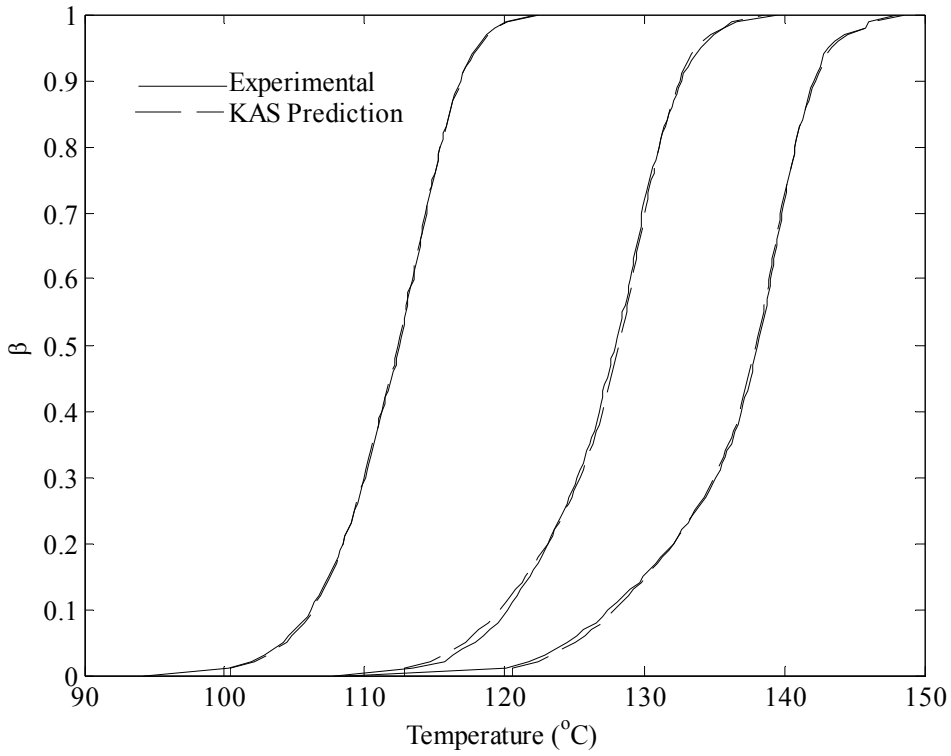

Figure 8.9 Comparison of experimental mechanical degree of cure at 1, 2, and 3 °C /min for aluminum foil-wrapped PF bonded wood joints and KAS predictions from ramp data.

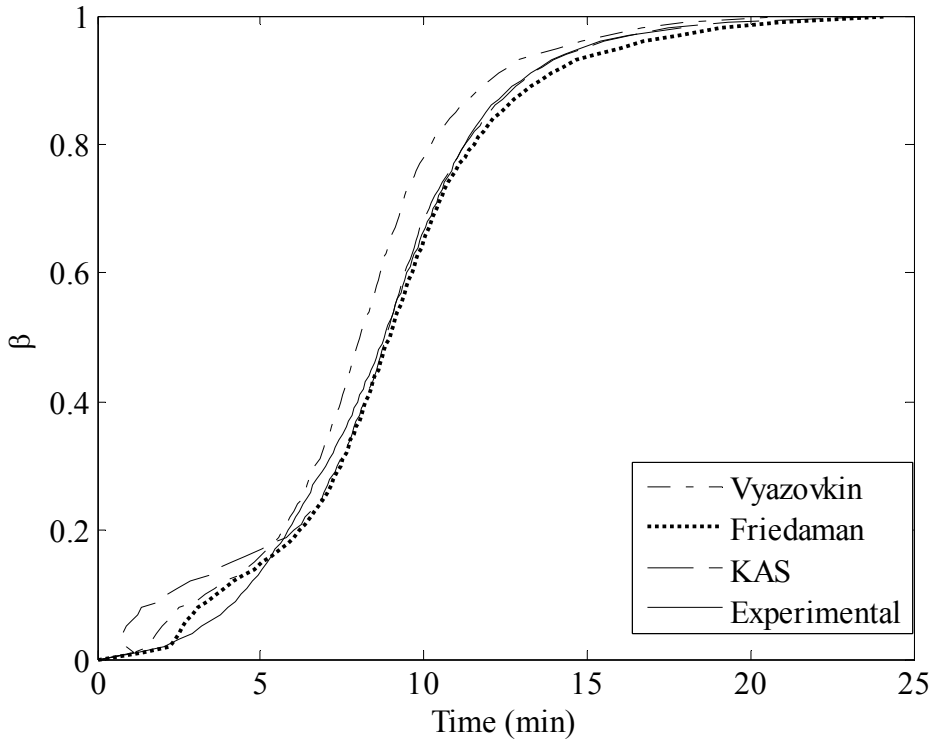

Figure 8.10 Comparison of experimental mechanical degree of cure at 120 °C for aluminum foil-wrapped PF bonded wood joints and predictions with parameters E_β and $C(\beta)$ from ramp data.

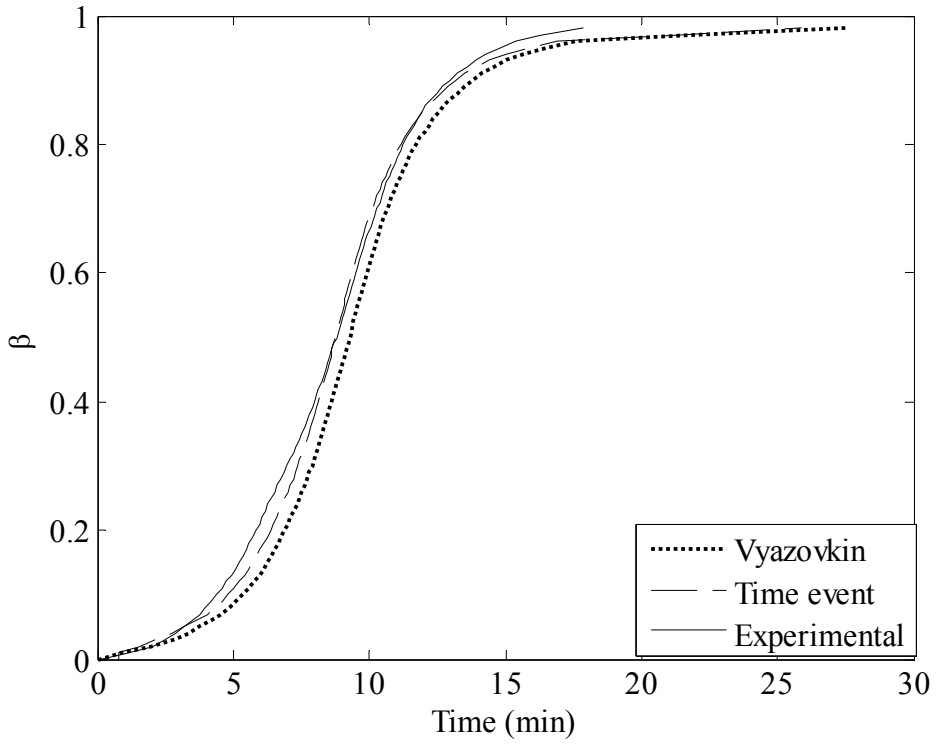

Figure 8.11 Comparison of experimental mechanical degree of cure at 120 °C for aluminum foil-wrapped PF bonded wood joints and predictions with the parameters from isothermal data.

CONCLUSION

Previous research has shown that foil-wrapped PF joints facilitated the detection of gelation peaks on tan δ curves under linear heating regime and cured slowly as compared with un-wrapped counterparts (Wang *et al*. 2007). It was then hypothesized that cure conditions in a foil-wrapped specimen was similar with those in hot-pressing where moisture loss is inhibited by a bulk of mass volume and platens

as well as those in sealed high pressure pans by DSC. Hence, mechanical degree of cure from foil-wrapped PF bonded wood joints was matched with chemical degree of cure determined by DSC. The mechanical cure was found to follow a sigmoidal relation with the chemical degree of cure and was fitted by a typical sigmoid function analogous to a two-parameter Weibull cumulative distribution function. The chemical degree cure at the gelation point as defined by DMA was relatively constant while the chemical degree of cure at vitrification points increased with isothermal temperature or linear heating rates. The maximum in $d\beta/d\alpha$ was coincident with the vitrification points.

The magnitude of activation energy represents an important established method of reporting and comparing kinetic data. The mechanical cure development was modeled by model-free models. The activation energies dependence of mechanical degree of cure has been obtained by model-free kinetic methods for foil-wrapped PF bonded joints. The average activation energy by each method was well in agreement with each other and with those by model-fitting methods (Wang *et al*. 2007). Although physical interpretation of activation energy dependence on mechanical cure advancement was illusive, two vector parameters from model-free kinetics provided a powerful predictive algorithm. The parameters extracted from isothermal data or ramp data all gave a good prediction for cure evolution across various isothermal temperatures. Therefore, after either mechanical or chemical cure development is characterized, the other can be estimated through connection of correlation function between mechanical and chemical degree of cure.

REFERENCES

Christiansen, A. W.; Follensbee, R. A.; Geimer, R. L.; Koutsky, J. A.; Myers, G. E. Phenol-formaldehyde resin curing and bonding in steam-injection pressing. Part II. Differences between rates of chemical and mechanical responses to resin cure. *Holzforschung (1993), 47*(1), 76-82.

Han, C. D.; Lem, K. W. Chemorheology of thermosetting resins I. The chemorheology and curing kinetics of unsaturated polyester resin. *Journal of Applied Polymer Science (1983), 28*(10), 3155-83.

He, G.; Yan, N. Effect of wood species and molecular weight of phenolic resins on curing behavior and bonding development. *Holzforschung (2005), 59*(6), 635-640.

Laborie, M.-P. G. Investigation of the morphology of the wood/phenol-formaldehyde adhesive interphase. Doctoral dissertation, Virginia Polytechnic Institute and State University, (2002), Blacksburg, VA.

Malkin, A. Ya.; Gorbunova, I. Yu.; Kerber, M. L. Comparison of four methods for monitoring the kinetics of curing of a phenolic resin. *Polymer Engineering and Science (2004), Volume Date 2005, 45*(1), 95-102.

Prime, R. B. Thermosets. In: Turi E.A, editor. Thermal characterization of polymeric materials. New York: Academic Press, (1997), p435–569.

Steiner P.R.; Warren, S. R. Rheology of Wood-Adhesive Cure by Torsional Braid Analysis, *Holzforschung (1981), 35* (6) 273-278.

Toffey, A; Glasser, W. G. Cure characterization of polyurethanes with lignin and cellulose derivatives. *Holzforschung (1997), 51*(1), 71-78.

Vazquez, G.; Lopez-Suevos, F.; Gonzalez-Alvarez, J.; Antorrena, G. Curing process of phenol - urea - formaldehyde -tannin (PUFT) adhesives. Kinetic studies by DSC and DMA. *Journal of Thermal Analysis and Calorimetry (2005), 82*(1), 143-149.

Wang, J.; Laborie, M.-P. G.; Wolcott, M. P. Comparison of model-free kinetic methods for modeling the cure kinetics of commercial phenol-formaldehyde resins. *Thermochimica Acta (2005), 439*(1-2), 68-73.

Wang, J.; Laborie, M.-P. G.; Wolcott, M. P. **C**omparison of model-fitting kinetic methods for modeling the cure kinetics of commercial phenol-formaldehyde resins.

Journal of Applied Polymer Science (2006), accepted.

Wang, J.; Wolcott, M. P.; Laborie, M.-P. G. Model-fitting kinetic analysis of phenol-formaldehyde bonded wood joints. Chapter 7, 2007.

Yu, H.; Mhaisalkar, S. G.; Wong, E. H.; Teh, L. K.; Wong, C. C. Investigation of cure kinetics and its effect on adhesion strength of nonconductive adhesives used in flip chip assembly. *IEEE Transactions on Components and Packaging Technologies, (2006), 29*(1), 71-79

Chapter 9 Summary and Conclusions

Two complementary methods of differential scanning calorimetry (DSC) and dynamic analytical analysis (DMA) were used to characterize the cure development of the core and face phenol-formaldehyde (PF) resol resins. Quantitative analyses with ^{1}H-, ^{13}C-NMR, and gel permeation chromatography demonstrated that the core PF resin has a higher molecular weight distribution than the face PF resin, and thereafter the core PF was labeled as PF-high and the face as PF-low. First, the resins were characterized in a neat state with DSC, in the blends of PF wood at various wood content levels with DSC, and in the thin film between two wood substrates, using DMA and the three-point bending test. The synergy of DSC and DMA techniques could pick up the intrinsic events and features of the PF curing processes, and characterization was comparable between the two techniques. Although the conclusions were based on PF resins, the developed kinetics and methodology should also be applicable to other thermosets.

In the neat state, both PF-high and PF-low resins exhibited two distinct exotherms that shifted to higher temperatures with an increasing heating rate. The PF-high resin reached similar degrees of cure, with *ca*. 10°C occurring earlier than that required for the PF-low resin. The chemical degree of cure was based on the reaction heat evolution recorded using DSC, and was assumed to be proportional to the crosslinking network formations. To model resin cure kinetics, model-fitting and model-free kinetics were used. Model-fitting kinetics of the nth-order Borchardt-Daniels (nth-BD), ASTM E698 (E698), autocatalytic Borchardt-Daniels

(Auto-BD), and modified autocatalytic methods (M-Auto) were evaluated on PF-high and PF-low resins. The n^{th}-BD, E698 and M-Auto methods all produced comparable values of activation energies (around 97 kJ/mol), while the Auto-BD method yielded aberrant values. For dynamic cure prediction, all model-fitting models failed to predict reaction rate, while degree of cure was reasonably well-predicted with all three methods. As a whole, the n^{th}-BD method best predicted the degree of cure for both resins. Due to the limitations of model-fitting kinetics, the Friedman, Vyazovkin and Kissinger-Akahira-Sunose (KAS) model-free-kinetics algorithms were applied to the same DSC data to model and predict the cure kinetics of commercial resoles. Results demonstrated that the model-free kinetics of the Friedman and Vyazovkin methods can provide insight into the cure mechanisms of PF resoles, and that the KAS method can predict cure development under isothermal and linear heating regimes. However, these methods were not as effective for n^{th}-BD predictions.

Although the cure development of neat PF resins can provide useful information for resin formulators, cure development in the presence of wood can elucidate wood-PF interactions, as well as the effects of wood presence on cure kinetics. DSC analysis showed that the curing behavior of the PF resin did not change significantly when wood content was below 20%. When wood content was over 35%, the overall DSC curve shapes and kinetic parameters changed. The wood addition accelerated one reaction and made it occur at a lower temperature; however, the main reactions did not change. Moreover, there was no significant difference in the effects of wood on PF curing behavior among the two species and their extracted

counterparts. Additionally, the paper cellulose and xylan hemicelluloses did not change the cure behavior of PF resin at 35% wood content, while lignin and southern yellow pine extractives delayed the cure development. Both southern yellow pine and aspen extractives released similar heat reactions, while all other fillers reduced the reaction heat significantly. This suggests that the resins did not reach the same cure extent in the presence of wood and wood constituents, as compared with PF alone.

The *in situ* shear moduli of the PF resins were estimated from 0.01 to around 16 MPa during the curing process, and were in a typical rubber range. The storage modulus ratio, defined as, $R = E'_{max} / E'_{min}$, maximum storage modulus (E'_{max}) , and loss tan δ after cure were recommended for direct evaluating the performance of wood-adhesive systems using DMA analysis. Theoretically, the ratio R should approach a value of 4. DMA curves. Results showed that the PF-low bonded wood joints cured slower and achieved a significantly higher shear modulus, E'_{max} and R as well as a lower tan δ after curing than the PF-high bonded wood joints. With a similar resin load, the PF-low formed a very thin bond layer as compared with PF-high, suggesting a good interphase response, which is related to good stiffness and low viscoelasticity for cured PF-low wood joints. The transition temperatures of the curing process and cure development could be clearly assigned to *tan δ*. Vitrification was probed in all samples, while gelation point was only detected for foil-wrapped wood joints under linear heating regime. It was assumed that moisture loss in unwrapped joints muffled the gelation points. The activation energy for gelation and vitrification were approximately 40 and 48 kJ/mol respectively.

The mechanical degree of cure is based on the storage modulus development recorded by DMA. The activation energies using model-fitting kinetics of the autocatalytic, Prout-Tompkins, and Avrami-Erofeev models were similar, and these results were in agreement with those using time events of vitrification with isothermal data. The activation energies obtained from linear heating data by the Kissinger equation were a bit larger than those from isothermal data. The activation energy obtained from these methods under both linear heating and isothermal regime are around 50-70 kJ/mol, which are less than those obtained from the neat resins by DSC (85-100 kJ/mol) and in agreement with those of PF/wood mixtures obtained by DSC. These results imply that the activation energy of cure processes decrease in the presence of wood.

The activation energy dependence of the mechanical degree of cure was obtained by model-free kinetics of Vyazovkin, Friedaman, KAS and isothermal time methods for aluminum foil-wrapped PF-high bonded wood joints. The average activation energy using each method were in good agreement with each other and with those using model-fitting methods. Two vector parameters from model-free kinetics provided a powerful predictive algorithm. The parameters extracted from isothermal data or ramp data all gave a good prediction for cure evolution across various isothermal temperatures.

The relationship between chemical cure and mechanical cure was correlated with an equation analog to the Weibull cumulative function. Therefore, when either mechanical or chemical cure development was characterized, the other can be

estimated. From this relationship, it was found that the chemical degree of cure at gelation was independent of cure regime, while the chemical degree of cure at vitrification increased with cure temperature. At vitrification points, the maximum change rate for the mechanical degree of cure with respect to the chemical degree of cure occurred.